THE AMERICAN MINERALOGIST
JOURNAL OF THE MINERALOGICAL SOCIETY OF AMERICA

Vol. 24 DECEMBER, 1939 No. 12, Part 1

POLYMORPHISM OF THE MICAS

STERLING B. HENDRICKS,

WITH OPTICAL MEASUREMENTS

MERRILL E. JEFFERSON,

Fertilizer Research Division, Bureau of Chemistry and Soils, U. S. Department of Agriculture, Washington, D. C.

Many systematic studies have been made of the compositions and optical properties of the micas, but failure of good face development other than the prominent cleavage has limited crystallographic work. Micas have been variously described, without real crystallographic evidence, as monoclinic, hexagonal, and triclinic; the preference usually being for monoclinic. *X*-ray diffraction patterns of muscovite show that it is monoclinic and the few published results on biotite lead to a similar conclusion.

It has been an objective of this laboratory to obtain structural information on minerals important in determining the properties of soils. The following study, while a part of this program, originated in an entirely accidental manner. One of several biotite samples that were being examined in a study of diffuse scattering from the micas showed an unexpectedly complicated diffraction pattern. A wealth of polymorphism was found upon digressing.

X-ray diffraction patterns were made from single crystals of more than a hundred specimens of micas. Crystal structure analyses were then carried out for the various polymorphic modifications. In presenting the results, however, it is more convenient first to describe the structures, and then to discuss the various specimens.

ACKNOWLEDGMENT

Work was greatly facilitated by the gracious cooperation of a number of mineralogists. Dr. W. F. Foshag, of the U. S. National Museum, Dr. C. S. Ross, Dr. W. T. Schaller and Miss Jewell Glass, of the U. S. Geological Survey, supplied the majority of the mica samples examined. They also took part in discussions of the question of composition and optical properties. Dr. H. E. Merwin, of the Geophysical Laboratory,

gave freely of his time in discussion. The best suite of samples available were the lepidolites that had been so carefully analyzed by Mr. R. E. Stevens of the U. S. Geological Survey. Dr. A. F. Hagner, of Columbia University, supplied a large number of samples, only a few of which were studied, and Dr. R. W. Webb, of the University of California at Los Angeles furnished a sample of alurgite that he has recently described. Possible significance of open groups of symmetry operations was discussed with Professor E. Teller, of George Washington University.

General Description of the Mica Structure

A general type of structure shown by many silicate layer minerals, including the micas, was first proposed by Pauling*[1] on the basis of his coordination theory. Mauguin[2] earlier had measured the units of structure and had discussed types of isomorphous replacement. He pointed out that the *c*-axis of biotite apparently was only half as long as that of muscovite. Jackson and West[3] made a detailed analysis of the structure of muscovite independent of Pauling's work.

The composition of muscovite approximates $[Al_2]\ (AlSi_3)O_{10}(OH, F)_2K$. Aluminum shown in brackets, $[Al_2]$, has octahedral coordination with respect to neighboring oxygen and hydroxyl ions. It is replaced by magnesium in phlogopite, $[Mg_3]\ (AlSi_3)O_{10}(OH, F)_2K$, and by magnesium, lithium, titanium, ferric and ferrous iron in various other micas related to biotite and lepidolite. An atom of a group $(AlSi_3)$ is surrounded by four oxygen ions at the corners of a tetrahedron. These tetrahedra are joined by the sharing of oxygen ions at three of the four corners into a hexagonal net having the composition $(AlSi_3O_{10})_n$ with the unshared oxygen ions coplanar as shown in Fig. 1*c*. Two such sheets are combined by octahedral coordination about aluminum, magnesium, iron, etc., of the unshared oxygen ions and of hydroxyl ions at the centers of the plane hexagons formed by the oxygen ions. A layer of this type having the composition $[Mg_3AlSi_3O_{10}(OH, F)_2]^-$ is shown in projection in Fig. 1*a*, and a similar one for muscovite $[Al_2AlSi_3O_{10}(OH, F)_2]^-$ is illustrated in Fig. 1*b*. The complete structure is formed by joining such layers with potassium ions at the centers of the hexagons in the projection of Fig. 1*a* and 1*b*, each of these potassiums having twelve neighboring oxygen ions, six being in the top of one layer and six in the bottom of another. The perfect cleavage, characteristic of the micas, is between the layers.

* Pauling indicated in a conversation with Foshag and Hendricks about five years ago that he suspected polymorphism among the micas.

[1] *Proc. Nat. Acad. Sci.*, **16**, 123 (1930).

[2] *C. R.*, **185**, 228 (1927); **186**, 879 and 1131 (1928).

[3] *Zeits. Krist.*, **76**, 211 (1930); **85**, 160 (1933).

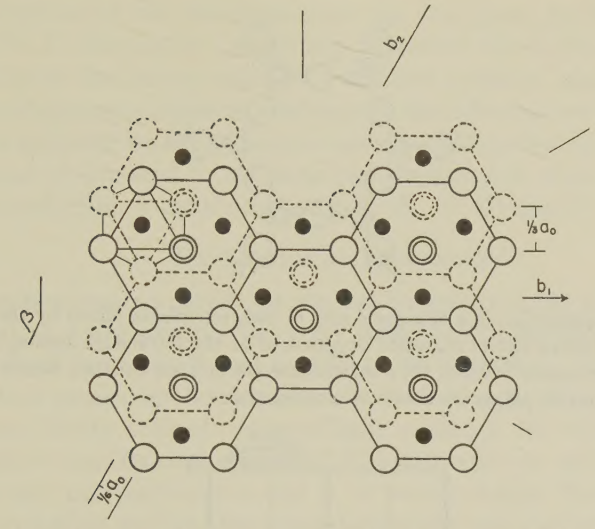

FIG. 1*a*. Projection on (001) of a portion of a phlogopite layer, $Mg_3AlSi_3O_{10}(OH,F)_2K$. In all the figures illustrating structure small black circles represent ions having octahedral coordination, in the plane of the projection: Mg, Li, Al, Fe, etc. Oxygen ions and hydroxyl groups 1.1Å from the plane of projection are shown as large circles; solid above, and dotted below. The hexagons are schematic representations of the atomic grouping of Fig. 1*c*. Potassium ions 5.0Å from the plane of projection are shown by small open circles. The *b* axis has the orientation b_1 in the single layer structure.

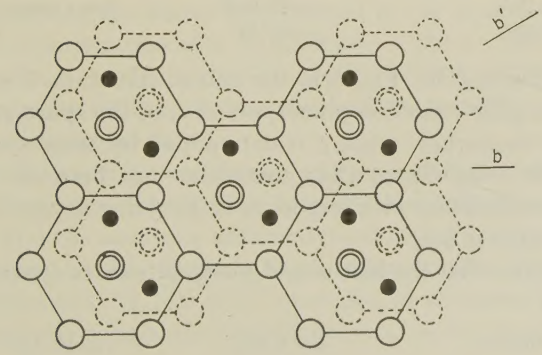

FIG. 1*b*. Projection on (001) of a portion of a muscovite layer $Al_2AlSi_3O_{10}(OH,F)_2K$.

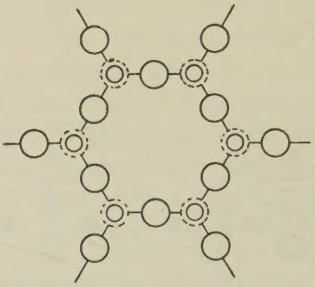

FIG. 1*c*. A projection of a hexagonal ring of SiO_4 tetrahedra joined by the sharing of oxygen ions. Dotted circles represent oxygen ions at the tetrahedra apexes, 2.2Å below the plane of projection in which the remaining oxygen ions are situated. Silicon ions 0.60Å below the projection planes are shown as small circles.

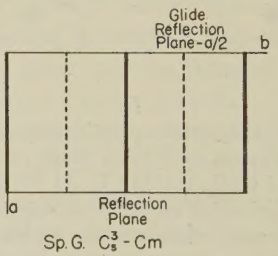

FIG. 1*d*. Symmetry elements of the space group C_s^3-m for the single layer structure. The layer has these symmetry operations.

Muscovite crystallizes in the monoclinic system and the $[[Al_2](AlSi_3)O_{10}(OH, F)_2]_n^{n-}$ layers are related as shown in Fig. 1*b* to the unique monoclinic axis *b*. The unit of structure of muscovite according to the measurements of Jackson and West has the constants

$a_0=5.18$Å	$c_0=20.04$Å	Space group C_{2h}^6-C2/c
$b_0=9.02$Å	$\beta=95°30'$	

with $2[Al_2(AlSi_3)O_{10}(OH, F)_2K]_2$ in the unit of structure. Two layers are related by the glide reflection planes, *n* and *c*, of the space group. (Note Fig. 3*b*.) The monoclinic angle β is determined by these symmetry elements and the requirement that potassium ions between layers have twelve-fold coordination with respect to neighboring oxygen ions; $c_0 \cos\beta$ being about equal to $\frac{1}{3}a_0$.

Mauguin states that the biotite and phlogopite units of structure have the constants

Biotite	$a_0=5.30$Å	$c_0=10.16$Å
	$b_0=9.21$Å	$\beta=99°3'$
Phlogopite	$a_0=5.32$Å	$c_0=10.24$Å
	$b_0=9.21$Å	$\beta=100°2'$

Descriptions of the mica structure are also given by W. L. Bragg[4] and by R. E. Stevens[5] in a paper that appeared recently in this journal.

Naming of the various micas is a difficult question, especially in the absence of complete chemical analyses. In the following work the mineral name as indicated on the specimen is given, and is probably trustworthy. The name biotite used in the structure discussion is often synonymous with octophyllite, a term originated by A. N. Winchell.[6]

Experimental Procedure

Crystals elongated parallel to various directions in the cleavage plane were cut to a size suitable for x-ray work, from cleavage sheets of the micas. These were usually cut parallel to the extinction directions if the sheets had observable birefringence in the cleavage plane. If the mica was very darkly colored, or practically uniaxial, the orientation was determined from Laue photographs. Crystals were cut with elongations parallel and perpendicular to the b- or pseudo b-axes. Some distortion was unavoidable and for this reason fragments were not always reduced to sufficiently small dimensions to avoid considerable absorption of x-rays. Some of the samples contained crystals less than .2 mm. in their maximum dimension and these were examined without cutting. Large folia were studied in several cases in order to eliminate any question of distortion.

Weissenberg x-ray goniometer equatorial zone photographs were taken for all the crystals with rotation about the a- or pseudo a-axes. In the majority of the cases equatorial zone photographs were also taken with rotation about the b- or pseudo b-axes, and rotating crystal photographs were taken about the a- and b- or pseudo a- and b-axes. Laue photographs were obtained from about twenty-five specimens.

Photographs of the above type as well as 1st layer line Weissenberg goniometer photographs with rotation about the a- and b- or pseudo a- and b-axes, and the 3rd layer line about the b- or pseudo b-axes were made in every case from at least two different specimens showing the structures examined in detail.

Cu K radiation was used throughout even though some of the micas contained large amounts of iron. Intensities of reflections were visually estimated and the accuracy obtained is adequate for this work. Atomic F values listed in the "International Tables for the Determination of Crystal Structures" (I.T.D.C.S.) were used in all intensity calculations. The Lorentz and polarization factors were taken into account, the factor

[4] *Atomic Structure of Minerals*, Cornell Univ. Press, Ithaca, N. Y., **1937.**

[5] *Am. Mineral.*, **23,** 607 (1938).

[6] *Am. Jour. Sci.* (V), **9,** 309 and 415 (1925).

depending upon the angle of diffraction being $\frac{1+\cos^2 2\theta}{\sin 2\theta}$. All calculated intensities listed are divided by 160 and are reduced by the necessary volume factor to make them comparable to that given for the single layer monoclinic unit of structure. Atomic coordinates are those listed in I.T.D.C.S.

Accurate measurements of crystal constants were outside the scope of this work. However, it was qualitatively observed that the values did not differ appreciably from those previously found except, of course, that there were various choices of β or its pseudo value. When β is given as 90° for a particular structure it is to be understood that the value is accurate to within $\pm 30'$.

The Single Layer Structure of the Micas (monoclinic hemihedral)

Biotite samples Nos. 78303 and 48309, phlogopite C3644, and lepidolite 93924 (analyzed) were thoroughly examined. Lattice dimensions of the phlogopite and biotite specimens were the same within the limits of error as those found by Mauguin, which requires $c_0 \sin \beta$ to be 10.0Å. The unit of structure therefore contains a portion of a single layer; which for phlogopite is $2[Mg_3AlSi_3O_{10}(OH, F)_2K]$, for biotite $2[(Mg, Fe, Al)_3AlSi_3O_{10}(OH, F)_2K]$ and for polylithionite $2[Li_2AlSi_4O_{10}F_2K]$ (which lepidolite 93924 approximates in composition).

The net of lattice points normal to the b-axis is shown in Fig. 2, and $ABCD$ is the projection of the unit cell selected. This, of course, is arbitrary, $GIJH$ etc. being equally satisfactory. More complex cells such as $GKLH$ crossing two layers, and $AEFD$ crossing three layers can be selected. The latter has the monoclinic angle β equal to 90°, the translation Bf being just one-third of a_0, BC. Rotating crystal photographs taken about AB, AE, and GK as axes of rotation give layer line periodicities 1×10Å, 3×10Å, and 2×10Å, respectively.

There is only one way in which the simplest unit of structure can contain a portion of one mica layer. Atomic coordinates of this arrangement having the orientation b_1, of Fig. 1a are given in Table I. The structure is isomorphous with the monoclinic hemihedral point group $C_s - m$, the space group being $C_s^3 - Cm$.

Relative intensities of various $(h0l)$, $(0kl)$, $(19l)$, and $(11l)$ reflections calculated for phlogopite, according to this structure, are listed in Tables II and III. All single layer mica samples have the same relative intensities of $(0kl)$, $k \neq n\times 3$, reflections, since the Al, Li, Mg, Fe, etc. atoms with octahedral coordination do not contribute to these reflections. A Weissenberg equatorial zone rotating about the a-axis is reproduced as Fig. 4a.

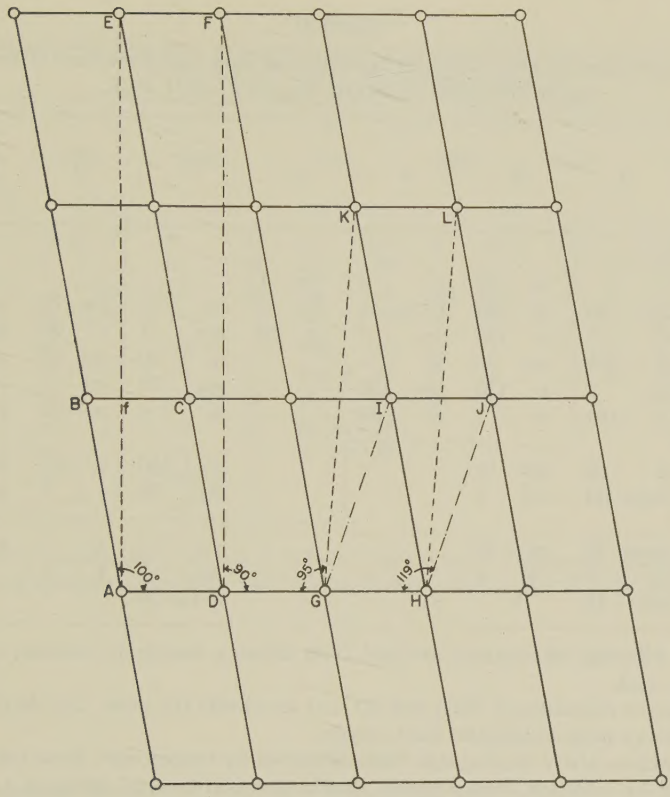

FIG. 2. Net of lattice points in (010) of the single layer monoclinic structure.

TABLE I

Atomic Coordinates for the Single Layer Structure. Space Group C_s^3-Cm, $\beta=100°$.

General Positions				Special Positions			
	x	y	z		x	y	z
4 O	.25	.25	.00	2 O	.00	.50	.00
4Si	.02	.33	.06				
4 O	.08	.33	.22	2(OH)	.08	.00	.22
4Mg	.44	.33	.34	2Mg	.44	.00	.34
4 O	.32	.17	.46	2(OH)	.32	.50	.46
4Si	.37	.17	.62				
4 O	.14	.25	.68	2 O	.39	.00	.68
				2K	.45	.50	.84

TABLE II

Approximate Observed and Calculated Intensities of Some ($h0l$) Reflections of the Single Layer Phlogopite Structure, $Mg_3AlSi_3O_{10}(OH, F)_2K$.

$h \rightarrow$ / $l \downarrow$	0		2^2		4		6		$\bar{2}$		$\bar{4}$		$\bar{6}$	
0			vs	170	a	2	vw	1						
1	ms[1]	80	vs	240	m-ms	50	vw	2	ms	70	ms	70	vw	1
2	w	9	s	130	vw	5	m	30	mw	5	s	90	ms	80
3	vs	250	mw	20	w	7			m	20	ms	40	mw	14
4	mw	7	s	170	ms	130			ms	70	vw	1	vw	4
5	vs	110	w	1	m	30			w	4	m	30	vw	2
6	m	60	mw	16					ms-s	150	s	90	m	30
7	m-ms	40	vw	2					ms	90	a	1	m	30
8	m-ms	50	m	30					vw	2	a	1	a	0
9	vw	2	vw	1					vw	2	a	1		
10	mw	15							m-ms	50				

[1] The following abbreviations are used in all tables: s, strong; m, medium; w, weak; vw, very weak.

[2] Observed intensities of ($20l_a$) and ($13\ l_{a+1}$) are closely the same. Calculated values differ only in a small contribution due to oxygen.

* Reflections above the line arise from diffraction by transmission, those below from diffraction by reflection, from a highly absorbing crystal (several tenths of a mm. in thickness). Reflections such as (20$\bar{7}$) are affected by absorbtion. Similar conditions hold in other tables.

A striking regularity of the diffraction photographs is the pseudo-hexagonal character of the reflections for which the k index is a multiple of three, such as ($20l_a$) and ($13l_{a+1}$). These planes are closely similar for the single layer structure as can be seen by referring them to the cell $AEFD$ of Fig. 2, which crosses three layers. The index transformations are as follows, the subscripts denoting layer multiplicity:

$$h_3 = h_1;\ k_3 = k_1;\ l_3 = 3l_1 + h$$

(201) becomes $(205)_3$ and (13$\bar{2}$) transforms to $(13\bar{5})_3$, which are equivalent hexagonal planes referred to orthohexagonal axes.

Intensity differences for some (hkl), $k = n \times 3$ reflections resulting from replacement of Mg in phlogopite by Li and Al, leading to lepidolite or polylithionite are shown in Table IV. Similar effects are observed and calculated for replacement of Mg by Fe, leading to biotite, annite, etc.

TABLE III

Approximate Observed and Calculated Intensities of Some Reflections of the Single Layer Phlogopite Structure, $Mg_3AlSi_3O_{10}(OH, F)_2K$.

$k \rightarrow$ / $l \downarrow$	(02l)		(04l)		(06l)		(19l)[1]		($\bar{1}$9l)[1]		(11$\bar{l}$)	
0	ms-m	60	m	40	vs	200	w	8			mw	15
1	w	2	m	40	mw	20	a	1	w	8	mw-w	11
2	s	120	mw	20	vw	1	mw	20	m	25	ms-s	90
3	ms	90	w	2	w	2	mw	16	w	7	s	130
4	vw	1	mw-w	5	mw	25	a	1	a	1	w	11
5	vw	2	vw	1	mw-w	15	m	50	m	30	vw	2
6	mw-w	4	mw	30	vw	2	m	50				
7	mw	12	mw	30	m-mw	35						
8	vw	1	vw	1	m-mw	30						
9	vw	0	mw-w	7								
10	w	2	vw	1								

[1] Structure factors of (19l) and (13l) reflections are equal. Differences in intensities are a result of different polarization and Lorentz factors and change of F values with sin θ/λ

TABLE IV

Approximate Observed and Calculated Intensities of Some Reflections of Phlogopite and Lepidolite.

Plane[1]	Phlogopite 4463		Lepidolite 86193	
203	mw	20	vw	3
20$\bar{3}$	mw	20	vw	2
20$\bar{4}$	ms	70	m	20
20$\bar{5}$	w	4	m	20
20$\bar{8}$	vw	2	vw	2
400	a	2	vw	3
40$\bar{5}$	m	30	w	15
062	vw	1	a	0

[1] (0kl), $k \neq n \times 3$, intensities are not influenced by substitution in the octahedral positions, i.e., Mg, Al, Fe, etc., by Li. Other (h0l) intensities show smaller variations, these listed being among the more pronounced ones.

The Two Layer Structure of the Micas; Muscovites, Biotites, Etc. (monoclinic holohedral)

Phlogopite sample 78218, biotite P. R. C. 395, and a commercial muscovite sample were thoroughly examined. The only possible two layer structure preserving the usual mica layer and twelve-fold coordination of potassium is that shown in Fig. 3*a*. It is isomorphous with point group $C2_h - 2/m$ and is derived from space group $C_{2h}^6 - C2/c$ (Fig. 3*b*) by choice of an appropriate value of β corresponding to cell *GKLH* of Fig. 2. This is the structure found for muscovites by Jackson and West and their parameter values are listed in Table V.

Table V

Atomic Coordinates for the Two Layer Structure, $\beta = 95°$. Space Group $C_{2h}^6 - C2/c$.

General Positions				Special Positions			
	x	*y*	*z*		*x*	*y*	*z*
8Mg	.25	.083	.000	4Mg(d)	.75	.25	.000
8Si	−.033	−.250	.135	4K(e)	.00	.083	.250
8Si	−.033	.417	.135				
8 O	.228	.333	.164				
8 O	.228	−.167	.164				
8 O	.480	.083	.164				
8 O	−.062	−.167	.055				
8 O	−.062	.417	.055				
8 (OH)	−.062	.083	.058				

Intensities of (*h*0*l*) reflections for the two layer phlogopite structure are the same as those given for the single layer structure in Table II after the necessary index transformation. Calculated and observed intensities of some (0*kl*) reflections for muscovite are listed in Table VII together with the structure amplitudes calculated by Jackson and West. A most important factor appears, namely (06*l*) reflections with *l* odd are observed and this is true for all the muscovite samples. Such reflections are required to be absent by the ideal structure and can only be explained by considerable departure from the structure given by Jackson and West. They are absent for the two layer biotite-like micas and none is observed for any of the micas that give the (*h*0*l*) intensities of the single layer structure (except muscovite). These characteristics are illustrated by the photographs reproduced as Figs. 4*a* and 4*d*.

TABLE VI

Approximate Observed and Calculated Intensities of Some (0*kl*) Reflections of the Two Layer Phlogopite Structure.

l ↓ \ *k*→	2		4		6		8	
0	w	$\bar{3}$	w	30	vs	200	a	2
1	m	40	mw−w	15	a	0	a	0
2	vw	2	w−	5	mw	20	a	0
3	s	120	w+	10	a	0	w−	10
4	m	50	w−	10	vw	1	vvw	3
5	ms	70	vw	5	a	0	vw	5
6	mw	25	vw	3	w	2	a	0
7	w	10	w	12	a	0		
8	a	0	vw	5	m	25		
9	a	2	a	0	a	0		
10	a	0	a	5	mw	15		
11	a	0	w	20	a	0		
12	a	2	vw	5	a	2		
13	w	15	w	20	a	0		
14	vw	3	vw	5	mw	35		
15	vw	3	vw	3	a	0		
16	a	0	a	0	m	30		
17	a	0	w−	5	a	0		

TABLE VII

Calculated Structure Amplitudes for Muscovite After Jackson and West. Observed Intensities for Cu K Radiation.

l ↓ \ *k*→	2		4		6	
0	w	4	w	18	vs	65
1	w	11	mw	18	w	0
2	mw	8	m		w+	16
3	m	21	mw	16	a	0
4	m+	24	m	14	a	1
5	ms	35	a	4	vw	0
6	a	7	w	9	w	4
7	w		vw		vw	0
8	a		a	0	m	26
9	a		a		w	
10	vw		vw		w	

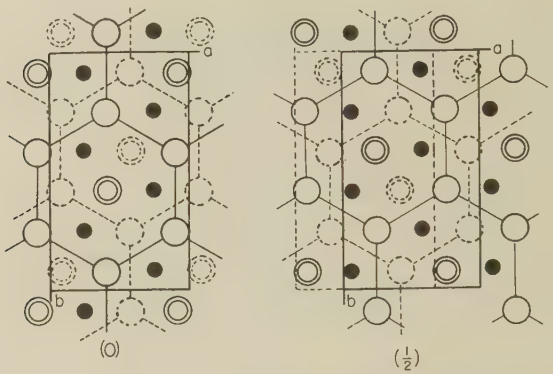

FIG. 3*a*. Sequence of layers in the two layer monoclinic holohedral structure.

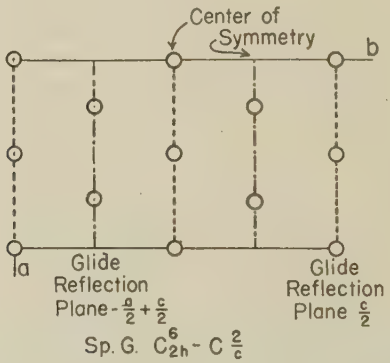

FIG. 3*b*. Symmetry elements of the space group.

Muscovite then has a distinctly different structure from the two layer biotites. It would be difficult to determine the exact departure from the ideal and for this reason a close analysis has not been made at this time. The coordinates given in Table V are accurate for the two layer biotite type structure.

Calculated intensities for (0*kl*) reflections listed in Table VI are very sensitive to choice of atomic scattering powers, particularly for oxygen. Several poor agreements in the table are explained in this manner. The poorest is (040), the calculated intensity of which is too high compared with the neighboring (041) and (043) reflections. The high calculated value of (04.10) is due entirely to a pronounced oxygen contribution which a thermal factor would greatly decrease. Similar effects appear in the various tables for the other micas.

FIG. 4. Weissenberg equatorial zone photographs of various micas with crystals rotating about a- or pseudo a-axes (except 4h), Cu K radiation.

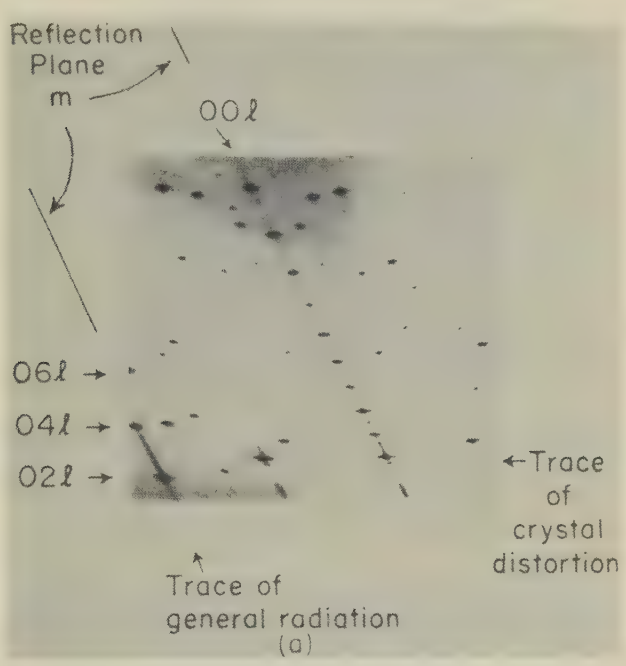

FIG. 4a. Single layer monoclinic hemihedral phlogopite that does not show diffuse scattering.

FIG. 4b. Single layer monoclinic hemihedral phlogopite with weak diffuse scattering.

FIG. 4*c*. Single layer monoclinic hemihedral biotite with very diffuse scattering.

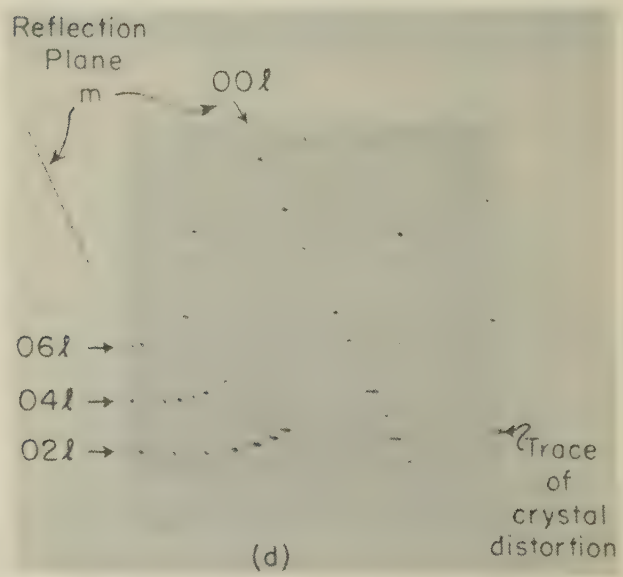

FIG. 4*d*. Muscovite, two layer monoclinic holohedral.

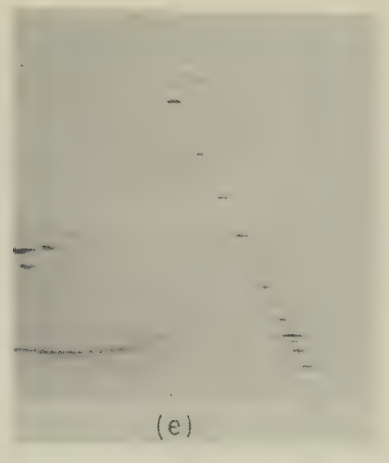

FIG. 4*e*. Two layer monoclinic holohedral biotite with very diffuse scattering.

FIG. 4*f*. Three layer rhombohedral enantiomorphic hemihedral phlogopite, weakly developed diffuse scattering.

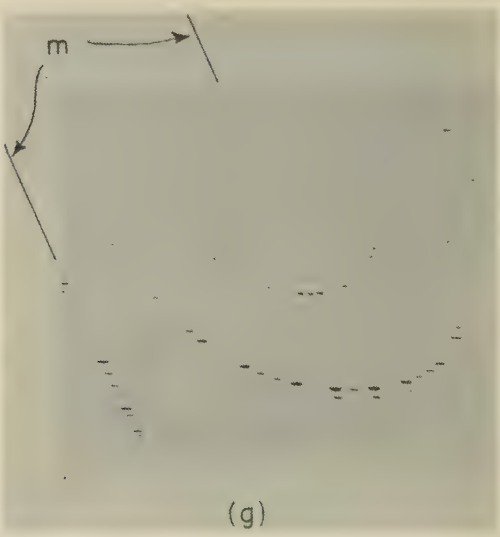

FIG. 4*g*. Six layer monoclinic hemihedral lepidolite (compare with 4*h*).

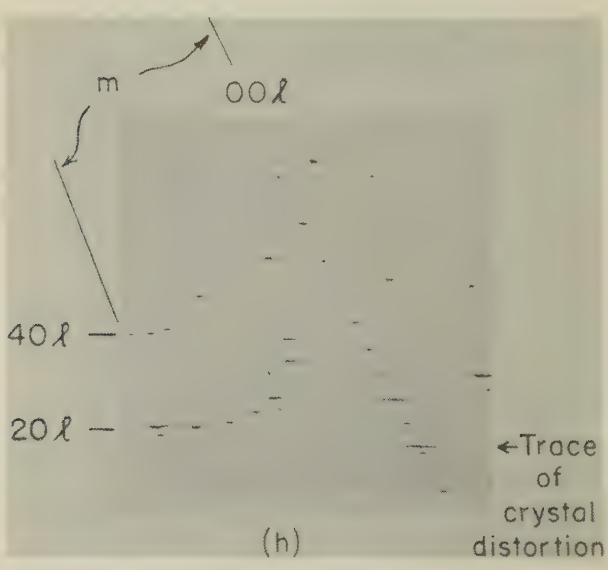

FIG. 4*h*. Single layer monoclinic hemihedral phlogopite with crystal rotating about *b*-axis.

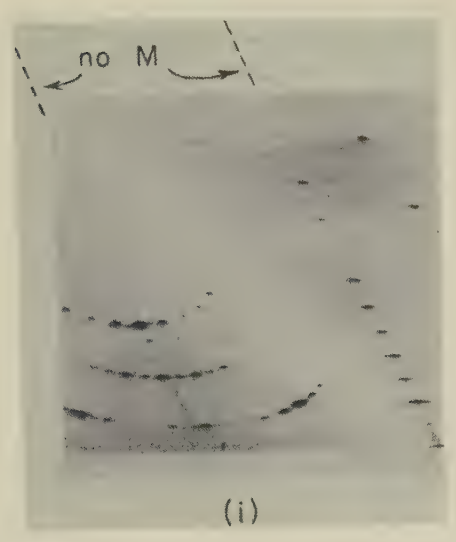

FIG. 4*i*. Six layer triclinic holohedral biotite. Note absence of reflection planes.

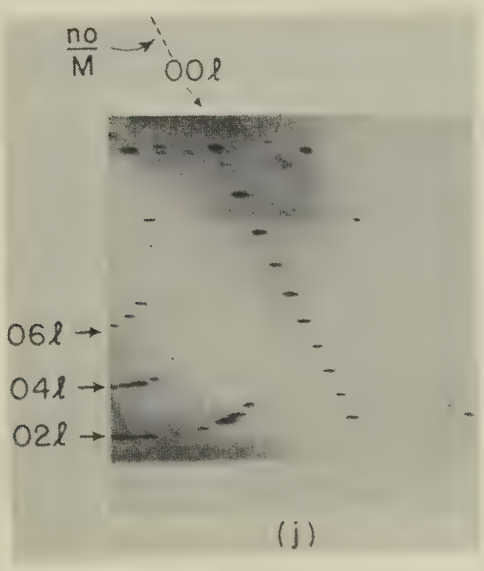

FIG. 4*j*. Twenty-four layer triclinic holohedral biotite.

The Three Layer Structure (rhombohedral enantiomorphic hemihedral. low-quartz class)

Phlogopite sample No. 4463 and lepidolite No. R4365 (analyzed) were carefully examined. All crystals of this type are closely uniaxial and Laue photographs with the x-ray beam normal to the cleavage appear to have a three-fold axis and three planes of symmetry (D_{3d}). Indices can be assigned to all reflections by use of a hexagonal unit of structure having $a_0 = a$ (single layer monoclinic structure) $= 5.3$Å, for phlogopite and $c_0 = 3 \times c$ (single layer monoclinic structure). Moreover $(2\bar{1} \cdot l_a)_{\text{Hex}}$ reflections have the same intensities as the $(h0l_a)_1$ reflections.

With the above limitations it is necessary to find a hexagonal or pseudo-hexagonal three layer structure having the same projection on (01.0) as does the single layer structure on $(010)_1$. This can only be done in two ways and these are enantiomorphic. Atomic coordinates of the resulting structure illustrated in Fig. 5*b* are listed in Table VIII. A particular layer is repeated about a three-fold screw axis normal to the cleavage. The space group is $D_3{}^3 - C3_112$ or $D_3{}^5 - C3_212$. (Fig. 5*a*).

Agreement between observed and calculated intensities is shown in Tables IX and II (after index transformation). Presence of lithium in the lepidolites modifies the intensities as shown by Table IV and as was discussed for the single layer structure; a Weissenberg goniometer photograph with rotation about the orthohexagonal b-axis is reproduced as Fig. 4*f* and a Laue photograph taken with the x-ray beam approximately normal to (00.1) is shown in Fig. 9*c*.

Table VIII

Atomic Coordinates for the Three Layer Structure. Space Group $D_3{}^3 - C3_112$. Rhombohedral Enantiomorphic Hemihedral.

General Positions				Special Positions		
	x	y	z		x	z
6Si	−.22	.22	.078	3K	.11(1/9)	.000(0)
6Si	.44	−.44	.078	3Mg	.11(1/9)	.167(1/6)
6O	.11	.39	.060	3Mg	−.22(2/9)	.167(1/6)
6O	−.39	−.11	.060	3Mg	.44(4/9)	.167(1/6)
6O	−.39	.39	.060			
6O	−.22	.22	.130			
6O	.44	−.44	.130			
6(OH)	.11	−.11	.130			

TABLE IX

Approximate Observed and Calculated Intensities of Some (0*kl*) Reflections of the Three Layer Rhombohedral Enantiomorphic Hemihedral Phlogopite Structure.

l ↓ \ *k*→	1		2		3		4
0	w	15	mw	20	vs	200	a
1	mw	20	mw	45	a	0	a
2	a	2	mw	20	a	0	vw
3	vw	5	mw	20	mw	20	a
4	m	30	mw	25	a	0	vw
5	ms	160	vw	5	a	0	vvw
6	s	200	w	7	a	1	vvw
7	ms	130	a	0	a	0	vvw
8	m	80	a	1	a	0	
9	mw	35	w	10	a	2	
10	w	20	vw	1	a	0	
11	vw	10	w	10	a	0	
12	a	0	vw	5	m	25	
13	a		vw		a	0	
14	a		a		a	0	
15	a		a		mw	15	

THE SIX LAYER LEPIDOLITE STRUCTURE (MONOCLINIC HEMIHEDRAL)

Lepidolite samples No. 97893 and Stevens No. 6, both of which were analyzed specimens, were carefully examined. Laue photographs taken with the *x*-ray beam normal to the cleavage although badly distorted show only a plane of symmetry. The crystals therefore must be monoclinic. Weissenberg equatorial zone photographs taken with crystals rotating about axes parallel to the extinction directions in the cleavage plane show that the *b*-axis is 5.3Å and the *a*-axis 9.2Å, which are interchanged in comparison with the other monoclinic micas. Moreover these lepidolites gave (0*kl*) reflections entirely different from the analogous (*h*0*l*) reflections of other micas examined as can perhaps be seen from the photographs reproduced in Figs. 4*g* and *h*. The monoclinic angle β can be taken as 90°.

The *c*-periodicity is six times c_0 of the single layer structure, therefore the unit of structure is crossed by six mica layers. Reflections so far as tested were present only from planes having $\frac{3k-h}{2}+1=3n$, which is the rhombohedral requirement for orthohexagonal indices. Reflections are absent from (*h*0*l*) with *l* odd, but are present from (11*l*) with *l* odd.

These conditions are strictly the same as were found for the kaolin mineral nacrite[7] which is monoclinic, the space group being C_s^4-Cc, but closely approaches the requirements of the rhombohedral space group C_{3v}^6-R3c. However while a kaolin layer in which positions with octahedral coordination are completely filled has a three-fold axis, the mica layer can not have this symmetry as perhaps can be seen from the various figures.

In order to determine the structure it is necessary to combine six mica layers according to the symmetry operations of space group $C_{3v}-Cc$ and still have the types of absent reflections indicated above. If there is a pseudo space group it cannot be rhombohedral since all rhombohedral groups have three-fold axes. The only groups that can be used are those having only three-fold screw axes, namely $C_3^2-C3_1$ and $C_3^3-C3_2$ (Fig. 6*b*). These combined with C_s^4-Cc (Fig. 6*a*) lead to the necessary structure.

This procedure is very interesting since it combines a three-fold screw axis with a glide reflection plane which converts it into a screw axis of opposite sense. The operations of such a group are not closed so that it is not one of the possible space groups. However it leads to a simpler description of the crystal than does the ordinary space group C_s^4-Cc. In short the symmetry operations of the crystal can be considered as right and left three-fold screw axes, with an *arbitrary origin*, repeated by a glide reflection of $c=\frac{1}{2}c_0$ about a plane including the axes.

Atomic coordinates referred to space group C_s^4-Cc are listed in Table X and it can be seen that 180 parameters are required to describe the structure. Agreement between observed and calculated intensities is shown in Tables XI and XII. The structure is illustrated in Fig. 6*c*.

[7] Hendricks, S. B., *Zeits. Krist.*, **100**, 509 (1939).

TABLE X

Atomic Coordinates of the Six Layer Pseudo-rhombohedral Monoclinic Lepidolite Structure. Space Group C_s^4-Cc.

	1st layer			2nd layer			3rd layer		
	x	y	z	x	y	z	x	y	z
4K	.00	1/3	a^1	1/3	2/3	1/6+a	1/6	5/6	1/3+a
4 O_1	1/4	1/12	b^1	1/12	5/12	1/6+b	1/6	1/3	1/3+b
4 O_2	1/4	7/12	b	1/3	1/6	1/6+b	5/12	1/12	1/3+b
4 O_3	1/2	1/3	b	1/12	7/12	1/6+b	5/12	7/12	1/3+b
4Si_1	1/3	1/3	c^1	0	2/3	1/6+c	0	1/3	1/3+c
4Si_2	1/6	5/6	c	1/6	1/6	1/6+c	1/3	1/3	1/3+c
4 O_4	1/3	1/3	d^1	0	2/3	1/6+d	0	1/3	1/3+d
4 O_5	1/6	5/6	d	1/6	1/6	1/6+d	1/3	1/3	1/3+d
4OH_1	0	1/3	d	1/3	2/3	1/6+d	1/6	5/6	1/3+d
4Mg_1	0	0	e^1	0	0	1/6+e	0	0	1/3+e
4Mg_2	1/6	1/2	e	1/6	1/2	1/6+e	1/6	1/2	1/3+e
4Mg_3	1/3	0	e	1/3	0	1/6+e	1/3	0	1/3+e
4OH_1'	1/6	1/6	f^1	0	1/3	1/6+f	1/3	2/3	1/3+f
4 O_5'	0	2/3	f	1/6	5/6	1/6+f	0	2/3	1/3+f
4 O_4'	1/3	2/3	f	1/3	1/3	1/6+f	1/6	1/6	1/3+f
4Si_2'	0	2/3	g^1	1/6	5/6	1/6+g	0	2/3	1/3+g
4Si_1'	1/3	2/3	g	1/3	1/3	1/6+g	1/6	1/6	1/3+g
4 O_3'	1/6	2/3	h^1	0	5/6	1/6+h	1/12	5/12	1/3+h
4 O_2'	5/12	5/12	h	1/4	1/12	1/6+h	1/12	7/12	1/3+h
4 O_1'	5/12	7/12	h	1/4	7/12	1/6+h	1/3	1/6	1/3+h

[1] In this table $a=.0825$, $b=.053=-h$, $c=.044=-g$, $d=.017=-f$, $e=.000$.

TABLE XI

Approximate Observed and Calculated Intensities of Some ($h0l$) Reflections for the Six Layer Pseudo-rhombohedral Monoclinic Lepidolite. Note that $a=9.0$Å, $b=5.3$Å.[1]

202	ms	30	$40\bar{2}$	m	20	600^2	vs	200
208	s	60	$40\bar{8}$	mw	10	606	m	20
$20\bar{1}4$	vs	200	$40\bar{1}4$	w	4	6012	a	0
$20\bar{2}0$	m	25	$40\bar{2}0$	mw	10	6018	a	0
$20\bar{2}6$	a	1	$40\bar{2}6$	a	3	6024	m	15
$20\bar{3}2$	a	0	$40\bar{3}2$	mw	20	6030	mw	6
$20\bar{3}8$	mw	20	$40\bar{3}8$	mw	15	6036	a	0
$20\bar{4}$	mw	10	404	ms	50			
$20\bar{1}0$	vs	150	4010	s	90			
$20\bar{1}6$	vs	150	4016	vw	6			
$20\bar{2}2$	w	4	4022	mw	20			
$20\bar{2}8$	vw	2	4028	a	2			
$20\bar{3}4$	w	5	4034	m	30			

[1] Only planes with pseudo-rhombohedral indices are present.

[2] ($60l$) and ($60\bar{l}$) observed and calculated intensities are identical.

TABLE XII

Observed and Calculated Approximate Intensities of Some (0*kl*) Reflections of the Six Layer Pseudo-rhombohedral Monoclinic Lepidolite. Note that $a=9.0$Å, $b=5.3$Å.

l ↓ \ k →	2		4		6	
0	mw	8	mw	15	vs	100
3	vs	100	ms	40	a	0
6	w	6	mw	8	a	0
9	s	60	mw	15	a	0
12	m	30	m	20	a	0
15	m	30	w	6	a	0
18	ms	50	a	2	a	0
21	w	5	a	0	a	0
24	a	1	a	0	w	3
27	ms	60	m	30	a	0
30	m	40	m	30	vw	2
33	a	0	vw	1	a	0
36	mw	30	vw	1		
39	mw	30	vw	1		
42	a	3	vw	1		

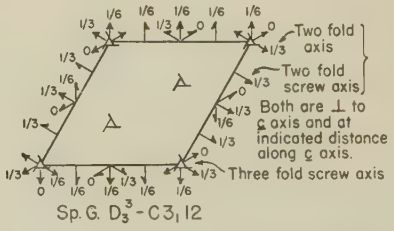

FIG. 5*a*. Symmetry elements of the space group.

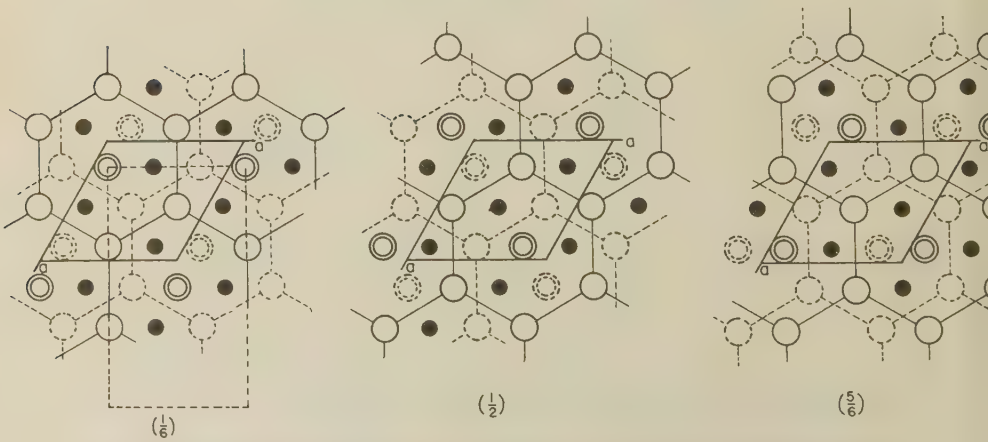

FIG. 5*b*. Sequence of layers in the rhombohedral enantiomorphic hemihedral structure.

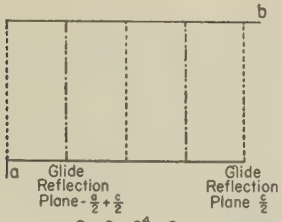

FIG. 6*a*. Symmetry elements of the space group.

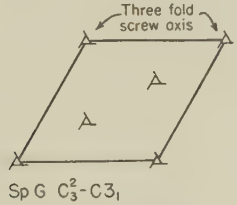

FIG. 6*b*. The pseudo subgroup $C_3{}^2-C3_1$.

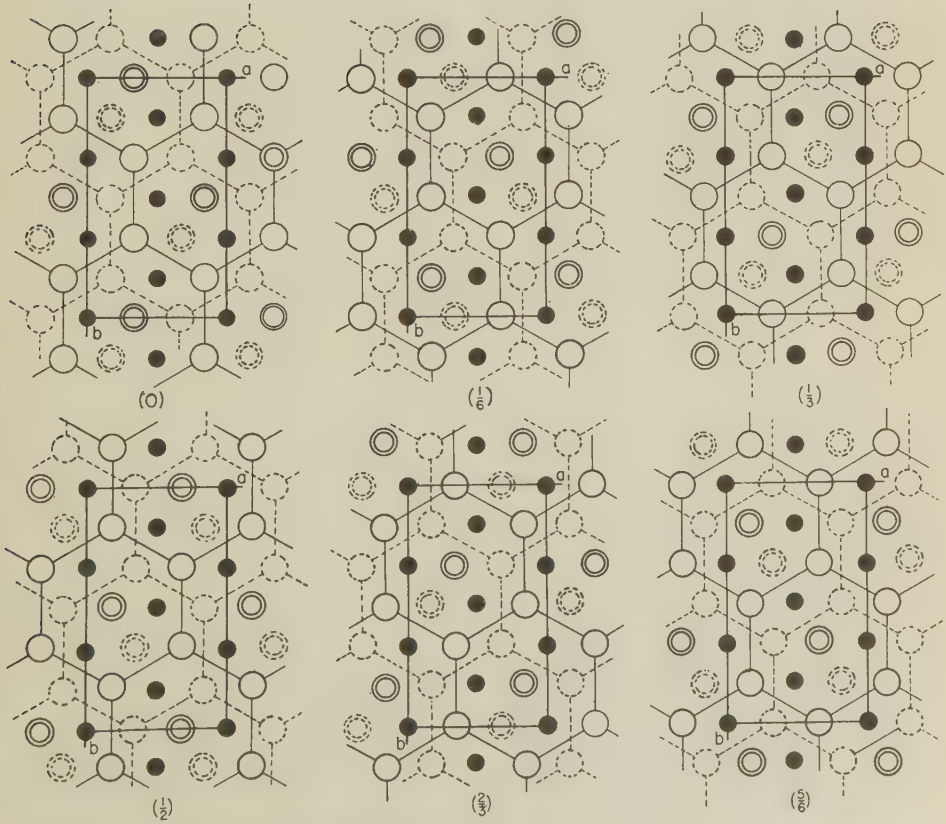

FIG. 6*c*. Sequence of layers in the monoclinic hemihedral six layer structure. The layers as a whole are repeated by these symmetry operations.

The Six Layer Biotite Structure (triclinic holohedral)

Biotite sample No. 3675 and one of the crystals from specimen No. 77436 were examined in detail. Laue photographs were too distorted for unambiguous determination of symmetry. The crystals were approximately uniaxial and Weissenberg equatorial zone photographs about the usual b- and pseudo b-axes were very similar. However neither these photographs nor ones taken about the a- and pseudo a-axes showed planes of symmetry normal to the cleavage.

A unit of structure can be selected that has the usual a- and b-dimensions of the one and two layer monoclinic micas. It has $c_0 = 6 \times c \sin \beta$ (single layer) and therefore is crossed by six layers. Moreover, reflections strictly analogous to the $(h0l)$ reflections of the single layer structure are observed with rotation about the pseudo b-axes. Assignment of indices to the various reflections according to this unit shows many types of general absences. Thus reflections are absent from $(0kl)$ (note Fig. 4i) with $2k+l \neq 3n$, and $(11l)$ with $l \neq 2+3 \times n$ among others.

In the structure analysis it is necessary to explain the observed systematic absences by an atomic arrangement having the same projection on (010) as the single layer structure. Since these conditions are to be satisfied by all atoms, they must be satisfied by the potassium atoms. Without loss of generality the potassium positions must include one out of each of the following six sets:

	1(0)	2(1/6c)	3(1/3c)	4(1/2c)	5(2/3c)	6(5/6c)
a	000	1/3 0 1/6	1/6 1/6 1/3	0 1/2 1/2	1/3 0 2/3	1/6 1/6 5/6
b		1/3 1/3 1/6	1/6 1/2 1/3	0 1/3 1/2	1/3 1/3 2/3	1/6 1/2 5/6
c		1/3 2/3 1/6	1/6 5/6 1/3	0 2/3 1/2	1/3 2/3 2/3	1/6 5/6 5/6

and $x+\frac{1}{2}$, $y+\frac{1}{2}$, z. There are $3^5 = 243$ possible combinations.

The condition that the general absences be explained is fulfilled only by combination 1, 2a, 3a, 4c, 5b, 6c, i.e., with potassium at 000, 1/3 0 1/6, 1/6 1/6 1/3, 0 2/3 1/2, 1/3 1/3 2/3, 1/6 5/6 5/6 and these values repeated at $x+\frac{1}{2}$, $y+\frac{1}{2}$, z. The structure is completely determined by the added requirement of a mica layer and twelve-fold coordination of potassium with respect to oxygen.

The structure is isomorphous with the triclinic holohedral point group $C_i - \bar{1}$, the space group being $C_i^1 - P\bar{1}$. (Fig. 7b). One of the simplest units of structure has $a = b = 5.3$Å, $c = 6 \times 10$Å, $\beta = \alpha = 90°$, $\gamma = 120°$. It corresponds to the usual hexagonal cells. Atomic coordinates referred to these axes are listed in Table XIII and the structure is illustrated in Fig. 7a. Observed and calculated intensities are listed in Tables II (after index transformation) and XIV.

TABLE XIII

Atomic Coordinates of the Six Layer Triclinic Biotite Structure. Space Group $C_i^1-P\bar{1}$.

	1st layer			2nd, 6th layer				3rd, 5th layer		
	x	y	z		x	y	z	x	y	z
4K	0	1/6	a[1]	4K	1/3	1/6	1/6+a	1/3	1/2	1/3+a
4Mg	1/3	1/6	e[1]	4Mg	0	5/6	1/6+e	0	1/6	1/2+e
2 Mg	0	1/2	e	4Mg	2/3	1/6	1/6+e	1/3	5/6	1/3+e
4 OH	0	1/6	d[1]	4Mg	1/3	1/2	1/6+d	2/3	1/2	1/3+d
4 O	1/3	5/6	d	4 OH	1/3	1/6	1/6+d	1/3	1/2	1/3+d
4 O	2/3	1/2	d	4 OH	0	1/6	1/6−d	1/3	1/6	1/3−d
4Si	1/3	5/6	c[1]	4 O	2/3	5/6	1/6+d	0	5/6	1/3+d
4Si	2/3	1/2	c	4 O	0	1/2	1/6+d	2/3	1/6	1/3+d
4 O	0	2/3	b	4 O	2/3	1/2	1/6−d	0	1/2	1/3−d
4 O	1/2	2/3	b	4 O	1/3	5/6	1/6−d	2/3	5/6	1/3−d
4 O	1/2	1/6	b							
	4th layer									
				4Si	2/3	5/6	1/6+c	0	5/6	1/3+c
4Mg	1/3	1/6	1/2+e	4Si	0	1/2	1/6+c	2/3	1/6	1/3+c
2Mg	0	1/2	1/2+e	4Si	2/3	1/2	1/6−c	0	1/2	1/3−c
4 OH	2/3	1/2	1/2+d							
4 O	0	1/6	1/2+d	4Si	1/3	5/6	1/6−c	2/3	5/6	1/3−c
4 O	1/3	5/6	1/2+d	4 O	5/6	2/3	1/6+b	5/6	0	1/3+b
4Si	0	1/6	1/2+c	4 O	5/6	1/6	1/6+b	1/3	0	1/3+b
4Si	1/3	5/6	1/2+c	4 O	1/3	2/3	1/6+b	5/6	1/2	1/3+b
4 O	1/6	0	1/2+b	4 O	0	2/3	1/6−b	5/6	1/6	1/3−b
4 O	2/3	0	1/2+b	4 O	1/2	2/3	1/6−b	5/6	2/3	1/3−b
4 O	1/6	1/2	1/2+b	4 O	1/2	1/6	1/6−b	1/3	2/3	1/3−b

[1] In the table $a=.0825$, $b=.053$, $c=.044$, $d=.017$, $e=.000$.

TABLE XIV

Approximate Observed and Calculated Intensities of Some (0*kl*) Reflections of the Six Layer Triclinic Biotite Structure. Note that $a=b=5.3$Å, $\gamma=120°$, $\alpha=\beta=90°$.

$l\downarrow$ \ $k\rightarrow$	1		$\bar{2}$		4	
2	w	8	w	10	a	1
5	a	0	mw	30	vw	3
8	mw	12	w	8	vvw	1
11	ms	30	w	6	w	5
14	m	40	vw	1		
17	s	60	a	2		
20	w	6	vw	2		
23	vw	3	w	5		

$l\downarrow$ \ $k\rightarrow$	$\bar{1}$		2		$\bar{4}$	
1	mw	35	mw	35	a	1
4	vvw	1	w	10	a	1
7	w	20	mw	25	vw	3
10	m	35	w	3	vvw	2
13	s	150	w	3	vw	3
16	m	30	a	0		
19	m	25	vw	5		
22	vw	1	vw	2		

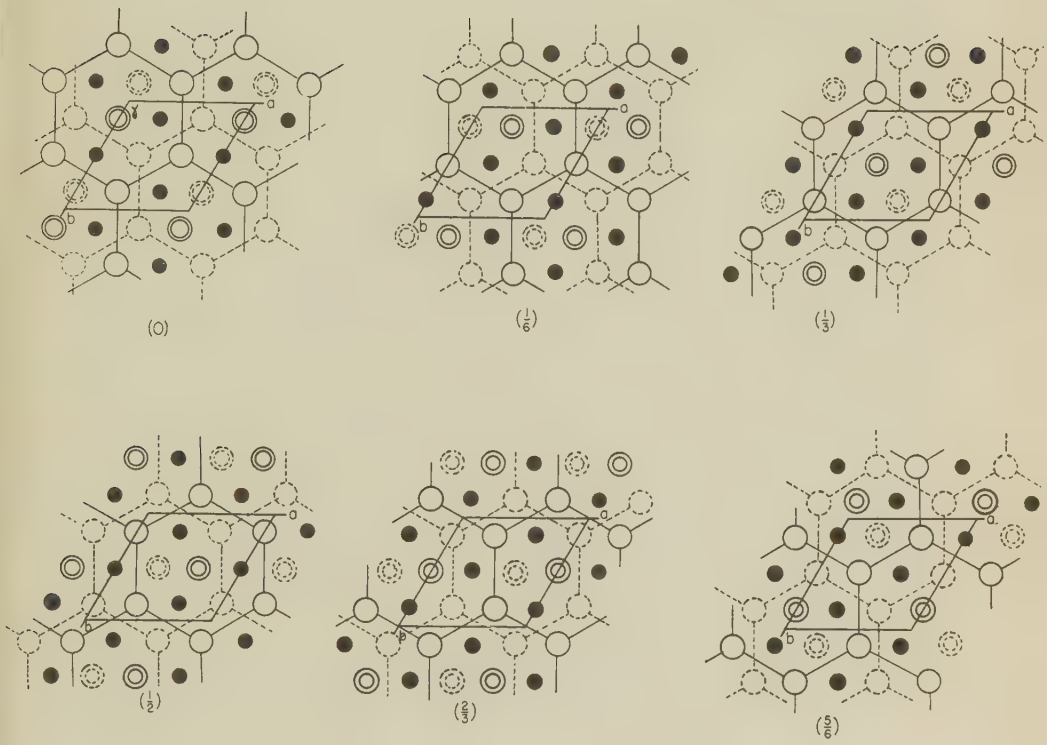

FIG. 7*a*. Sequence of layers in the six layer triclinic structure.

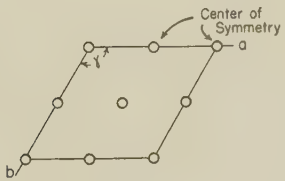

Sp.G. $C_1^1 - P\bar{1}$

FIG. 7*b*. Symmetry elements of the space group.

A Twenty-Four Layer Triclinic Structure

Sample No. 77436 from Ambulawa, Ceylon, contained a single mica crystal showing a very high layer periodicity. Photographs about the usual single layer pseudo a- and b-axes indicated that the symmetry is triclinic as also did Laue photographs one of which is reproduced as Fig. 9*d*. It is thus permissible to take the usual a- and b-directions as axes of the unit cell, the dimensions being $a=5.3$Å, $b=9.2$Å, $c=n\times 10$Å, $\gamma=90°$, and $\beta=90°$ with some question about α.

Reflections from (hkl) with $k=n\times 3$ are the same as were observed for the single layer structure. It is therefore necessary that the projection on (010) be the same as that of the single layer structure. A Weissenberg equatorial zone photograph with the crystal rotating about the triclinic a-axis is reproduced in Fig. 4*j*. It can perhaps be seen that the periodicity normal to the layer is very high and that an unambiguous index assignment would be difficult. After careful examination it was established that the (0kl) reflections closely reproduced the (0kl) reflections of the six layer triclinic structure as a partial group. Moreover the heavy trace of continuous scattering from (060) on an over-exposed photograph did not pass through any (02l) reflection but rather at a distance of about one-third the periodicity from the closest reflection.

Table XV

Observed Intensities of Some (0kl) Reflections of the Twenty-four Layer Triclinic Biotite and (in parentheses) the Six Layer Triclinic Structure $a=b=5.3$Å, $\gamma=120°$, $\alpha=\beta=90°$.

l	$k=1$	l	$k=1$	l	$k=2$	l	$k=2$
2	vw	59	vw	76—(19)	w(w)	133	a
5	vw	62	a	79	a	136—(34)	w(w)
8—(2)	w(w)	65	vw	82	a	139	vvw
11	vw	68—(17)	ms(ms)	85	a	142	vvw
14	a	71	w	88—(22)	w(w)	145	vw
17	a	74	vw	91	vvw	148—(37)	w(vw)
20—(5)	a(a)	77	vw	94	vvw	151	a
23	a	80—(20)	w(w)	97	w	154	a
26	a	83	vvw	100—(25)	w(w)	157	a
29	vw	86	a	103	a	160—(40)	w(w)
32—(8)	m(mw)	89	a	106	a	163	vw
35	a	92—(23)	vw(vw)	109	a	166	vw
38	a			112—(28)	a(a)	169	w
41	a			115	a	172—(43)	w+(w+)
44—(11)	ms(ms)			118	a		
47	mw			121	vw		
50	w			124—(31)	w(w)		
53	w			127	a		
56—(14)	m(m)			130	a		

There are thus good reasons for supposing that the unit of structure is crossed by twenty-four mica layers. It is consistent with the above observations that the structure be triclinic holohedral with the cell dimensions

$a=b=5.3$Å $\quad c=24\times10$Å
$\alpha=\beta=90°$ $\quad \gamma=120°$

similar to those of the six layer triclinic structure.

Observed intensities of some ($0kl$) reflections are listed in Table XV together with analogous ($0kl$) reflections of the six layer triclinic biotite. No attempt was made to complete the structure analysis although it does not appear impossible. There are 3^{23} combinations of twenty-four mica layers that will give the (010) projection.

Optical Properties and Frequency of Occurrence of Various Structures

Partial descriptions of the micas examined are listed under structure types in Tables XVI to XIX. It is realized that complete chemical analyses would have been desirable although they are not absolutely necessary. Many of the specimens were type materials from the Roebling collection of the U. S. National Museum. The lepidolite samples analyzed and described by R. E. Stevens[5] were available and are indicated under his numbers in the tables. Analyses also had been made of the taeniolite[8] sample, zinnwaldite from Amelia, Va.[9], alurgite from Cajon Pass, California[10] and muscovite from the Harding Mine, N. M..[11]

Some optical properties of the micas studied are listed in Tables XVI to XX. The maximum refractive index was measured either by immersion under the microscope, or by the Abbe total reflectometer when the Na_D absorption was not too great. Only the latter method was used to obtain the minimum refractive index. The optic axial angle was measured by the Mallard method and is probably accurate to $\pm 2°$ where a greater limit is not required by variability. It was thought that the refractive indices might be of some value as a rough measurement of the amount of iron present in the samples. The optic orientation was determined by examination of samples the crystallographic orientation of which had been determined by means of x-ray diffraction photographs.

[8] Miser, H. D., and Stevens, R. E., *Am. Mineral.*, **23**, 104 (1938).
[9] Glass, J. J., *Am. Mineral.*, **20**, 741 (1935).
[10] Webb, R. W., *Am. Mineral.*, **24**, 123 (1939).
[11] Analysis of Rocks and Minerals, *U. S. Geol. Survey, Bull.* **878**, 108 (1937).

TABLE XVI

Optical Properties and Numbers of Samples with the Single Layer Structure (monoclinic hemihedral).

		α	γ	2V	Optic Orientation	Degree of Diffuseness
Biotites	U. S. N. M.					
78303	Wakefield, P. Q.	1.563	1.609	0°–5°		none
48309	Rossie, N. Y.	1.537	1.568	9°		none
48305	Pierrepont, N. Y.	1.54	1.59	8°–12°		VWD
R4454	Easton, Pa.	1.548	1.595	5°	‖ to (010)	WD
14459	Portland, Conn.	1.551	1.592	9°–10°	‖ to (010)	none
96204	Miask, Russia	1.566	1.618	6°–8°	‖ to (010)	VD
C3647	Succasunna, N. J.	1.557	1.612	6°–8°		VWD
82253	Grand Calumet Is., Can.		1.585	6°–8°	‖ to (010)	WD
P.R.C.1501	From a leucite monchiquite		1.61	0°–3°		none
P.R.C.266	From a nepheline syenite		1.63	3°–6°		WD
R4448	Anomite, Chester, Mass.		1.592	6°–9°	‖ to (010)	WD
R4449	Anomite, Greenwood Furnace, N. J.	1.560	1.604	5°–7°		MD
45960	Cryophyllite, Rockport, Mass.	1.545	1.57	20°–22°		none
R4472	Lepidomelane, Litchfield, Me.		1.64	3°		VD
Phlogopites						
C3644	Franklin, N. J.	1.530	1.558	7°		
13946	South Burgess, Ontario	1.543	1.582	8°–9°	‖ to (010)	none
86772	Franklin, N. J.			3°–5°	‖ to (010)	none
82023	Vroomans Lake, N. Y.	1.533	1.574	1°–3°	‖ to (010)	VD
78211	Somerville, N. Y.		1.565	5°–7°	‖ to (010)	none
92833	Pierrepont, N. Y.	1.544	1.582	0°		none
78216	Muscalunge Lake, N. Y.		1.575	5°–6°		VWD
103226	Magnet Cove, Ark.	1.590	1.613	0°–2°	‖ to (010)	none
R4468	Ogdensburg, N. J.	1.539	1.566	5°–6°	‖ to (010)	none
48300	DeKalb, N. Y.		1.575	5°–6°		none
82459	Burgess, Ontario	1.552	1.597	5°–7°	⊥ to (010)	WD
78214	Hammond, N. Y.		1.576	6°–8°	‖ to (010)	none
48278	Edwards, N. Y.		1.575	1°–2°		MD
Lepidolites, Polylithionites						
93924	Ramona, Calif., Stevens #15	1.533	1.555	45°	‖ to (010)	WD
86193	Haddam, Conn., with muscovite		1.56	48°–50°		none
84942	Mesa Grande, Calif.		1.562	50°		none
96239	Alaeschka, Russia		1.558	40°		MD
R4420	Haddam, Conn., with muscovite		1.558	35°–40°		none
R4425	Mt. Apatite, Me.		1.555	35°		none
94314	Kangerluar Suk, Greenland, Stevens #17		1.569	40°	‖ to (010)	none
Zinnwaldite						
86008	Zinnwald	1.539	1.564	30°	‖ to (010)	none
R4436	Brambach, Saxony		1.572	25°–35°	‖ to (010)	none
Samples from U. S. Geological Survey:						
Biotite	Magnet Cove (C. S. Ross) from nepheline pegmatite		1.625	10°–15°	‖ to (010)	none
Talniolite	Magnet Cove (W. T. Schaller)	1.523	1.553	0°		none
Phlogopite	Mendham, N. J. (Miss Glass)	1.538	1.570	5°–8°	‖ to (010)	MD

		α	γ	2V	Optic Orientation	Degree of Diffuseness
	U.S.N.M.					
Lepidolite	Stevens #8		1.56	30°–40°	‖ to (010)	
	Stevens #9		1.555	55°–58°	‖ to (010)	none
	Stevens #10 U.S.N.M. 96012		1.562	30°	‖ to (010)	none
	Stevens #13		1.558	25°–30°	‖ to (010)	none
	Stevens #16		1.558	45°	‖ to (010)	none
Zinnwaldite	Amelia, Va. (Miss Glass)					

TABLE XVII

Optical Properties and Numbers of Samples with the Muscovite Structure (monoclinic holohedral).[1]

		α	γ	2V	Optic Orientation
Muscovites	U.S.N.M.				
R4366	"Dutch East Africa"	1.570	1.615	37°–38°	⊥ to (010)
86193	Haddam Conn., with lepidolite		1.59	45°–47°	⊥ to (010)
89190	Pala, Calif.		1.578	43°–44°	⊥ to (010)
83775	Custer Co., S. D., with biotite	1.560	1.592	45°	⊥ to (010)
82021	Portland, Conn.	1.565	1.605	36°–38°	⊥ to (010)
46127	with biotite				
96460	Spruce Pine, N. C.	1.557	1.597	48°–50°	⊥ to (010)
C3677	with biotite				⊥ to (010)
C3648	Lincoln Co., N. C.	1.564	1.600	43°	⊥ to (010)
14349	Middleton, Conn., with biotite				
84430	Henry Co., Va.	1.563	1.605	38°–40°	⊥ to (010)
R4420	Haddam, Conn., with lepidolite	1.550	1.591	45°	⊥ to (010)
R4354	Catawaba Co., N. C.	1.556	1.605	34°	⊥ to (010)
96458	Oje Caliente, N. M.				
R7106	Mörefjar, Norway		1.61	42°	⊥ to (010)
Muscovites	U. S. Geological Survey				
	Spruce Pine, N. C. (W. T. Schaller)	1.568	1.610	50°	⊥ to (010)
	Harding Mine, N. M. (W. T. Schaller)		1.59	47°–48°	⊥ to (010)
	Amelia, Va. (Miss Glass)	1.550	1.585	43°	⊥ to (010)
	North Carolina with biotite (C. S. Ross)	1.563	1.600	40°	⊥ to (010)
Lepidolite, Stevens #1			1.57	38°–40°	⊥ to (010)
Alurgite, Cajon Pass, Calif. (R. W. Webb)					

[1] None of the samples with the muscovite structure showed observable diffuse scattering in the $[h_a k_b l]$, $k_b \neq n \times 3$, zones.

TABLE XVIII

Optical Properties, Numbers, and Degree of Diffuseness of Samples with Various Multilayer Structures.

	α	γ	2V	Optic Orientation	Degree of Diffuseness
Two layer structure (monoclinic holohedral) U.S.N.M.					
Biotite P.R.C395, Montgomery Co., Ark.		1.625	10°–15°		none
Lepidomelane 7117, Brevig, Norway		opaque	ca 5°		none
Phlogopite 78218, Burgess, Ontario	1.54	1.57		$\perp$ to (010)	WD
Manganophyllite R4452, Pajsberg, Sweden		1.60	0°–2°		VD
Biotite 77436, Ambulawa, Ceylon					WD
Three layer structure (rhombohedral enantiomorphic hemihedral) U.S.N.M.					
Biotite, 93228, Torrington, New S. Wales		1.62	0°–3°		VD
C3677, with muscovite	1.585	1.635	0°–1°		VD
14349, Middleton, Conn. with muscovite	1.580	1.635	0°–5°		MD
Alurgite 93915, St. Marcel, Italy		1.607	0°		none
Phlogopite R4463, Masham, P. Q.		1.59	0°–3°		WD
Zinnwaldite 97374, Amelia, Va.	1.550	1.584	0°		none
Lepidolite R4365, Western Aust., Stevens #14	1.525	1.558	0°		none
Biotite, Avery, N. C., (C. S. Ross)	1.597	1.64	0°–3°		VD
Six layer structure (monoclinic hemihedral) U. S. Geological Survey					
Lepidolite, Stevens #6		1.550	25°–30°	$\parallel$ to (010) (b=5.3Å)	none
Stevens #7 U.S.N.M. 97893		1.562	25°–40°	$\parallel$ to (010) (b=5 3Å)	WD
Stevens #12		1.554	35°	$\parallel$ to 010 (b=5.3Å)	WD
Six layer structure (triclinic holohedral) U.S.N.M.					
Biotite 3675, Sterling, N. Y.	1.59	1.645	0°–3°		WD
46127, with muscovite					VD
Biotite 77436, Ambulawa, Ceylon					VWD
Twenty-four layer structure (triclinic holohedral) U.S.N.M.					
Biotite 77436, Ambulawa, Ceylon		1.64	0°–3°		MD

TABLE XIX

Samples with Mixed Structures.

	α	γ	2V	Degree of Diffuseness
From U.S.N.M.				
Biotite 103149, Varnitskaya Bay, Russia	1.59	1.64	0°–3°	MD
R4451, Houghtonite, Respond, Scotland	1.581	1.63	10°–15°	MD
12291, Vesuvius, Italy		1.585	0°–3°	MD
83775, Custer, S. D., with muscovite				WD
11852, Yena Gori, Japan	1.585	1.625	1°–3°	VD
Phlogopite C3686, Sparta, N. Y.				M.D.
R7115, Uhlen Snarum, Norway		1.58	5°–10°	completely D
Campbell Quarry Texas, Md.		1.59	8°–12°	M.D.

From U. S. Geological Survey:					
Biotite	Franklin, N.C., with muscovite (C. S. Ross)				V.D.
	Amelia, Va. (Miss Glass)		1.64	2°–4°	M.D.
From Columbia University:					
Biotite	Moravia		1.59	0°–3°	WD.
	Larchmont Manor, N. Y.	1.586	1.64	0°–3°	VD
	Tyrol		1.59	3°–7°	MD

TABLE XX

Summary of Observations on Analyzed Lepidolites.

	Six fold Coordination Al	Li	Σ	Structure Type	Orientation of Plane of O.A. and 2V
1	1.59	0.73	2.48	Muscovite	⊥ to (010) (b=9.0Å) 38°–40°
2	1.55	0.95	2.54	Too fine grained for study	wavy extinction, distorted interference figures
3	1.55	1.00	2.60		
4	1.54	1.02	2.58		
5	1.51	1.07	2.63		
6	1.32	1.36	2.73	6 layer monoclinic	‖ to (010) (b=5.3Å) 25°–30°
7	1.30	1.39	2.86	6 layer monoclinic	‖ to (010) (b=5.3Å) 25°–40°
8	1.35	1.35	2.71	Single layer	‖ to (010) (b=9.0Å) 30°–40°
9	1.36	1.44	2.81	Single layer	‖ to (010) (b=9.0Å) 55°–58°
10	1.10	1.50	2.94	Single layer	‖ to (010) (b=9.0Å) 30°
11	1.35	1.50	2.85	None available	
12	1.31	1.52	2.85	6 layer monoclinic	‖ to (010) (b=5.3Å) 35°
13	1.30	1.56	2.91	Single layer	‖ to (010) (b=9.0Å) 25°–30°
14	1.25	1.62	2.94	3 layer hexagonal	uniaxial
15	1.11	1.68	2.95	Single layer	‖ to (010) (b=9.0Å) 45°
16	1.05	1.85	2.98	Single layer	‖ to (010) (b=9.0Å) 45°
17	0.98	1.94	2.97	Single layer	‖ to (010) (b=9.0Å) 40°

Nineteen of the samples studied were muscovites and all these had the same two layer monoclinic structure. This structure was also shown by the lepidolite sample that approached closest to muscovite in composition and by the analyzed alurgite from California. The optic axial angles (2V) of all the specimens were between 34° and 50° and the plane of the optic axes was perpendicular to (010) in every case.

Forty-five of the remaining seventy-eight biotite-like (octophyllite) micas have the single layer monoclinic structure. They include many phlogopites and seven of the analyzed lepidolites as well as several zinnwaldites. The iron contents of the biotites vary over wide limits as shown by the value of the maximum refractive index and by the presence of such varieties as anomite, cryophyllite, and lepidomelane. The plane of the optic axes was parallel to (010) in all of the samples tested, except

one—phlogopite No. 82459. The optic axial angles of the biotites and phlogopites were very small. Lithium-bearing members, on the other hand, had optic axial angles in the same region as did the muscovites, namely 25–60°.

The single layer structure is often a component present in the mixed type structures given by the thirteen specimens listed in Table XIX. The optic axial angle of all these micas was found to be small.

The five unusual types of structures described earlier in the paper are represented among the remaining twenty specimens examined. Eight of these had the rhombohedral enantiomorphic hemihedral structure. Several of these are strictly uniaxial even in a conoscope with low divergence of the illumination. However, others show a small opening of the interference figure. All give some diffuse scattering, the significance of which will be discussed later. There is no doubt but that the hexagonal description is accurate as a limiting case. This three layer structure was found for a wide variety of compositions including an analyzed lepidolite. The four biotite samples were very darkly colored and had a high maximum index of refraction, which suggests that they had a high iron content.

Five specimens have the two layer monoclinic structure related to that of muscovite but differing from it in the absence of $(0kl)$, l odd reflections. There were three examples of each of the six layer structures and a single case of the twenty-four layer structure.

General Discussion

Three questions naturally come to the fore. What are the factors determining the polymorphism of the micas? What are the relationships between optical properties and structure? In what manner does diffuse scattering arise?

Before addressing any of these, attention should be called to several papers by A. N. Winchell.[12] He recognized a group distinction among the micas which he summarized in the terms heptaphyllite and octophyllite. These terms simply mean that seven and eight positive ions, respectively, are present for twelve negative ions. Muscovite is the type heptaphyllite mica having the formula $[KAl_2AlSi_3O_{10}(OH, F)_2]$ and phlogopite the type octophyllite mica $[KMg_3AlSi_3O_{10}(OH, F)_2]$. This distinction is entirely consistent with the present and previously published information on the mica structures. Another way of expressing it is that micas related to muscovite (heptaphyllites) have only two-thirds

[12] *Am. Jour. Sci.*, (V), **9**, 415 (1925); *Am. Mineral.*, **17**, 551 (1932); **20**, 773 (1935).

of the positions with octahedral coordination relative to oxygen filled while phlogopite (octophyllite) has all such positions filled. Finally, Winchell has made two further statements of use here: "It is important to note that no evidence of crystal solubility between octophyllite and heptaphyllite has been found; on the contrary any good analysis belongs definitely to one or the other, and not to both." "Also certain lithia micas are reported to be triclinic, while others (even in the same rock) seem to be monoclinic. Apparently these micas are dimorphous, and that condition would doubtless entail variations in optical properties, the extent and character of which are at present unknown."

Muscovite in accord with Winchell's concept was found to be invariant in structure and none of the other micas had the same structure. The most characteristic feature of the structure is that it is distorted from the ideal as shown by the presence of reflections from (06l) with l odd. The exact character of the distortion is not known but it undoubtedly is the factor that leads to a unique requirement on the successive stacking of layers. In other words, muscovite has a unique structure because of its distorted layer while the biotites (octophyllites) have variable structures because their layers are symmetrical. The distortion of the layer in muscovite is a result of incomplete filling of the octahedral positions. Thus some octahedral edges will be differently surrounded than others and there will be changes of the type predicted by Pauling's coordination theory. In the biotites (octophyllites) all octahedral positions are filled and the octahedral edges are equivalent.

The distortion of the muscovite layer also probably contributes to the partial birefringence in the cleavage plane and thus increases the optic axial angle. It is apparently for this reason that the partial birefringences $(\gamma-\beta)$ of muscovites are greater than those of other micas.

Results obtained from the lepidolites analyzed by Stevens as summarized in Table XX serve to illustrate the limited solid solutions of muscovite and lepidolite. In Table XX, Σ is the number of atoms having octahedral coordination for every twelve negative ions in a mica; it should be 2 for muscovite (heptaphyllite) and 3 for polylithionite (octophyllite). Sample 1 having $\Sigma = 2.48$ still has the muscovite structure and it is tantalizing to think that samples 2 to 5 owe their poor crystal development to their close approach to the limit of the lepidolite solid solution in muscovite. Samples 6 to 17 show three different structures without evident correlation with composition. These can be considered as solid solutions of muscovite in polylithionite, or better as lithium micas in which more than 11/12 ($\Sigma = 2.75$) of the octahedral positions are filled.

The six layer monoclinic structure is reported in the tables as only being observed for lepidolites and it thus might be thought to be peculiar to them. However, at least two of the mixed types of Table XIX appear to contain a part of this structure type and the absence of a biotite or phlogopite representative appears accidental. The structure is most interesting in that it alone of all the types found, effects an interchange of the usual a- and b-axes. In Table XX it would appear that the optic orientation for this structure is similar to that of the single layer and three layer structure. Actually, it is more comparable with muscovite as represented by sample 1 on account of the interchange of axes. The optic axial angles of the six layer, one layer, and muscovite types of lepidolite are all of the same magnitude as that of muscovite. However, this is really a result of the low birefringence $(\gamma-\alpha)$, the partial birefringence $(\gamma-\beta)$ being about two-thirds to one-half that of muscovite.

While the six layer and single layer lepidolites cannot be distinguished optically, the three layer hexagonal structure is immediately evident. This particular sample (Stevens #14, U.S.N.M. R4365) is a very large sheet from Londonderry in Western Australia. The sheet is predominantly uniaxial but in a few parts the optic axes (2V) open up to 20–40°. These parts upon examination by x-ray diffraction are found to have the single layer structure. If the change is to be accounted for by composition, then it is varying on a small scale and the composite nature of the analyzed material would obscure any correlation between structure and composition. A similar situation was encountered in a zinnwaldite sheet from Amelia, Va., that was kindly supplied by Miss J. J. Glass of the U. S. Geological survey. The optic axial angle (2V) of different parts of the sheet varied from uniaxial to 25°. A uniaxial part had the three layer structure while mixed structure types combining the single layer and three layer structures were found in two of the biaxial parts.

The six layer monoclinic structure is rather analogous to the nacrite structure, as was pointed out in the structure analysis. In fact, the distinction between the various mica structures is more pronounced than that between the kaolin minerals, kaolinite, dickite and nacrite. Absence of appreciable variation of composition among the kaolin minerals made it possible to interpret the optical properties with more certitude than was the case for the micas. In a sense, however, the presence of a uniaxial lepidolite is an indication of polymorphism among the micas.

The truly hexagonal three layer structure is by no means unusual and in fact it occurred with about one-fifth the frequency of the predominant single layer structure among the biotites (octophyllites). The six layer monoclinic structure is related to it in a sense that it too has three-fold screw axes even though these are eliminated as symmetry

operations of the space group by the glide reflection plane. In fact the hexagonal structure can be considered as a combination of two $C_3^2-C3_1$ or $C_3^3-C3_2$ subgroups with two-fold axes normal to the hexagonal axis (note I.T.D.C.S.) while the six layer monoclinic structure combines either of the same groups with a glide reflection plane with a glide component along the three-fold screw axis. As pointed out before this is of most interest in that it forms an unclosed group of operations.

Remaining structure types are the two layer monoclinic, the six layer triclinic, and the twenty-four layer triclinic. The triclinic ones are of interest in that they give a summary answer to the question of the possible existence of a triclinic mica. As a group they are a motley array without apparent interrelationship except that they are predominantly biotites with probably a high iron content. However, each structure is characterized by having centers of symmetry, an element of symmetry which is absent for the three lepidolite structures.

Good evidence that these three structures are probably related was found in an entirely accidental manner. The crystal taken from the Ambulawa, Ceylon, biotite specimen was among the first examined and it showed the twenty-four layer structure which was merely appreciated as being complex at the time. Later, when a closer examination was to be made, a second crystal from the same specimen was accidentally selected. It proved to have the six layer triclinic structure.

The Ambulawa, Ceylon, specimen which is marked a thoranite-bearing pegmatite, is shown in Fig. 8. Structures of various crystals are indicated in the accompanying diagram (Fig. 8*b*). It is to be noted that only

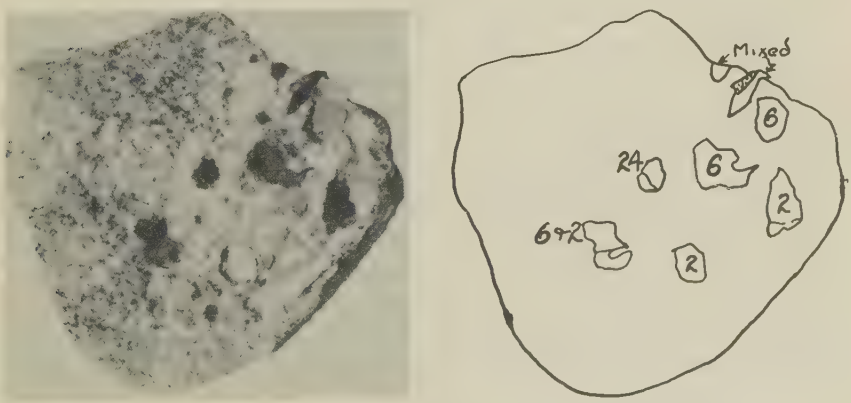

FIG. 8*a*. Biotite specimen from thoranite-bearing pegmatite, Ambulawa, Ceylon.

FIG. 8*b*. Drawing of crystals in specimen with indicated layer multiplicities in structures.

two layer monoclinic and six and twenty-four layer triclinic structures are represented, together with mixtures of these. The crystals appear to be closely similar and they probably do not vary appreciably in composition. It would seem therefore that whatever factors determine the structures, composition probably being important, operate for all cases.

The only phlogopite specimen, No. 78218, having one of these structures, is not typical. It is weathered as shown by poor coherence of the cleavage sheets and absence of an interference figure. Moreover, the surface is too drusy for use on the total reflectometer and there are a tremendous number of acicular inclusions.

In general the partial birefringence $(\gamma-\beta)$ of the octophyllite micas other than the lepidolites is so low that the optical character is probably determined more by variation in composition than by structure. The three layer hexagonal micas are closely uniaxial, but so are representatives of the other structures.

A number of specimens were examined, in some of which biotite crystals were included in muscovite and in others muscovite was zoned with lepidolite. In none of these did the biotite or lepidolite take up the muscovite structure. In fact the octophyllite parts of the seven specimens examined afforded examples of four structure types while the muscovite was invariant. Moreover, crystallographic orientations were not the same for the component crystals but rather had other simple relationships.

Mixed Structures and Relationship of Diffuse Scattering of X-Radiation to Structure

It was mentioned that portions of the zinnwaldite specimen from Amelia, Va., and lepidolite R4365 were mixtures of the single layer and three layer structures. Mixtures of a more complex nature and involving other structures were observed for a number of samples which are listed in Table XX. Since the diffraction photographs are difficult to analyze correctly, no attempt was made to determine the exact type of mixing. The three samples from Columbia University were selected for study on account of their close approach to uniaxial character, this being a qualitative criterion for some structure other than the single layer one.

Different components in a mixed structure maintain parallel orientations, except for variation in the c-axis. Thus the orthohexagonal b-axis of the three layer component in zinnwaldite from Amelia, Va., is parallel to the b-axis of the monoclinic part.

Appreciable development of diffuse scattering along $(h_a k_a l)$, $k \neq n \times 3$, curves was noted on Weissenberg photographs of all samples with mixed structures. Such scattering was also observed for many other micas

examined as indicated in Tables XVI and XVIII, but, significantly, was not found for any of the muscovites. The phenomenon was first noted by Mauguin[2] who, without detailed knowledge of the structures, concluded that it was a result of some type of randomness in positions of the heavy ions. Others have observed similar scattering from various layer silicate minerals; among the most recent being Hutton and Fankuchen in their work on stilpnomelane.[13] A probable explanation of the effect was given in the paper on the structures of vermiculites[14] and elaborated in the more recent work on cronstedite.[15] Both of these minerals as well as the chlorites show pronounced development of the general scattering. The work on the micas focuses attention on several factors that merit discussion.

The concept of a mosaic crystal was introduced by C. G. Darwin[16] in his classical work on diffraction of x-rays by crystals. He demonstrated that the observed intensities of x-ray diffraction maxima required crystals to consist of many small elements of volume deviating slightly from perfect alignment. According to this concept a mica crystal would consist of parts each of which was a perfect crystal in itself but which scattered x-rays independent of neighboring parts except insofar as they form a screen. The total reflection is the summation of the x-rays scattered from the different parts, but one part does not give interference with another. Magnitudes of the perfect volumes are unknown and in fact the whole phenomenon has not been very susceptible of study.

In micas, as in other layer minerals, the diffuse scattering is restricted to those Weissenberg curves along which the h and k indices are constant and the k index not a multiple of three, $(h_a k_b l)$, $k_b \neq n \times 3$. Several typical Weissenberg goniometer photographs taken with the crystal rotating about the a-axis, or pseudo a-axis, are shown in Fig. 4. The diffuse scattering is always associated with the strong reflections along a curve. In this connection it is interesting to compare the diffuse scattering from phlogopite R7117 and biotite 11852, photographs of which are reproduced in Fig. 4c and 4e, respectively. The first closely resembles the usual pattern of a two layer biotite while the second is related to the photographs of the single layer and others.

Laue photographs of micas taken with the incident x-ray beam normal to the cleavage plane show radial streaks that usually have been explained as "asterism." Such streaks, which are illustrated by Fig. 9, are

[13] *Mineral. Mag.*, **25**, 172 (1938).
[14] Hendricks, S. B., and Jefferson, M. E., *Am. Mineral.*, **23**, 851 (1938).
[15] Hendricks, S. B., *Am. Mineral.*, **24**, 529 (1939).
[16] *Phil. Mag.*, (6), **27**, 325 (1914).

analogous to the continuous Weissenberg curves. Both can be explained in terms of constant h and k indices with an apparently continuous variation of the l index. Qualitatively the entire effect appears to involve a variable length in the stacking of the mica layers that leaves those planes with the k index a multiple of three undisturbed.

Inspection of the various drawings and tables of coordinations will perhaps make it evident that translation of one-half of a mica layer by $nb/3$ with respect to the other half leaves the layer unchanged but results in a change of the relationship of successive layers. This is really the factor that permits the polymorphism of the octophyllite micas. Now if this process is carried out in a random instead of a regular manner there will be no definite c periodicity unless the k index is a multiple of three, in which case the periodicity is that of a single layer. As a result diffuse scattering of the observed type will necessarily appear, and its intensity will depend upon the number of the random shifts.

In the structure analysis of dickite,[17] pyrophyllite, and talc[18] it was found that while intensities of reflections from (hkl), $k=n\times 3$, could be explained, those from (hkl), $k\neq n\times 3$, could not. The explanation advanced was that random shift of one layer with respect to another by $nb/3$ within an element of a crystal mosaic introduced an indefinite shift of phase. In the micas, however, as seen above, calculated intensities in agreement with observed values can be found for (hkl), $k\neq n\times 3$ reflections. It is necessary, therefore, to assume that many elements of a mosaic in a mica crystal showing a well developed structure are perfectly regular and any diffuse scattering is due to random shifts in a limited number of the mosaic elements. Similarly in dickite, pyrophyllite and talc the majority of the elements would have at least one random displacement and none would have many, since no diffuse scattering is observed.

Mica crystals having the single layer structure, for instance might consist of perfect mosaic elements and show no diffuse scattering, or a sufficiently large number of the mosaic elements might have many random elements leading to completely diffuse (hkl), $k\neq n\times 3$ reflections. The presence of mixed structures further serves to support these concepts in that they indicate that different parts of the crystal mosaic can vary in structure.

In the end it is all too evident that the first question has not been answered. What are the factors determining the polymorphism of the micas? Surely it is most surprising that they have fixed structures at all.

[17] Hendricks, S. B., *Am. Mineral.*, **23**, 295 (1938).
[18] Hendricks, S. B., *Zeits. Krist.*, **76**, 211 (1930).

FIG. 9. Laue photographs with the x-ray beam approximately normal to the plane of micaceous cleavage. Symmetry planes are indicated by M. All photographs were taken with the same crystal to plate distance and peak voltage.

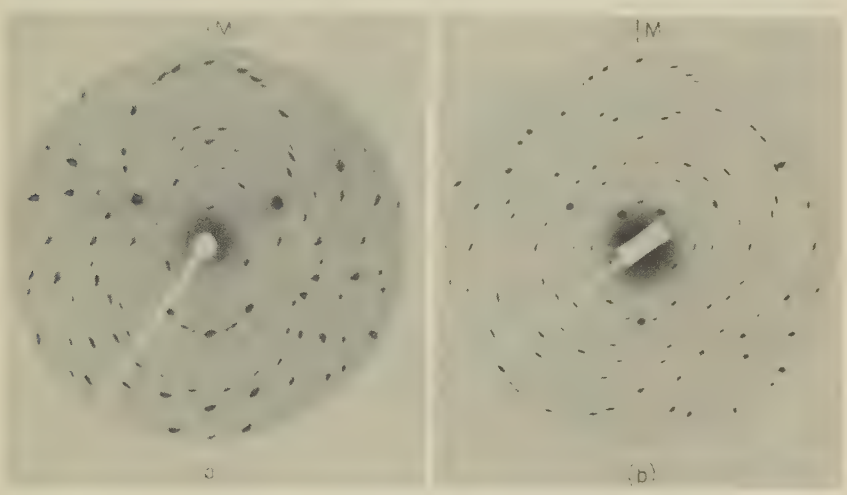

a. Single layer monoclinic hemihedral phlogopite.
b. Muscovite, two layer monoclinic holohedral.

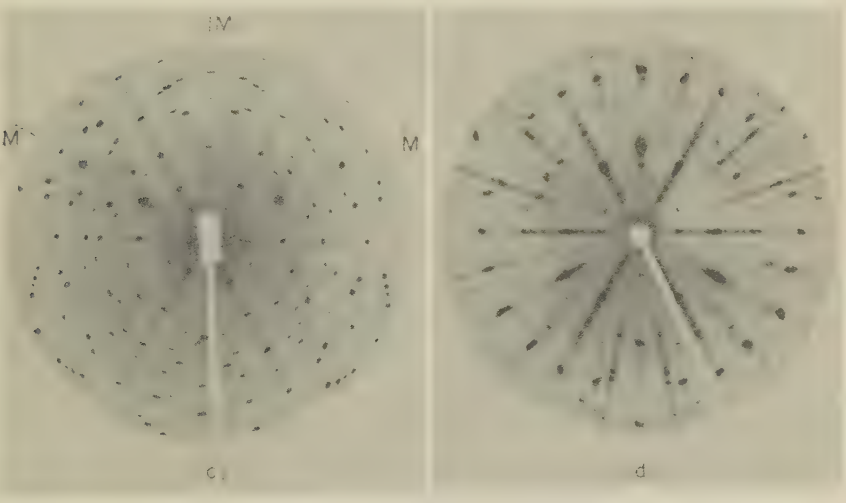

c. Three layer rhombohedral enantiomorphic hemihedral lepidolite. Note radial streaks.
d. Twenty-four layer triclinic holohedral biotite.

Summary

Seven different crystalline modifications were discovered among one hundred specimens of mica that were examined by x-ray diffraction methods. Constants of these various forms and their frequency of occurrence are:

Single layer monoclinic hemihedral (45)
$2[R_3(Al, Si)_4O_{10}(OH, F)_2K]$ in unit of structure
$R = Mg^{++}$, Fe^{++}, Fe^{+++}, Li^{+}, Ti^{++++}, etc.
$a = 5.3$Å $c_0 = 10.2$Å Sp. G. $C_3^3 - Cm$
$b = 9.2$Å $\beta = 100°$
(A. C.) Atomic Coordinates, Table I
(Struc.) Structure, Fig. 1.
(Photo.) X-ray diffraction patterns, Figs. 4a, b, c, h, 9a.

Two layer monoclinic holohedral, muscovite type (21)
$4[(Al, R)_2(Al, Si)_4O_{10}(OH,F)_2K]$,
$a = 5.2$Å $c_0 = 20.0$Å Sp. G. $C_{2h}^6 - C2/c$
$b = 9.0$Å $\beta = 95° 30'$
(A. C.) Table V, (Struc.) Figs. 1b, 3b.
(Photo.) 4d, 9b.

Two layer monoclinic holohedral, octophyllite type (5)
$4[R_3(Al, Si)_4O_{10}(OH,F)_2K]$
$a = 5.3$Å $c_0 = 20.2$Å Sp. G. $C_{2h}^6 - C\,2/c$
$b = 9.2$Å $\beta = 95°$
(A. C.) Table V, (Struc.) Fig. 3a.

Three layer rhombohedral enantiomorphic hemihedral (8)
$3[R_3(Al,Si)_4O_{10}(OH,F)_2K]$
$a = 5.3$Å $c_0 = 30.0$Å Sp. G. $D_3^3 - C3_112$ or $D_3^5 - C3_212$
(A. C.) Table VIII, (Struc.) Fig. 5b. (Photo.) 4f, 9c.

Six layer monoclinic hemihedral (3)
$12[R_3(Al,Si)_4O_{10}(OH,F)_2K]$
$a = 5.3$Å $c = 60.0$Å Sp. G. $C_s^4 - Cc$
$b = 9.2$Å $\beta = 90°$
(A.C.) Table X, (Struc.) Fig. 6., (Photo.) 4g.

Six layer triclinic holohedral (3)
$6[R_3(Al,Si)_4O_{10}(OH, F)_2K]$
$a = 5.3$Å $\alpha = 90°$ Sp. G. $C_i^1 - P\bar{1}$
$b = 5.3$Å $\beta = 90°$
$c = 60.0$Å $\gamma = 120°$
(A.C.) Table XIII, (Struc.) Fig. 7, (Photo.) 4i

Twenty-four layer triclinic holohedral (1)
$24[R_3(Al,Si)_4O_{10}(OH,F)_2K]$
$a = 5.3$Å $\alpha = 90°$ Sp. G. $C_i^1 - P\bar{1}$.
$b = 5.3$Å $\beta = 90°$
$c = 240.0$Å $\gamma = 120°$
(Photo.) 4j, 9d. Structure not determined.

Mixtures (13) of the various structures were found and a general explanation is given for the diffuse scattering of x-rays in some crystal zones. Underlying reasons are given for Winchell's successful grouping of micas as heptaphyllite, or muscovite-like, and octophyllite, or phlogopite-, lepidolite-, biotite-, etc., like.

The general reader and mineral collector will perhaps find the part of the paper after "Optical Properties etc." of most interest. For his use it can be stated that two triclinic, four monoclinic, and one hexagonal modification of mica were discovered. There is some correlation between crystal optics and structure, particularly for lepidolites.

MIARGYRITE CRYSTALS FROM RANDSBURG, CALIFORNIA

Joseph Murdoch, *University of California at Los Angeles*

Abstract

A study of recently collected miargyrite from Randsburg, California, has shown crystals richer in forms than from any other locality except Bräunsdorf, Saxony. Forty-seven forms in all have been observed by the writer, of which T (313) and Σ (322) are new, and α ($\bar{2}33$) and Z (205) confirm forms which have been reported as doubtful by earlier workers. A few of the crystals are as much as one centimeter across, but most of them are considerably smaller.

The mineral miargyrite is noted for its richness in crystal forms and complex crystals. Fifty-nine forms have been accepted up to the present as established, another 25 or so have been noted as probable or uncertain, and 17 more have been observed as untypical or vicinal.

The crystallography of miargyrite has been studied by many authors,[1] notably in recent years by Rosický, who has made an exhaustive investigation of the known forms.

Various orientations of this species have been suggested: Naumann followed the modern orientation, but with the a-axis $\frac{1}{3}$ of its present length: $a : b : c$ 0.9977:1:2.91, $\beta = 81°36'$. In the orientation of Weisbach the base corresponds to present c, but o ($10\bar{1}$) was taken as the orthopinacoid (100), (100) as (101), and ($31\bar{3}$) as the prism (110). This orientation appears in an early edition of Dana's *Textbook* (1868), and was accepted by Friedlander, Vrba and G. vom Rath. This gave an axial ratio of:

$$a : b : c \quad 1.0136:1:1.3026, \beta = 48°38'.$$

Miller and Lewis used the present orientation, which has been followed

[1] Miller, W. H., In *Phillips Elementary Introduction to Mineralogy*, 1837.
Naumann, C., Ueber die Krystallformen des Miargyrits: *Pogg. Ann. Physik und Chemie*, **XVII,** 142 (1829).
Weisbach, A., Beitrag zur Kentniss des Miargyrits: *Pogg. Ann. Physik und Chemie*, **CXXV,** 441 (1865).
Weisbach, A., Beitrag zur Kentniss des Miargyrits: *Zeits. Kryst.*, **II,** 55 (1877).
Vom Rath, G., Ein Beitrag zur Kentniss der Krystallform des Miargyrits: *Zeits. Kryst.*, **VIII,** 25 (1884).
Lewis, W. J., Ueber die Krystallform des Miargyrit: *Zeits. Kryst.*, **VIII,** 545–567 (1884).
Eakle, A. S., Miargyrit von Zacatecas, Mexico: *Zeits. Kryst.*, **XXXI,** 209–215 (1899).
Spencer, L. J., Notes on some Bolivian minerals: *Mineral. Mag.*, **XIV,** 339–340 (1907).
Rosický, V., Ein Beitrag zur Morphologie des Miargyrits: *Bull. Inter. de l'Acad. des Science de Boheme*, **XVII,** 1912.
Shannon, E. V., Miargyrite silver ore from the Randsburg District, California. *U. S. Nat. Mus. Proc.*, **LXXIV,** Art. 21 (1929).

by observers since that time. Lewis calculated the elements from 32 measured angles. Dana, recalculated many observed angles, modified Lewis' values slightly, and obtained: $a : b : c = 2.99449 : 1 : 2.90951$, $\beta = 81°22'35''$.

These are the present accepted values, and have been used in this paper.

Lewis grouped the crystal habits in seven types, as follows:

1. Bräunsdorf type: *a o c* large, *d s t* small, the latter intersecting an analogous zone in the rear octants to form a sharp angle on the *b*-axis.
2. ξ strongly developed, also faces in the symmetry zone [*a o c*].
3. *a o c* large, *d*, *g* almost as large, producing orthorhombic development.
4. [*d s t*] and [β *z k t*] zones equally developed, with either β or *x*, or both, present.
5. Tabular, with large *c*. [*o p g*] zone more strongly developed than [*d s t*].
6. Kenngottite type—base large, all other faces small, and belonging to [*o p g*] or [*d s t*] zones.
7. Minute crystals with *o* and *b* well developed, *g* large, *a* triangular, *c* lacking, [*d s t*] zone subordinate.

Rosický has discussed at length the zones and dominant combinations from all the prominent localities (Bräunsdorf, Felsöbanya, Príbram, Zacatecas, Potosi) and has grouped them into three types.

1. Isometric habit: equidimensional crystals with the orthodiagonal zone ordinarily prominent. *c a o* the largest faces. *A* and *g* fairly large. This is the commonest habit in crystals which have been illustrated.
2. Tabular habit—base largest face, or less commonly *a* or *o*.
3. Columnar habit. Generally the zone [*o g A*] is developed, which determines the columnar form. He did not observe this type, personally, but noted it in the literature.

Rosický also has listed all known forms up to the time of writing, 59 certain, 16 doubtful, and 16 vicinal or untypical. Since then Shannon[2] has observed three probable new forms from Randsburg, (722), (733), (433), although the observed readings of ϕ vary by over 1° from the calculated values.

It has been the writer's good fortune recently to obtain crystallized material from Randsburg, much of it quite different in character from Shannon's, and the present paper is the result of a study of these crystals. The geologic occurrence has been described by Hulin[3] and by Shannon.[2] The crystals range in size from about a millimeter across up

[2] Shannon, E. V., *loc. cit.*

[3] Hulin, C. D., Geology and ore deposits of the Randsburg Quadrangle, California: *Calif. State Min. Bur., Bull.* **XCV**, 97–102 (1925).

to a maximum of one centimeter, although the larger crystals, usually, are not complete. Some of them are quite complex, one crystal showing 27 forms, with 48 faces, another 25 forms with 39 faces.

In habit they fall into three classifications:

1. Small crystals like those described by Shannon, with few distinct faces. The *a* pinacoid keystone shaped, the base large, and the [*d s t*] zone represented by a heavily striated band, with one or two definite facets. Any number of observations may be made in this zone, but only a few places give a definite signal. This corresponds to Rosický's No. 1 type. Little evidence appeared of the fracturing and recementing of crystals noted by Shannon, except that here and there a zone of signals is offset a trifle.

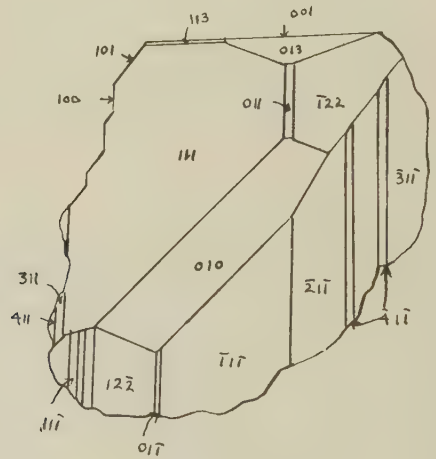

FIG. 1

2. Large crystals, beautifully formed, but incomplete, planted approximately on one end of the symmetry axis. These do not show the maximum number of forms, but there are no heavily striated zones as in type 1. The face *b* is often heavily lined, and some of the other faces may be somewhat curved and striated. The [*d s t*] zone is prominently developed, commonly in characteristic panels, although some of the faces are dull or corroded by etching, and the junction between faces is often marked by a series of narrow lines, or vicinal faces, giving no separate reflections. This type is shown in Fig. 1, which is a projection of one of the large crystals on *b*. This type occurs in a rather vuggy matrix of massive miargyrite and quartz, the latter being bluish, transparent, and forming a drusy coating on the cavity walls. The miargyrite crystals rest on the quartz, and are in general later. This material, with glistening

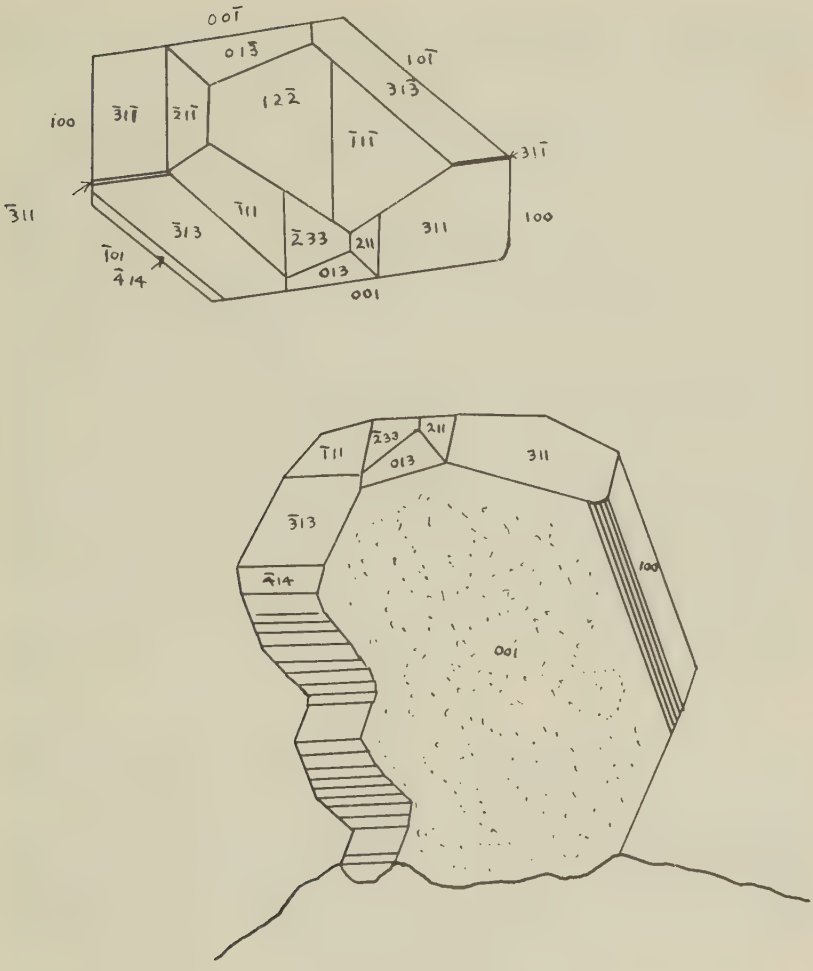

FIG. 2

miargyrite and sparkling quartz, makes very showy specimens. This type is not represented in Rosický's classification, but may approach Lewis' No. 4.

3. Small crystals, tabular, parallel to *c*. They correspond to Rosický's type 2, but are somewhat elongated and are perched on the matrix by an extreme end of the symmetry axis, so that they stand up like posts on the surface. One end is perfectly terminated and many faces are visible on the other. Only two crystals of this type were found, and proved to be very complex, one of them having the greatest number of forms (26)

observed from the region. Another crystal had 24. The *c* face is ordinarily roughened, dull or studded with minute crystals, with other faces in the orthodome zone (except perhaps *a* or *o*) poorly developed or represented by a series of striations. One of these crystals is shown in Fig. 2.

No difficulty was experienced in orientating crystals of types 1 and 3 although type 3 is more easily set in the second inversion position.[4]

Crystals of type No. 2 are very difficult to adjust, particularly those in in which *b* is absent, or as is often the case when present, deeply grooved, so that it cannot be used as a pole face. Under such conditions it was found easiest to place the [*d s t*] zone in a prism position, make a stereographic projection from the readings, and by rotation match these points with a series of known pole positions similarly plotted. Then the projection is tilted, by means of stereographic protractors, into a normal position, or second inversion position, whichever is more convenient. From this readjusted projection, the faces can be identified. In many instances the preliminary orientation will enable a normal setting to be made, so that the ϕ and ρ angles may be plotted directly and more accurately.

Measurements on 14 crystals showed 42 forms, two of which are new. If we add to this number two known and three new forms observed by Shannon, but not by the writer, we have a total of 47 forms for miargyrite from this locality.

New Forms

T (313)—occurs as three faces on a single crystal. The reflections are rather poor, but reasonably consistent. Calculations from the average of observed angles give a value of 3.02 instead of 3 for the indices.

Σ (322)—a single face, with good signal and fair agreement with the calculated position. This form occurs also on crystals from Ungemach's collection, measured by Palache[5] and is considered by him as established.

Confirmed Forms

In addition to these new forms, several were observed which confirm doubtful forms noted by Rosický and others, or add to the evidence in favor of some he calls untypical or vicinal.

α ($\bar{2}33$)—present as two faces on one crystal and one on another, confirming the identity of this form. This is accepted by Palache, and earlier had been noted by Rosický as a doubtful form.

Z (205)—a single very narrow face, with a poor signal. This is listed by Rosický as untypical, but has been found on Ungemach's material by Palache, and may be considered as established.

[4] Peacock, M. A., A suggested form of crystallographic presentation: *Am. Jour. Sci.*, XXVIII, 244 (1934). [5] Charles Palache, personal communication.

Doubtful Forms

δ (13.4.4)—present as two faces on one crystal and one on another. This has been listed by Rosický as untypical and vicinal, and is probably to be so considered.

W (1.0.12)—present as a single very narrow face. It is noted by Rosický as untypical, and cannot as yet be considered as an established form.

$\bar{7}$.10.10—faces with these indices were observed in three instances, but never in the same quadrant as α ($\bar{2}33$). The values are so close to those of α that probably they could not be separated, and should all be grouped under the accepted form.

144—a single face in this position. Probably should be taken as (133).

524—a single face with good signal, and fair agreement with calculated position. Since this occurs only once, it would be better to consider it as a possible but not established form.

A number of other faces occur only once, poorly developed, narrow, and with very unreliable readings. They are ($\bar{1}\bar{0}$.1.3), (623), ($\bar{5}44$), ($\bar{6}12$), and (315). They should be considered as very doubtful forms.

In Table 1 are given the measured and calculated values for these forms.

Table 1

			Measured		*Calculated*	
Letter	Symbol		ϕ	ρ	ϕ	ρ
T	(313)		49°48′	56°12′		
			49 40	56 16		
			48 44	57 10		
		Average	49 24	56 35	49°10′	55°05′
Σ	(322)		31 50	73 30	29 11½	73 18
α	($\bar{2}33$)		−10 34	71 14		
			− 9 28	71 16		
			− 8 42	71 30		
		Average	− 9 35	71 20	− 9 49	71 17½
			ϕ_2	ρ_2	ϕ_2	ρ_2
	(In 2[d] inversion)		114 50	20 16	116 42½	21 02
Z	(205)		60 29	90 00	61 25	90 00

			Measured		*Calculated*	
			ϕ	ρ	ϕ	ρ
δ	(13.4.4)		49 16	77 16		
			49 00	77 32		
		Average	49 08	77 24	48 59	77 17
W	(1.0.12)		90 00	13 00	90 00	13 09
	(524)		42 30	63 49	43 31	63 29½
	($\bar{1}0$.1.3)		−72 48	73 00	−72 44	72 59
	(623)		47 00	70 00	47 29½	70 47½
	($\bar{5}44$)		−20 00	72 16	−20 19	72 08
	($\bar{6}12$)		−63 28	73 07	−63 03½	72 42
	(315)		50 08	44 09	51 52	43 18½
	($\bar{7}$.10.10)		−11 10	71 36		
			−11 08	71 36		
			−11 30	70 44		
			−10 46	69 48		
		Average	−11 08½	70 56	−10°40′	71°20½′
	(144)		7 46	70 53	7 46	71 11½

In Table 2 are given the calculated crystallographic data for the new and confirmed forms according to the presentation method suggested by Peacock.[6]

TABLE 2

Letter	Symbol	ϕ	ρ	ϕ_2	$\rho_2 = B$	C	A
T	(313)	49°10′	55°05′	41°23½′	57°34½′	81°23′	51°39′
Σ	(322)	29 11½	73 18	31 35	33 15	69 15	62 09
α	($\bar{2}33$)	−9 49	71 17½	116 42½	21 03	72 58	99 17½
Z	(205)	90 00	28 35	61 25	90 00	19 57½	61 25

In Table 3 are listed the observed forms from Randsburg, with the number of faces of each form and on each crystal.

[6] Peacock, M. A., *loc. cit.*

TABLE 3

Letter	Form	1	2	3	4	5	6	7	8	9	10	11	12	13	14	Total faces	Number of crystals
c	(001)	1	1	1	1	2	1	1	1	2		1	1	1	1	15	13
b	(010)		1		1	1	1	1		1					1	7	7
a	(100)	2	1	2	1	2	1	1	1	2	1	2	2	1	1	20	14
β	(013)	2	1	1	1		1		1				1			8	7
ω	(011)		2	1		2	1						1			7	5
W	(1.0.12)	1														1	1
G	(105)(S)																
Z	(205)														1	1	1
m	(101)	1	1	1	1	1	1	1							1	8	8
o	(1̄01)	2		2	2	1	1	1	1	2	1	1	1		1	16	12
h	(113)		1			1		1	1							4	4
t	(111)		3	1		2	1						1	1	1	10	7
ρ	(1̄13)								1							1	1
A	(1̄11)	2	1	2	2			3	1					1		12	7
z	(137)						1									1	1
k	(124)					1							1		1	3	3
Γ	(133)					1		1								2	2
X	(122)					1										1	1
x	(1̄22)	2	2	2		3	1		1			1				12	7
ξ	(2̄15)														1	1	1
α	(2̄33)	1		4	2								1			8	4
p	(6̄16)			2		1	1	2	1							7	5
π	(5̄15)	1		1							1					3	3
γ	(4̄14)	2		3	1	2	2	1			1		1			13	8
T	(313)					3										3	1
g	(3̄13)	3		1	2	3	1	2		1	1	1			1	16	10
χ	(2̄12)			1		1	1									3	3
	(524)					1										1	1
ψ	(4̄13)			1		1										2	2
Σ	(322)													1		1	1
	(433)(S)																
s	(211)	2	1	3		2	2		1	1		1	1	1		15	10
σ	(2̄11)					3		1	1							5	3
V	(11.5.5)			1		2										3	2
Q	(733)(S)																

Letter	Form	1	2	3	4	5	6	7	8	9	10	11	12	13	14	Total faces	Number of crystals
ϵ	(522)											1				1	1
d	(311)	3	2	3	1	3	2	1	1	2	1	1				20	11
i	($\bar{3}11$)	1		1		3		1	1	1	1	1			1	11	9
δ	13.4.4 (722)(S)					1								1	1	3	3
ϕ	(411)	2	2	2		3	1			1	1			1		13	8
H	($\bar{4}11$)							1								1	1
f	(922)													1		1	1
F	(511)	2		1						1						4	3
η	(611)			1							1		1			3	3
D	(711) (15.1.1)(S)										1	1				2	2
Total forms		15	14	24	12	26	17	16	13	11	10	9	12	9	12		

47 = total for district. (S) indicates form observed by Shannon but not by the writer. *a*, *c*, *o*, *d*, *g*, *s* appear on practically all crystals, but there are 12 forms each of which appear only on one crystal, showing the highly variable character of these combinations. These odd faces are, however, in general small or unimportant, so that they do not notably affect the crystal types.

Comparison of the total number of forms from various localities shows that Randsburg, with 47 forms is second in the list, exceeded by Bräunsdorf with 70 (including doubtful forms), and followed by Zacatecas with 40, Příbram with 28, Potosi with 13, and Parenos, Mexico, with 13.

TABLE 4

Analyses

	1	2	3	4	5	6
S	21.96	21.54	19.27	21.68	21.95	21.9
Sb	41.07	41.73	42.46	41.15	39.14	40.5
Ag	36.97	36.57	36.20	36.71	36.40	33.9
Cu		0.07	0.02	—	1.06	2.6
Fe		(tr)	0.56	tr	0.62	1.0
Pb		—	0.95	—	—	0.6
As		—	—	—	—	—

(1) Theory; (2) Randsburg, F. A. Gonyer; (3) Randsburg, E. V. Shannon; (4) Příbram, R. Andreasch; (5) Bräunsdorf, H. Rose; (6) Potosi, Bolivia, L. J. Spencer.

The analysis made for the writer by Gonyer was on selected crystals, mostly of type 2. A spectroscopic analysis confirmed the chemical tests but showed a very slight trace of iron.

Acknowledgment

The writer wishes to express his appreciation to Professor Charles Palache of Harvard University for his helpful suggestions in the preparation of this paper and to Mr. F. W. Royer, manager of the Kelly-Rand mine. The chemical analysis was made possible by a grant from the Research Fund of the University of California.

RESORBED FELDSPAR IN A BASALT FLOW*

Carl Fries, Jr., *University of Wisconsin, Madison, Wisconsin*

Introduction

During a study of feldspar twins in a thick flow of basalt, an interesting occurrence of partly assimilated feldspar of the fundamental composition of andesine was noted. The distribution and physical characters of these included crystals were studied because of their relation to twin-origin. These characters will be described, and an attempt will be made to interpret their significance.

It is hoped to show that the basalt had sufficient heat to resorb the andesine, thus producing skeleton and honeycombed remnants. Before all the feldspar had been assimilated, however, temperature had dropped to the point where the normal crystallization of the basalt began. The skeletons were filled and surrounded by bytownite in crystallographic continuity. The outer borders of the newly crystallized feldspar show gradational zoning.

Description of Basalt

The basalt in which the andesine occurs is known as the Cape Spencer flow, 556 feet thick. It is the thickest of a series of five Triassic flows which form the headland of Cape d'Or, Nova Scotia, and which have been named the North Mountain basalt. The flows have been described by Powers and Lane (1916), from drill cores, to show evidence of magmatic differentiation in effusive rocks. Later work by Lund (1930), based on the same cores, gave further evidence of differentiation in the Cape Spencer flow. A brief résumé of their work is given here.

The basalt is composed of four chief constituents—feldspar, 34–59%; pyroxene, 32–48%; magnetite and glass, 2–30%. The present study indicates that quartz occurs in the central third of the flow, and becomes important near the center. Chlorite, limonite, hematite, zeolites and olivine are minor constituents. Feldspar content is highest between the 136 and 248 foot depths. Pyroxene increases from the top downward. Magnetite and glass are highest in the top 100 feet.

It has been concluded by Lund (1930, p. 562) that pyroxene has settled during cooling, and that feldspar has concentrated near the center. Some of it may have risen. During cooling there has been enrichment of soda in the liquid fraction, and the feldspar of lowest anorthite content occurs near the 248 foot depth. The highest anorthite content occurs near the base.

* This work has been supported in part by a grant from the Wisconsin Alumni Research Foundation.

Method of Study

The basalt was studied from drill core A, which Professor Lane kindly sent to the University of Wisconsin some years ago. The thin sections which were used were in some cases the same as those used by Lund, but in other cases new sections were taken at intervals corresponding to those listed in his paper. The numbers and depths of these sections are given in Table 1.

Table 1

Section no.	Depth below flow top	No. of determinations of composition
A-13	36 feet	3
A-14	61	4
A-15	86	9
A-15a	86	2
A-17	136	11
A-19a	188	7
A-20	248	29
A-22a	288	10
A-25	361	12
A-28	436	6
A-31	511	14
A-34	561	5

All determinations were made from sections mounted on a Bausch and Lomb universal stage, and were incidental to a study of twin laws. One unit of a feldspar was oriented in such position that the optic symmetry planes were in the cardinal positions—one horizontal, the second vertical and north-south, the third vertical and east-west. From this recorded position the feldspar was rotated until a twin composition face, or cleavage, was vertical and north-south. The pole of this face was plotted on a stereographic net whose three diameters represented the three vibration directions: α, β, and γ. This was then superposed on the Fedorov-Nikitin stereograms, which give composition of the feldspar and identity of the cleavage or composition face. Accuracy is believed to be $\pm 2\%$ An.

Description of Feldspar

Variation in grain size of the feldspar is considerable. Excluding phenocrysts, which become important in the lower half of the flow, size is least at the top, reaches a maximum through the third quarter, and becomes intermediate near the bottom. The phenocrysts increase in abundance from the first third downward. The groundmass feldspar is generally

tabular parallel to 010. A small percentage is elongate in the direction 001, and others are nearly equidimensional. The phenocrysts are equidimensional in small part, but they are generally elongated about $2\frac{1}{2}:1$ in the direction 010.

The feldspar of the basalt is almost exclusively plagioclase of intermediate to calcic composition. No potash feldspar was identified. Since the chemical analyses show less than 1% K_2O, the potash is probably in solid solution with the plagioclase. The normal plagioclase ranges in composition from An_{35} to An_{85}, although it is rare for any crystal to be entirely below An_{55}. Variation in a single crystal embraces the entire range. Variations within the sections are indicated in Table 2. It is believed that the higher figure is very nearly the maximum in all cases, although the lower figure is not always the minimum. The minimum composition occurs in the lower central portion of the flow. The maximum is very nearly the same in all sections, except at the top.

TABLE 2

Slide no.	Depth below flow top	Composition range	
		Normal feldspar	Cores
A-13	36 feet	58–69% An	40% An
A-14	61	59–78	30–38
A-15, A-15a	86	40–70	35–38
A-17	136	51–80	37–38
A-19a	188	56–80	
A-20	248	40–85	
A-22a	288	35–75	
A-25	361	40–85	
A-28	436	55–81	
A-31	511	60–80	
A-34	561	62–80	

As suggested above, zoning is important in all the feldspars, excluding the cores. Two types of zoning occur—an early "line zoning" (oscillatory), and a later "gradational zoning." The line zoning is due to extremely fine bands of slightly different and alternating composition. Alternating variation of composition is probably within the limit of error of the method used, $\pm 2\%$ An, although the outer layers become progressively more sodic. Line zoning is limited to feldspar above An_{70}, so that it is most noticeable in the more calcic phenocrysts. It occurs, also, only in the inner portions of these crystals. The innermost lines enclose perfectly euhedral crystals. In some cases later lines indicate

that two crystals have come together along crystal faces and have then grown as a single unit. Twin lamellae are crossed by these lines with but slight change in direction. In some cases the form changes from one twin to the next, although delineated by the same line. In other words, the twins grew as twins.

It has been indicated that line zoning is confined to the more calcic feldspar. Gradational zoning, however, occurs universally, from the tiniest visible crystal to the largest phenocryst. It is extremely marked in the larger crystals and is generally confined to the outer third or quarter of the units. Table 3 gives some examples of range of composition within single crystals. The minimum composition is not always known because of difficulty in orienting narrow units.

TABLE 3

Specimen no.	Range in composition	Specimen no.	Range in composition
A-14 (26)	78–59% An	A-22a (35)	61–35% An
A-15a (54)	70–40	A-25 (5)	60–40
A-17 (50)	80–56	A-25 (42)	83–52
A-19a (1)	70–56		

CORED FELDSPAR

It has been necessary to describe the feldspar in some detail in order to develop a background for description and interpretation of the partly assimilated andesine, which is the main thesis of this paper. The andesine occurs in sections of the upper 175 feet of the flow. It decreases in abundance from the top downward. In sections A-13 and A-14 the larger part of the feldspar contains some of the included material, while in section A-17 only a few of the larger phenocrysts have small core remnants.

The old feldspar is irregular in outline and is abundantly dotted with elongate cavities filled with bytownite or magnetite. Plate I illustrates two typical specimens from section A-14. If the bytownite were destroyed the core would consist of a ragged-edged, honeycombed structure with little semblance of feldspar form. The trend of destruction of the andesine is sometimes well defined and may be in the planes 010, 001, 100 or a brachydone. Apparently, unless fractures were present, the direction of easiest solution or replacement was in the planes of the chief crystallographic forms assumed by feldspar.

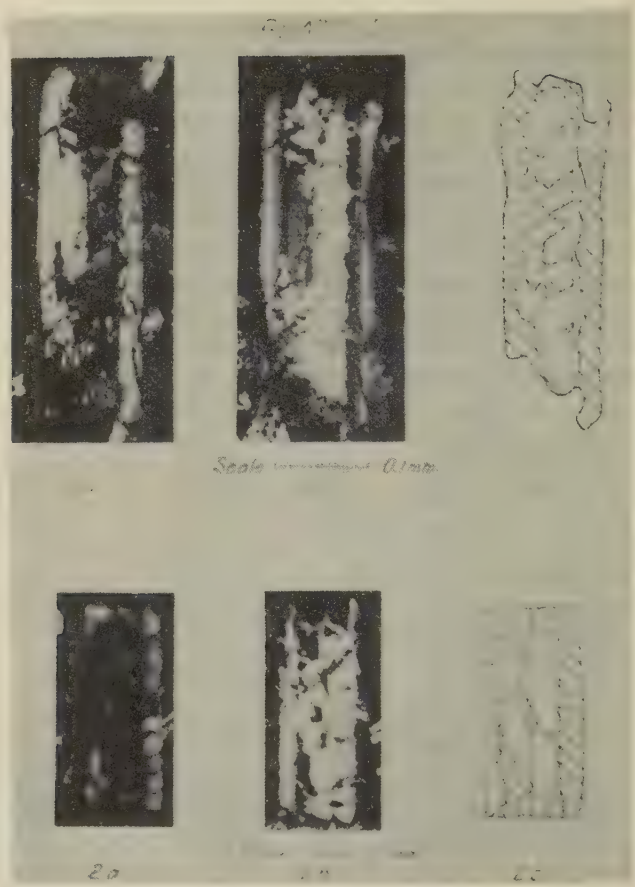

1. Specimen A-14 (26), under crossed nicols. 1*a* shows calcic border lighted. 1*b* shows andesine core lighted. Both line and gradational zoning can be seen in outer feldspar. 1*c* is a diagram which illustrates the ragged, honeycombed structure of the core (unruled), position of twin lamellae, and calcic border feldspar (ruled).

2. Specimen A-14 (42), under crossed nicols. Figures correspond to those of No 1.

The composition of the cores varies within a narrow range, about An_{30-40}, and the majority of this feldspar is An_{35-38} (Table 2). Excluding the newly crystallized borders, no zoning is present. The cavities in the andesine are filled with feldspar of high anorthite content, indicating that they were filled at the time the phenocrysts were being formed. Where the cores are small, the new feldspar exhibits line zoning in the interior, which gives way to gradational zoning in the borders. If the core is excluded, zoning and composition variation in the new feldspar is

exactly comparable to the phenocrysts which occur throughout the flow. Evidence indicates that growth tended to produce euhedral form. The cavities and irregularities were filled in first. Later the crystals were enlarged in the regular manner.

The twins of the andesine are not markedly different from those of the feldspar of the basalt. There is a tendency, however, for the units to be broader and less numerous. Specimen A-14 (26) (Plate I-1) is composed of three Carlsbad units. Two narrow albite units are on either side of the central Carlsbad. These are in albite relation to the central unit. As indicated by the diagram accompanying the photograph, the new feldspar has crystallized in continuity with the twin structure of the older andesine. Specimen A-14 (42) (Plate I-2) shows only albite lamellae. Here, also, the new feldspar preserves the twin fabric of the old.

Composition of specimen A-14 (26) is An_{30} for the core, while the new material drops from An_{78} near the center to An_{59} near the border. In specimen A-14 (42) the core is An_{38} and the outer part An_{62}. As in other determinations, the lowest value of the border cannot always be determined by the method used. The photograph of specimen A-14 (26) illustrates both line and gradational zoning in the outer feldspar. Composition data of other crystals are given in Table 4.

TABLE 4

Specimen no.	Composition range	
	Core	Exterior
A-13 (3)	40% An	58% An
A-14 (32)	35	63
A-15 (9)	36	60
A-15 (10)	38	60
A-15 (11)	35	64
A-15a (54)	38	70–40
A-17 (49)	38	71–58
A-17 (50)	37	80–56

DISCUSSION OF FELDSPAR HISTORY

The Ab:An ratio of the basaltic magma was probably between Ab_{40}-An_{60} and $Ab_{35}An_{65}$, as suggested by the composition range of the feldspar of the quickly cooled upper surface of the flow, section A-13. This is in agreement with Bowen's (1928, p. 141) statement that "the most calcic composition of the total plagioclase of a uniformly fine-grained or aphanitic, basaltic rock appears to be about Ab_1An_2."

Evidence has been given to indicate that feldspar crystallization has occurred through a considerable time range. The first feldspar which crystallized from the basaltic magma has the composition An_{80-85}. This separated while much of the basalt was yet liquid, as shown by perfect euhedral form of the central zones of the phenocrysts. The line zoning, due to slight alternation of composition, suggests that these crystals formed while there was considerable movement of the basalt, or probably before the flow came to final rest. Thus, possibly slightly varying temperatures may have been experienced during their early growth. The early formed, high anorthite crystals showed a slight tendency to settle, which is expressed by their increasing abundance in the lower portions of the flow.

As cooling continued, the remaining liquid became progressively enriched in soda. The outer borders of all the feldspars were formed from this more salic material. The feldspar of lowest anorthite content occurs on the borders of those crystals just below the center of the flow, together with interstitial quartz (refer to Table 1). This suggests that the final liquid phase was last present there. Solidification progressed inward from the top and the bottom. Temperatures were slightly higher in the lower central portion of the flow during the later stages of cooling. Differentiation in the plagioclase series is, thus, well exhibited.

It has been indicated that the andesine cores of the feldspars in the upper portion of the basalt were present as crystals before the phenocrysts began to form, since they are filled and surrounded by the high calcic feldspar which first crystallized from the basaltic liquid. Furthermore, they were partly destroyed by resorbtion before any feldspar had crystallized from the magma, as indicated by their honeycomb structure. It is possible that there may have been some direct replacement in the solid phase, but inasmuch as line zoning occurs in the newer feldspar of these assimilated units, it would seem that the cavities existed, as such, at some time. This is in agreement with principles discussed by Bowen (1928, pp. 199–201), wherein he states that, "inclusions can become part of the liquid only when they have a composition toward which the composition of the liquid can vary by spontaneous differentiation." The quantity of included material is small, and it is probable that its effect on the gross composition of the basalt was not great.

The structure and twin fabric of the cores have apparently been followed and rebuilt by the later feldspar. It is possible that the cores were recrystallized during and after the addition of the feldspar from the basalt. In this case, they may have assumed the twin pattern of the border. In view of the slightly different twin pattern of the cored crystals

to that of the normal feldspar of the basalt, it is believed that the former is the more plausible explanation. It is believed that the addition of calcic feldspar in and around the core protected it from further attack by the magma. There was probably not enough heat to form a melt after the bytownite had begun to crystallize.

The source of the andesine is unknown. There is no normal feldspar of the basalt which has the composition or character of the andesine. Feldspar of this composition occurs only in the outer zones of crystals well within the flow and of later origin. The fact that it was already present in crystal form when the calcic phenocrysts of the basalt first began to crystallize suggests that it was picked up by stoping before or during extrusion of the magma. Apparently the process of resorbtion was a slow one. The interval of time between acquisition of the andesine and initiation of crystallization of the feldspar normal to the basalt must have been a short one. In other words, there could not have been much excess of heat when the andesine was included.

The partly resorbed feldspar occurs within the upper 175 feet of the flow and increases in abundance upward. Both the proportion of cored to uncored, and of core to total of each unit increase toward the top. It is believed that evidence is sufficient to conclude that these crystals rose while the basalt was yet largely fluid. With the exception of this cored feldspar, and possibly some of the early large phenocrysts, it is believed there was little tendency for the feldspar crystals to migrate either upward or downward.

Summary

The feldspar of a thick, normal basalt has been described, as a background for description and discussion of partly resorbed andesine which occurs in the upper portion of the flow. The following conclusions have been reached.

(1) A basaltic magma has picked up andesine, source unknown, which has the composition An_{30-40}. The magma has partly resorbed the included feldspar—some was probably entirely resorbed—and has furnished the more calcic material which fills and surrounds the ragged and honeycombed structures in crystallographic continuity.

(2) Early crystallized plagioclase, An_{70-80}, shows line zoning, due to slight oscillation in composition. This is surrounded by gradationally zoned material which drops to as low as An_{35} near the center of the flow. Thus, differentiation in the plagioclase series is well exhibited. The normative feldspar probably lies in the range An_{60-65}.

(3) Early formed phenocrysts are largely bytownite and have shown

a tendency to settle toward the bottom. Cored feldspar which occurs within the top 175 feet of the flow shows definite evidence of having risen. There was probably little or no differential movement of the remaining feldspar.

Acknowledgments

This work was an outgrowth of a study of feldspar twins in a basalt, which was supported by funds from the Wisconsin Alumni Research Foundation and the Graduate School of the University of Wisconsin, to which thanks are due. The writer is indebted to Dr. R. C. Emmons for suggesting the problem and for helpful criticism.

References

Bowen, N. L., *Evolution of the Igneous Rocks*, Princeton University Press, **1928.**

Lund, R. J., Differentiation in the Cape Spencer flow: *Am. Mineral.*, **15,** 539–565 (1930).

Powers, S., and Lane, A. C., Magmatic differentiation in effusive rocks: *Trans. A.I.M.E.*, **54,** 442-457 (1916).

GRANITE PEGMATITES OF THE MT. ANTERO REGION, COLORADO

GEORGE SWITZER, *Harvard University, Cambridge, Mass.*

ABSTRACT

A granite stock in the region of Mt. Antero, Chaffee County, Colorado, contains numerous, small, closely associated beryllium-rich pegmatites and veins. The pegmatites have the typical magmatic minerals microcline and quartz, and a variety of later hydrothermal minerals—beryl, phenakite, albite, bertrandite and fluorite. The veins are shown to be equivalent to the hydrothermal phase of the pegmatites. The upper temperature limit of formation of the pegmatites is approximately 600°C., as shown by frequent development of trigonal trapezohedron faces on smoky quartz crystals. The lower temperature limit of crystallization of the vein minerals is less than 200°C., as indicated by the position of adularia in the sequence of mineralization.

A new angle table has been calculated for bertrandite. Twinned octahedra of fluorite are described. The relation between the structure and morphology of phenakite is pointed out, and the crystallographic elements of phenakite recalculated in a new, preferred setting.

INTRODUCTION

The region of Mt. Antero, Colorado has been known for many years as a locality for fine crystallized specimens of beryl (aquamarine), phenakite and bertrandite. Descriptive notes on these minerals have been published by Cross (1887), Smith (1887), Penfield (1887, 1888, 1890), Penfield and Sperry (1888), Over (1928, 1935), Pough (1935, 1936), and Montgomery (1938). However, no detailed study has been made of the occurrence of these minerals. For this purpose the writer spent six weeks during the summer of 1938 in the Mt. Antero region, in company with Mr. Arthur Montgomery of New York City, and Mr. Edwin Over of Colorado Springs, Colorado.

The writer wishes to acknowledge his indebtedness to Professor Charles Palache, who suggested this study and made it possible by a grant for field expenses from the Holden Fund of the Department of Mineralogy of Harvard University. The coöperation of Messrs. Montgomery and Over, who spent their 1938 collecting season in the Mt. Antero region, was greatly appreciated.

LOCATION AND GENERAL GEOLOGY

The pegmatites and veins of the Mt. Antero region are almost entirely confined to a granite stock which is roughly elliptical in outline and approximately three miles across. The summits of Mt. Antero (14,245 ft.) and White Mountain (13,900 ft.) lie within the stock. These two mountain peaks are near the southern end of the Sawatch Range of the Southern Rocky Mountains, and are about 15 miles northwest of Salida, Chaffee County, Colorado.

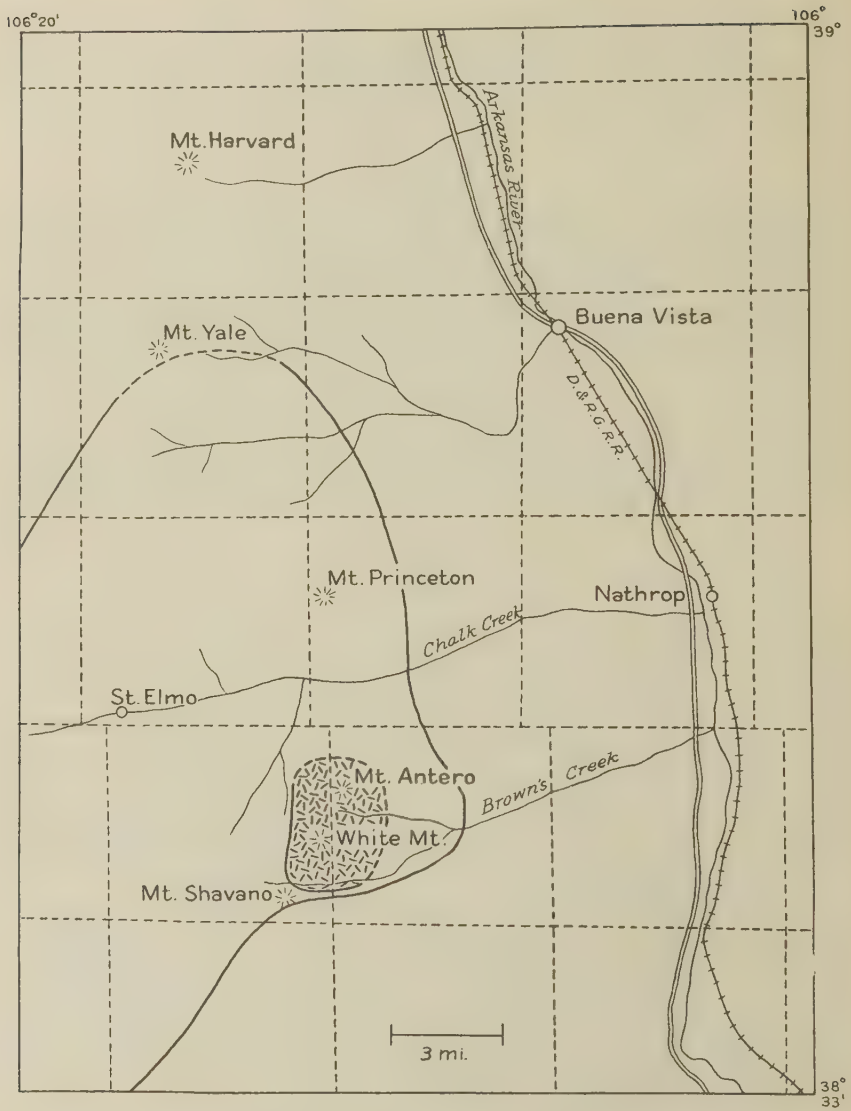

FIG. 1. Map showing location and geologic setting of Mt. Antero, Colorado.

The granite stock is part of a much larger batholith of quartz monzonite, called by Crawford (1924) the Princeton batholith, and dated by him as being late Mesozoic or Tertiary in age. On the map, Fig. 1, the boundary of the Princeton batholith is shown as given by Crawford, and the smaller hatched area represents the granite stock in which the pegmatites and veins are found.

The quartz monzonite is typically rather dark in color, of medium to coarse grain, and composed of subhedral andesine and green hornblende, anhedral orthoclase, quartz and biotite. The minor accessories are sphene, apatite and iron oxides. The granite is medium grained, and composed of subhedral oligoclase, anhedral orthoclase and quartz. The mafic minerals, green hornblende and biotite, are present in only small amount. Numerous fine-grained aplite dikes cut the granite and quartz monzonite.

The minerals that have been described from Mt. Antero are found both in pegmatites and veins. All of the pegmatites seen were within the granite stock. The veins are in both granite and quartz monzonite.

PEGMATITES AND VEINS

The pegmatites are uniformly small in size, seldom exceeding 3 feet in width and extending laterally for only a few feet. Clean-cut exposures are few because of extreme frost action. All of the pegmatites and veins are found well above the timber line, in an area entirely covered with a mantle several feet deep of disintegrated rock. However, several outcroppings in vertical cliffs showed the pegmatites to be isolated lenticular bodies having sharp contacts with the granite enclosing them. Complete excavation of these pegmatites revealed that they are roughly disk-shaped or cylindrical bodies of limited extent in all directions.

FIG. 2. Typical pegmatite exposure, in deeply disintegrated granite.

About 15 pegmatites and veins were studied in detail. The distinction between pegmatite and vein is made chiefly on the basis of mineralogy, the differences in mineralogy being taken as a direct connotation of the physico-chemical conditions of deposition. On the same basis the pegmatites and veins have been further subdivided. This subdivision is done not only to facilitate description, but to point out that, although all of the pegmatites and veins arose from a common source, there are significant differences in their paragenesis, which will be discussed in a later section of the paper.

The pegmatites and veins have been divided into the following types:

A. Pegmatites
   1. Beryl pegmatites
      (a) Beryl-smoky quartz
   2. Phenakite pegmatites
      (a) Phenakite-colorless quartz
      (b) Phenakite-smoky quartz
   3. Beryl-phenakite-bertrandite pegmatites
      (a) Beryl-phenakite-bertrandite
      (b) Beryl-phenakite-bertrandite-fluorite
   4. Topaz pegmatites

B. Veins
   1. Muscovite-quartz vein
   2. Phenakite-quartz-fluorite vein
   3. Beryl-quartz-molybdenite vein

Beryl Pegmatites

Pegmatites characterized by beryl are the most abundant of the complex pegmatites of the region. The beryl pegmatites are of two types, those that have "pockets" and those that do not. The pegmatites having no pockets are small dikes or lenses of common pegmatite, with some subhedral beryl, but with no open-space deposition. The pegmatites containing pockets have been further complicated by successive deposition of fine euhedral crystals of microcline, beryl, smoky quartz, albite and fluorite on the walls of the pockets.

Beryl-smoky quartz pegmatites. Several pegmatites of this type which had pockets containing a variety of well crystallized minerals were found. One of the best exposed of these pegmatites was found by Over, near the summit of White Mountain. It out-cropped on a vertical cliff, and, therefore, was one of the least weathered of all the pegmatites seen. The pegmatite was a lens-shaped body approximately 12 inches across and had a roughly cylindrical central cavity extending back about 4 feet into the cliff. The pocket minerals were attached to the walls of the central opening and projected into it. The open space was partially filled

with "pocket dirt," most of which was formed by surface weathering. The periphery of the pegmatite was graphic granite several centimeters thick, to which was attached the pocket minerals.

Fine crystals of perthitic microcline ranging up to 10 cm. in length were found both as single individuals and as *Carlsbad* and *Baveno* twins. Beryl started to crystallize at the close of the microcline deposition. The beryl crystallized in fine green to deep blue transparent crystals up to 7 cm. in length. Smoky quartz followed beryl, and formed sharp crystals up to 10 cm. in length and of deep smoky color. The smoky quartz formed as low-quartz, as shown by frequent development of faces of a trigonal trapezohedron. Muscovite followed quartz and in part was deposited contemporaneously with it. Albite closely followed muscovite and can be seen replacing muscovite. However, some of the muscovite is definitely later than the albite. It is not known whether this represents continuous deposition of muscovite, or two separate generations. Albite in some cases formed complete replacement pseudomorphs of microcline; in others it only partially replaced it, or formed shells about the microcline crystals. Most of the microcline was then removed by solution, leaving hollow shells of albite. Abundant sericite was formed by the alteration of microcline. Fluorite, colorless quartz and limonite were present in small amount. A tabular summary of the paragenesis of this pegmatite is given in Table 1, column 1.

Phenakite Pegmatites

Next in abundance to pegmatites characterized by the presence of beryl are those which have only phenakite as a beryllium mineral, and show no evidence of beryl having been present. All of the pegmatites of this type contain pockets, but the complexity of the pocket-mineralization is greater where smoky quartz is present. Here, as in the beryl pegmatites just described, the presence of a cavity containing smoky quartz seems to indicate a center of more prolonged mineralization, with gradually decreasing temperature.

Phenakite-colorless quartz pegmatite. The simplest of the phenakite pegmatites are in a pegmatitic area exposed on a cliff on the southeast side of Mt. Antero. The pegmatites are highly siliceous, being composed dominantly of milky quartz, with some subhedral microcline. The phenakite is found in small pockets lined with crystals of colorless or light smoky quartz ranging up to several centimeters in length. The phenakite crystals are both single and twinned and have a maximum length of about 5 mm. They are found either loose in the pockets or partially embedded in quartz. The only other mineral present is a small amount of muscovite.

Phenakite-smoky quartz pegmatite. In the same pegmatitic area just described one smoky quartz pocket was found by Over. The pocket was approximately 18 inches across and 4 feet deep, and was lined with large crystals of microcline and smoky quartz.

Euhedral crystals of microcline with a maximum dimension of 22 cm. show an etched peripheral zone about 2 cm. wide formed by the solution of the albite lamellae of the perthite. Muscovite was not abundant and in part overlapped with microcline in its deposition. Smoky quartz was very abundant and formed crystals ranging up to 30 cm. in length. Some of the crystals are greatly distorted by flattening parallel to a prism face, and many smaller ones are completely doubly terminated and show no place of attachment to the walls of the pocket. Phenakite crystals ranging up to 1 cm. across were very abundant. The phenakite is fixed in the sequence of mineralization by the fact that the crystals are commonly emplanted on, but not embedded in, smoky quartz. Both single and twin crystals were present, but the single crystals were more abundant. A late-stage introduction of albite followed quartz and phenakite, but the amount of albite introduced, mainly by replacement of microcline, was small. Fluorite was present in good octahedral crystals ranging up to 5 cm. in size. Colorless quartz formed as either small individual crystals or as "caps" on some of the smoky quartz crystals. A tabular summary of the paragenesis of this pegmatite is given in Table 1, column 2.

Beryl-Phenakite-Bertrandite Pegmatites

Two of the pegmatites examined contained all three of the beryllium minerals—beryl, phenakite and bertrandite. These two pegmatites varied considerably in their paragenesis and will be described separately.

Beryl-phenakite-bertrandite pegmatite. This pegmatite is located on the south slope of Mt. Antero. It has been almost entirely excavated by previous collectors, but abundant material on the dump, and information furnished by Over, who collected some fine bertrandite specimens there on previous trips, made it possible to build up a fairly complete picture. The original pegmatite was apparently comparatively large, with occasional small pockets several centimeters across.

The pocket minerals of this pegmatite were crystallized on a smaller scale than in most of the other pegmatites seen. The smoky quartz crystals were sharp and well formed but with a maximum length of 3 cm. Beryl formed well-terminated bluish-green crystals up to 3 cm. in length. Crusts of phenakite formed on unetched beryl crystals. Fluorite was present in small colorless and purple octahedra. Bertrandite in both single and twinned crystals up to 1 cm. in length formed as a late-stage alteration of beryl, as shown by its association with deeply etched beryl

crystals, or in cavities left by the complete removal of beryl by etching. A tabular summary of the paragenesis of this pegmatite is given in Table 1, column 3.

Beryl-phenakite-bertrandite-fluorite pegmatite. The second pegmatite of this type was found by Montgomery on the northwest face of Mt. Antero. It was completely disintegrated and may not have been in place as seen in the field. It consisted of a cavity about one foot across completely filled with debris, in which the various minerals were buried. None of the material was attached to the walls of the cavity.

Microcline was present only in small amount, and was clearly the first formed mineral. It has been deeply etched, with the removal of the perthite lamellae, and later partially replaced by albite. Beryl is not now present in the pegmatite, but its existence at one time is indicated by numerous hexagonal-shaped casts of phenakite. Muscovite in part forms the casts and, therefore, followed beryl in its crystallization. After the removal of the beryl, the phenakite casts were often partially refilled by more phenakite. This later phenakite may have formed directly from the beryl as it was removed by solution. As a general rule, long prismatic twin crystals of phenakite formed later than did the more abundant short prismatic single and twinned crystals. Albite was introduced in small amount toward the close of the period of deposition of phenakite. Fluorite was quite abundant in sharp, well-formed octahedra, and in multiple disk-shaped twins, greatly flattened parallel to an octahedron face. Bertrandite formed in small amount very late in the hydrothermal stage. Quartz is almost entirely lacking. Only two small colorless quartz crystals were found, and their exact place in the sequence of mineralization is not known. A tabular summary of the paragenesis of this pegmatite is given in Table 1, column 4.

Topaz Pegmatites

Topaz was found in only one pegmatite, on the south side of Mt. Antero. The pegmatite was completely disintegrated and consisted of a mass of fragments in the broken rock. Fragments of graphic granite composed of white microcline and smoky quartz indicated that the walls of the pegmatite were made up of this material. Numerous loose crystals were found of microcline and smoky quartz. There was a small amount of muscovite and fluorite. The topaz was brown in color and consisted of deeply etched crystal fragments. The original crystals must have been several centimeters in length.

Vein Deposits

Three veins were examined in the Mt. Antero region. Two of these are

in the granite stock and closely associated with pegmatites. The third vein is in the quartz monzonite, about one half mile from the granite contact.

Muscovite-quartz vein. This vein was found by Montgomery on the northwest slope of Mt. Antero. It was a narrow, irregular vein with highly altered granite wall-rock on which had crystallized abundant deep green muscovite in clusters of small crystals, and deep smoky quartz in crystals ranging up to 20 cm. in length. Immediately following the smoky quartz, but sharply separated from it, was colorless quartz, which formed either as a capping layer on the smoky quartz or as small druses. Phenakite started to crystallize at this time and in part overlapped with the colorless quartz, as is shown by specimens of phenakite crystals partially or wholly embedded in the colorless quartz which caps the smoky quartz crystals. A small amount of albite was deposited at about this time and is the only feldspar present in the vein.

As is shown in Table 1, column 5, phenakite crystallized over a wide range, contemporaneous with quartz, and with colorless and deep purple fluorite. The colorless fluorite built octahedra as large as 10 cm. on an edge. There was then a halt in the crystallization of fluorite, but phenakite continued to form as a surface coating on the colorless fluorite crystals. Purple fluorite was then deposited by building on the colorless fluorite octahedra, and outlasting the period of deposition of phenakite. A pale green coating of fluorite then formed on some of the larger fluorite crystals. Some of the smoky quartz and fluorite crystals are dusted with a drusy coating of purple fluorite, which in this case is cubo-octahedral in habit. Limonite was very abundant, and a small amount of residual pyrite served to demonstrate its origin. When the limonite formed from pyrite it was deposited primarily as a replacement pseudomorph of fluorite. A small amount of native sulphur was also formed. The exact position of the pyrite and limonite in the sequence of mineralization is not known. A tabular summary of the paragenesis of this vein is given in Table 1, column 5.

Phenakite-quartz-fluorite vein. On the northwest slope of Mt. Antero a vertical vein about 4 feet wide is exposed over a length of 20 feet. It is composed dominantly of milky quartz but contains numerous pockets that range in size up to 14 inches across, lined with colorless or light smoky quartz crystals.

Phenakite was very abundant, and in part overlapped with quartz in its deposition, as shown by phenakite crystals partially embedded in the quartz that lines the pockets of the vein. Muscovite was present in minor amount, and was followed by orthoclase, variety adularia. Albite was

TABLE I. PARAGENESIS OF MT. ANTERO PEGMATITES AND VEINS

	1 BERYL-SMOKY QUARTZ PEGMATITE	2 PHENAKITE-SMOKY QUARTZ PEGMATITE	3 BERYL-PHENAKITE-BERTRANDITE PEGMATITE	4 BERYL-PHENAKITE-BERTRANDITE FLUORITE PEGMATITE	5 MUSCOVITE-QUARTZ VEIN	6 PHENAKITE-QUARTZ FLUORITE VEIN
MICROCLINE	——	——	——	——		
BERYL	——		——	——		
QUARTZ[1]	——	——	——		—	——
MUSCOVITE	——------—	—	------	—	——	—
PHENAKITE		——	——	—------	——	——
ORTHOCLASE						—
ALBITE	——	------ ---	—	—	---	—
FLUORITE	—	—	——	—	—— ——	——
BERTRANDITE			---	—		
QUARTZ[2]		—		—	—	
CALCITE	—					
SERICITE	---					
LIMONITE	--		---		-----	

1 SMOKY QUARTZ
2. COLORLESS QUARTZ
--- MINERAL PRESENT BUT POSITION DOUBTFUL

next introduced, principally as a pseudomorph of the adularia crystals. Fluorite was very abundant, sometimes completely filling the pockets. It formed in sharp octahedra up to 10 cm. across. Phenakite is shown to have persisted over a long range in its crystallization by the fact that it is found partially embedded in fluorite.

Beryl-quartz-molybdenite vein. This deposit has already been described by Landes (1934). It is only mentioned here to complete the picture of the apparent gradation in the Mt. Antero region from pegmatite to vein. The beryl-quartz-molybdenite vein is not found within the granite stock to which all previously described localities were confined. It is in the surrounding quartz monzonite, about one half mile from the granite contact. The presence of beryl in the vein indicates that the mineralizing solutions arose from the granite stock in which so many beryllium-rich pegmatites are found, and that it can, therefore, be considered as an outlying part of the same general zone of mineralization.

SUMMARY AND CONCLUSIONS

With the exception of the *beryl-quartz-molybdenite vein*, the pegmatites and veins of the Mt. Antero region are all found entirely within a single small granite stock, and presumably, therefore, arose from a common source. The paragenetic table (Table 1) of the various deposits described brings out the broad similarity between them, and also several significant differences. These differences are an expression of the physicochemical conditions obtaining during the formation of any particular pegmatite or vein. The most important factors that may have governed the paragenesis of the pegmatites and veins are: (1) chemistry, (2) pressure, (3) temperature and rate of change of temperature, (4) wall-rock control.

The paragenetic table shows all of the pegmatites and veins to be similar chemically in that they contain essentially the same elements, as might be expected since they arose from a common source. However, the relative proportions of the elements vary widely in different occurrences. It is probable that the most important influence of variation in chemistry of the primary solutions has been to control the amounts of the various minerals present.

Speculation about pressure effect upon the paragenesis of the pegmatites and veins is difficult. All of the bodies are found within a horizon 500 feet thick, and the difference in pressure due to load was not, therefore, very large. More important than this, however, would be the variation in hydrostatic pressure of the solutions, which might be governed by the size of the channelways through which the solutions moved. However, since the direct effect of reduced pressure would be to lower the

temperature of the solutions, these two factors may be considered to be interdependent.

The granite in which the pegmatites and veins are found is very uniform throughout, and the possibility of wall-rock control is slight.

The major dissimilarity in paragenesis is between the two groups which have been described as *pegmatites* and *veins*. Included in the pegmatite group are all those dikes or lenses of coarsely crystalline microcline and quartz, either together as graphic granite or as individual crystals; that is, those bodies whose early phase at least, was probably magmatic. Included in the vein group are three dikes that are vein-like in shape, and are composed chiefly of typical milkvein-quartz, with graphic granite and microcline entirely lacking. There can be little doubt that the fundamental differences between pegmatites and veins were caused by temperature of formation. This is brought out clearly in Table 1, assuming that from top to bottom in the table is a direction of decreasing temperature. In the true pegmatites (columns 1–4) microcline and beryl were the first minerals to form, and were, therefore, formed at the highest temperature and probably crystallized from a medium close in its properties to a true magma. Following the crystallization of microcline and beryl in the pegmatites came the typical hydrothermal introduction of lower temperature minerals. The veins in their entirety are essentially equivalent to the hydrothermal phase of the pegmatites.

The *muscovite-quartz vein* has highly silicified and altered granite wall rock, and its general nature gives the impression that it was created by the early hydrothermal solutions of a typical pegmatite which escaped from the pegmatite magma chamber into a crack or fissure in the granite. The close association of this vein with several true pegmatites supports this idea. The *phenakite-quartz-fluorite vein* has unaltered, sharp contacts with the granite wall rock and, therefore, appears to have formed at a still lower temperature than the *muscovite-quartz vein*. For the same reason the *beryl-quartz-molybdenite vein* apparently formed at a relatively low temperature.

Apparently all the pegmatites started to crystallize at about the same temperature. The paragenesis of the individual pegmatites is broadly similar. The lack of certain minerals in some which are present in others, and the differing amounts of the various minerals, can be attributed to slight compositional differences in the solutions which introduced the hydrothermal minerals, and to a varying rate of change of temperature. The paragenetic table (Table 1) shows phenakite to be stable at a lower temperature than beryl, and quick cooling past the stability range for beryl might prevent its crystallization, resulting in the formation of phenakite at a lower temperature.

Temperature of formation. Any precise statement as to the temperature of formation of a pegmatite is of doubtful value. However, for at least some of the pegmatites of the Mt. Antero region (the *beryl-smoky quartz* type), it is known that the smoky quartz formed as low-quartz, and thus crystallized at some temperature below 573°C.[1] Since smoky quartz was the third mineral to start to crystallize it seems probable that the upper temperature limit of the pegmatites could not have been much greater than 600°C. It has been established by various investigators that the temperature of formation of adularia is about 230°C. On this basis the lower temperature of formation of the *phenakite-quartz-fluorite vein* will be some figure below this value, perhaps as low as 100°C.

DESCRIPTION OF THE MINERALS

The common pegmatite minerals microcline, muscovite, quartz and albite of the pegmatites of the Mt. Antero region have no features requiring a detailed description. A description will be given, however, of the less common minerals bertrandite, beryl, fluorite and phenakite.

Bertrandite

Bertrandite was first described from Mt. Antero by Penfield in 1889. The material collected by the writer can add nothing to Penfield's description. However, a structural study of bertrandite by Ito and West (1932) has shown that the unit chosen by Penfield does not correspond to the true unit as revealed by x-ray study. The change necessary for correspondence is a minor one, and consists only of halving the c-axis of the Penfield setting. The transformation is given by $100/010/00\frac{1}{2}$.

The unit cell dimensions of Ito and West are $a_0 = 15.19$Å, $b_0 = 8.67$Å, $c_0 = 4.53$Å. From this the axial ratio $a_0 : b_0 : c_0 = 0.571 : 1 : 0.298$ is obtained. (To obtain this conventional form for the axial ratio the a_0 and b_0 lengths of Ito and West must be interchanged.) This is in good agreement with the axial ratio obtained by halving c of Penfield's original values.

A new angle table has been calculated for all known forms on bertrandite, using the elements required by the structural study of Ito and West. It is evident that the change made in morphology requires no revision of previous statements of physical and optical properties.

Bertrandite from Mt. Antero is found in platy crystals tabular parallel to $c\{001\}$ and usually elongated parallel to the a-axis. The crystals are white or colorless and transparent, and range in size up to 1 cm. in length. Their hemisymmetric character is indicated by the fact that one basal plane is commonly flat, while the other is rounded and striated

[1] The exact value of this inversion is, of course, unknown, since the pressure at the time of formation is not known.

TABLE 2. BERTRANDITE—$Be_4Si_2O_7(OH)_2$

Orthorhombic: pyramidal—*m m* 2

$a:b:c=0.5688:1:0.2987$; $p_0:q_0:r_0=0.5251:0.2987:1$

$q_1:r_1:p_1=0.5688:1.9044:1$; $r_2:p_2:q_2=3.3478:1.7581:1$

Forms		ϕ	$\rho=C$	ϕ_1	$\rho_1=A$	ϕ_2	$\rho_2=B$
c	001	—	0°00′	0°00′	90°00′	90°00′	90°00′
b	010	0°00′	90 00	90 00	90 00	—	0 00
a	100	90 00	90 00	—	0 00	0 00	90 00
f	130	30 22	90 00	90 00	59 38	0 00	30 22
m	110	60 22	90 00	90 00	29 38	0 00	60 22
g	320	69 14	90 00	90 00	20 46	0 00	69 14
h	310	79 16	90 00	90 00	10 44	0 00	79 16
i	089	0 00	14 52	14 52	90 00	90 00	75 08
ϵ	021	0 00	30 51½	30 51½	90 00	90 00	59 08½
η	041	0 00	50 04½	50 04½	90 00	90 00	39 55½
e	061	0 00	60 50½	60 50½	90 00	90 00	29 09½
k	102	90 00	14 42½	0 00	75 17½	75 17½	90 00
d	101	90 00	27 42	0 00	62 18	62 18	90 00
l	302	90 00	38 13½	0 00	51 46½	51 46½	90 00
$\bar{x}$	16$\bar{1}$	16 20	118 10	60 50½	75 39	62 18	32 13

Doubtful:

o 265

308

parallel to the *a*-axis by the oscillatory combination of the basal plane with a dome, probably $\epsilon\{021\}$. Twin crystals are relatively common. The twin plane is (021). The twins are heart-shaped in cross section, with the smooth basal plane on the outside. The appearance of single and twinned crystals of bertrandite from Mt. Antero is illustrated by Figs. 3 and 4.

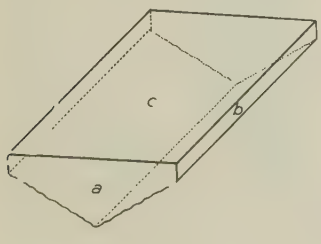

3

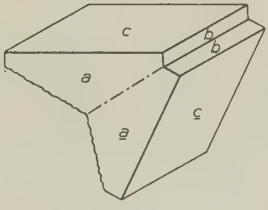

4

FIG. 3. Bertrandite from Mt. Antero, Colorado.

FIG. 4. Bertrandite, twin crystal. Twin plane (021). Mt. Antero, Colorado.

Beryl

Beryl, variety aquamarine, is the principal mineral for which Mt. Antero has long been known. Only the beryl which has grown freely in open pockets of the pegmatites is transparent and flawless, and, therefore, of value as gem aquamarine. Unfortunately much of the beryl is found frozen into the pegmatite and is then always translucent and worthless.

The color of the beryl from the Mt. Antero region varies from pale greenish blue to fairly deep aquamarine. The largest crystals ever found in this region were found by Over in 1932, on White Mountain. The contents of this pocket are now in the Mineralogical Museum of Harvard University. The largest crystal is 3.5×20 cm., gemmy in part. Several others almost as large were also taken from this pocket, and many more of smaller size.

Some pegmatites contain beryl crystals that are totally unetched. In others the degree of etching may vary to the extreme case in which the crystals have been reduced to a mass of fibres of beryl, or have been completely redissolved.

Commonly the beryl crystals are terminated only by a basal plane. The terminal forms $p\{10\bar{1}1\}$ and $s\{11\bar{2}1\}$ were also observed on numerous crystals. Sometimes the prism zone is sharp and other times deeply striated parallel to the length of the crystals. Figure 5 illustrates part of the beryl crystals found in the *beryl-smoky quartz pegmatite*.

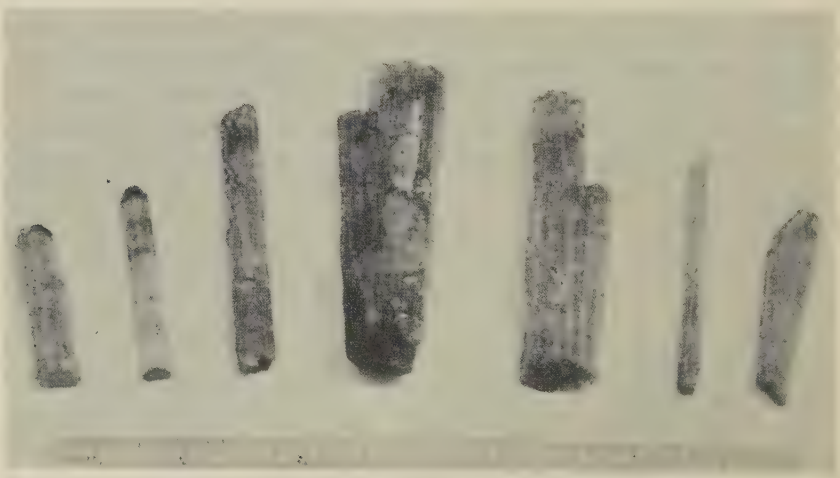

Fig. 5. Beryl from White Mountain, Colorado.

Fluorite

The fluorite of the pegmatites and veins of the Mt. Antero region is always octahedral in habit. Octahedra of fluorite were found ranging in size from 1 mm. to 20 cm. Deep purple is the most common color but small colorless crystals were also found, and occasionally light green fluorite formed as a thin coating on earlier formed crystals.

Fluorite crystals were found in the *beryl-phenakite-bertrandite* pegmatite which are twinned on an octahedron face, and show dominantly the octahedron form, with occasional small truncating faces of the dodecahedron. About 15 twin crystals were found in this pegmatite. Most of these are much flattened parallel to an octahedron face, and with one individual of the twin developed to a much greater degree than the other, as shown in Fig. 6. Others are disk-shaped and made up of several individuals.

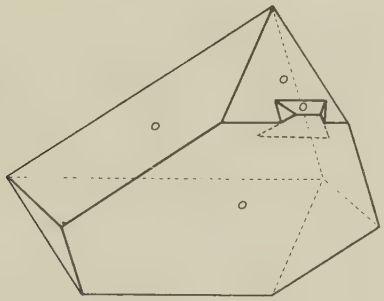

Fig. 6. Fluorite twin from Mt. Antero, Colorado.

Two fluorite twins were found in the *muscovite-quartz vein*. These twins are typical "spinel" twins, made up of two equally developed octahedra, twinned on an octahedron face. The best formed of these two twins is about 5 cm. across and deep purple in color, with a surface coating of pale green color.

Also found in the *muscovite-quartz vein* were drusy coatings of minute purple fluorite crystals upon smoky quartz and fluorite. These drusy coatings are cubo-octahedral in habit, with the cube and octahedron faces nearly equally developed. Since the drusy crystals were clearly the last formed fluorite of the vein, and, therefore, formed at the lowest temperature, it seems probable that temperature was the dominant factor in controlling the habit of the fluorite, and that octahedral habit is favored by high temperature. What the temperature of crystallization of the cubo-octahedral crystals was is not known. However, the association of octahedral fluorite with adularia in the *phenakite-quartz-fluorite vein* in-

dicates that octahedral fluorite can develop at a temperature somewhat less than the temperature of crystallization of adularia. Temperature as a controlling factor of the habit of fluorite has also been suggested by Drugman (1932).

Phenakite

Introduction. In order to properly describe the phenakite from Mt. Antero it was found necessary to make a general survey of the whole phenakite problem, principally in order to determine whether the present morphology and crystal structure were in agreement.

The unit cell and structure of phenakite was determined by Bragg in 1927, and the unit cell dimensions by Gottfried at about the same time (1927). Later (1930) Bragg and Zachariasen further elaborated on the phenakite structure. Pough (1935, 1936) made a detailed study of the morphology of phenakite but failed to point out the direct tie-up between morphology and structure.

Symmetry. Following the method outlined by Buerger and Parrish (1937), a series of equi-inclination Weissenberg photographs about the *c*-axis permits one to resolve the reciprocal lattice into stacks of plane reciprocal lattices normal to the *c*-axis. The projections of these lattices are displaced over each other by $\frac{1}{3}$ of the long mesh diagonal of each layer, thus fixing the space lattice type as rhombohedral.

The symmetry class is determined by the relation of the third-order terminal planes on both top and bottom of the crystals. Such planes are only repeated by a three-fold axis and an inversion center. The Weissenberg photographs also clearly reveal the absence of any vertical symmetry planes. The crystal class is, therefore, C_{3i} ($R3$). Of the two space groups based on this crystal class only one is based on a rhombohedral lattice; thus the space group is C_{3i}^2 ($R\bar{3}$).

Unit Cell. The unit cell chosen by Bragg is a rhombohedron with the length of the rhombohedron edge 7.684 Å and $\alpha = 108°01'$. In order to bring out the relation between structure and morphology a structural cell based upon a hexagonal network must be used. The rhombohedral unit cell dimensions of Bragg transformed to the corresponding hexagonal cell are shown in Table 3. Also listed are the unit cell dimensions determined by the writer.

Table 3

Unit Cell Dimensions of Phenakite

	Bragg	Switzer
a_0	12.33 Å	12.40Å (±0.02)
c_0	8.23	8.24 (from rotation picture)

The hexagonal unit cell of the writer has $V_0 = 1097$ cubic Å and contains 18 (Be_2SiO_4). The calculated density is 2.98 (measured 2.97–3.00).

From the unit cell dimensions a calculation of the axial ratio yields $a_0:c_0 = 1:0.6645$, and the polar elements $p_0:r_0 = 0.7673:1$, which is in good agreement with the morphological elements of Goldschmidt and Schröder (1909).

Morphological elements. The morphological presentation of a rhombohedral mineral can be greatly simplified by omitting a treatment of Goldschmidt's alternative G_1 and G_2 positions, as has been pointed out by Peacock and Bandy (1938). This has been done in the new morphological elements for phenakite given below. The elements of Goldschmidt and Schröder (1909) have been used, but recalculated to the proper position. Since the ϕ and ρ angles remain as given by Pough (1936) a complete new angle table is not required.

TABLE 4

Morphological Elements of Phenakite

Hexagonal—R;	Rhombohedral—$\bar{3}$
$a:c = 1:0.6636$; $\alpha = 107°56'$;	$p_0:r_0 = 0.7662:1$; $\lambda = 63°24'$

It is interesting to note that seven forms of the list of certain forms given by Pough do not fit the rhombohedral rule, which states that $h+i+l = 3n$. These are $c\{0001\}$, $m\{10\bar{1}0\}$, $d\{10\bar{1}2\}$, $r\cdot\{01\bar{1}1\}$, $H\{2\bar{1}\bar{1}2\}$, $v\cdot\{17\bar{8}5\}$, and $V\cdot\{\bar{1}8\bar{7}5\}$. These forms only fit the rhombohedral rule when given multiple indices, and, as is to be expected from this, all but $m\{10\bar{1}0\}$ are rare and are found only as small crystal faces.

Phenakite from Mt. Antero. Phenakite is found at Mt. Antero in a variety of habits and sizes. The crystals are opaque white to colorless, sometimes transparent and with a faint yellow tinge. Both single and twin crystals are abundant. In size they range from $3\frac{1}{2}$ cm. to $\frac{1}{2}$ mm.

The forms measured on Mt. Antero crystals by the writer, listed in order of importance, are: prisms $a\{11\bar{2}0\}$, $m\{10\bar{1}0\}$, terminal forms $X\cdot\{\bar{1}3\bar{2}2\}$, $r\{10\bar{1}1\}$, $S\{21\bar{3}1\}$, $p\{11\bar{2}3\}$, $d\cdot\{01\bar{1}2\}$, $c\{0001\}$, $\Lambda\{31\bar{4}2\}$, $\Sigma\{32\bar{5}1\}$. Interpenetration twins are common. The twin plane is (0001).

By far the most common habit of phenakite from Mt. Antero is short prismatic single crystals, as shown in Figs. 7 and 8. It is characteristic of practically all Mt. Antero phenakite to be terminated dominantly by $X\cdot\{\bar{1}3\bar{2}2\}$, with all other forms small. A few small crystals were found on which the dominant form was $r\{10\bar{1}1\}$. Less commonly single crystals have fairly long prisms. Twin crystals, on the other hand, are decidedly prismatic in habit. The prismatic twin crystals sometimes go to the ex-

treme of being needle-like in appearance. A typical twin is shown in Fig. 9.

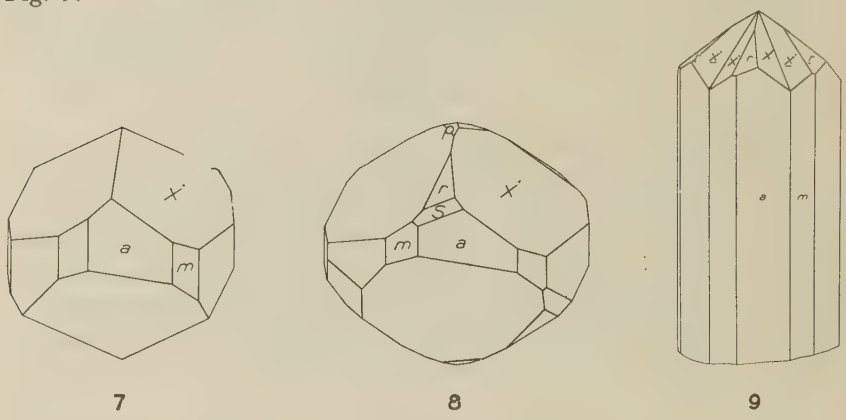

7 8 9

Fig. 7. Crystal of phenakite from Mt. Antero. The commonest type of crystal.
Fig. 8. Crystal of phenakite from Mt. Antero.
Fig. 9. Interpenetration twin of phenakite from Mt. Antero. Twin plane (0001).

Although no exact rule can be formulated, in general it appears that low temperature of crystallization favors development of twin crystals of phenakite, and also favors the most extreme development of prismatic habit of the twins.

References

Bragg, W. L., The structure of phenacite: *Proc. Royal Soc.*, A, **113,** 642–657 (1927).

Bragg, W. L., and Zachariasen, W. H., The crystalline structure of phenacite and willemite: *Zeits. Krist.*, **72,** 518–528 (1930).

Buerger, M. J., and Parrish, W., The unit cell and space group of tourmaline: *Am. Mineral.*, **22,** 1139–1150 (1937).

Crawford, R. D., A contribution to the igneous geology of central Colorado: *Am. J. Sci.*, (5), **7,** 365–388 (1924).

Cross, R. G., Notes on aquamarine from Mt. Antero: *Am. J. Sci.*, (3), **33,** 161–162 (1887).

Drugman, J., Different habits of fluorite crystals: *Mineral. Mag.*, **23,** 137–144 (1932).

Goldschmidt, V., and Schröder, R., Phenakit aus Brasilien: *Zeits. Krist.*, **46,** 465–470 (1909).

Gottfried, C., Über die Struktur der Phenakitdioptasgruppe: *Neues Jahrb. Min., Beil. Bd.* **55,** A, 393–400 (1927).

Ito, T., and West, J., The structure of bertrandite: *Zeits. Krist.*, **83,** 384–393 (1932).

Landes, K. K., The paragenesis of the granite pegmatites of central Maine: *Am. Mineral.*, **10,** 355–411 (1925).

———, The beryl-molybdenite deposit of Chaffee County, Colorado: *Ec. Geol.*, **29,** 697–702 (1934).

Montgomery, A., Storm over Antero: *Rocks and Minerals*, **13,** 355–369 (1938).

Peacock, M. A., and Bandy, M. C., Ungemachite and clino-ungemachite: New minerals from Chile: *Am. Mineral.*, **23,** 314–328 (1938).

PENFIELD, S. L., Phenacite from Colorado: *Am. J. Sci.*, (3), **33,** 131–134 (1887).
———, Bertrandite from Mt. Antero: *Am. J. Sci.* (3), **36,** 52–55 (1888).
———, Some observations on the beryllium minerals from Mt. Antero: *Am. J. Sci.*, (3), **40,** 488–491 (1890).
PENFIELD, S. L., and SPERRY, E. S., Mineralogical notes: *Am. J. Sci.*, (3), **36,** 32 (1888).
POUGH, F. H., The morphology of phenacite from two new occurrences: *Am. Mineral.*, **20,** 863–874 (1935).
———, Phenakit, seine Morphologie und Paragenesis: *Neues Jahrb. Min., Beil. Bd.* **71,** A, 291–341 (1936).
OVER, E., JR., Mineral localities of Colorado: *Rocks and Minerals*, **3,** 110–111 (1928).
———, Further explorations on Mt. Antero, Colorado: *Rocks and Minerals*, **10,** 27–29 (1935).
SMITH, W. B., Mineralogical notes, 1, 2, and 3: *Colorado Sci. Soc., Proc.*, **2,** 177–179 (1887).

NOTES AND NEWS

Dr. Edward S. Simpson, Government Mineralogist and Analyst for the State of Western Australia, died at his home in South Perth on August 30.

Dr. Waldemar Lindgren, emeritus professor of economic geology at the Massachusetts Institute of Technology, died on November 4 at the age of seventy-nine years.

Correction

By mistake an abstract of the mineral *Priceite* was included in the list of abstracts for "New Mineral Names" in the November issue of the Journal. The mineral *Priceite* is not new, being included in the 6th edition of Dana's *System.*

INDEX TO VOLUME 24

Leading articles are in **bold face type**; notes, abstracts and reviews are in ordinary type. Only minerals for which definite data are given are indexed.

Abukumalite (Shin Hata)..... 66
Adinoles of Dinas Head, Cornwall. (Agrell)..... 63
Agrell, S. O..... 63
Alderman, A. R..... 277
Allen, V. T..... 194
Alurgite from California, new occurrence of. (Webb)..... 123
Ammonium mica synthesized from vermiculite. (Gruner)..... 428
Anderson, B. W..... 528
Angewandte Kristallstrukturlehre. (Brandenberger) [Book review] 276
Antlerite. (Palache)..... 293
Apatite, fluorescent, from Center Strafford, N. Hamp. (Stewart) 274
Australites of unusual form. (Singleton)..... 63
Awariute. (Owens, Burns)..... 528

"Baddelyite" from Alno—an error. (vonEckermann)..... 528
Bannister, F. A.....64, 66
Barksdale, J. D. Silicified wood in dolomite.....181, 699
Bavenite, new occurrence of. (Claringbull)..... 277
Behre, C. H., Jr..... 181
Beliankin, D. S..... 279
Bell, J. F..... 181
Berman, H. Torsion microbalance for determining specific gravity of minerals.....182, 434
——— and Gonyer, F. A. Re-examination of colusite..... 377
Berry, L. G..... 182
Bertrandite..... 802
Beryl..... 804
β-uranotile. (Steinocher, Nováček). 324
Bidalotite. (Rao, Rao)..... 350
Bloom, M. C. Mechanism of the genesis of polymorphous forms......182, 281
Bøgvad, R..... 278
Botryogen. (Quentenite)..... 525
Bowles, O. The stone industries. [Book review]..... 461
Brandenberger, E. Angewandte Kristallstrukturlehre. [Book review]..... 276
Bray, J. M. Ilmenite-hematite-magnetite relations in some emery ores.....162, 183
Brochantite. (Palache, Richmond). 463
Brunckite. (Herzenberg)..... 350
Buerger, M. J. Crystal structure of gudmundite..... 183
Bullard, F. M. Rosebud meteorite, Milam Co., Texas.....184, 242
Burns, B. D..... 528

Calcite, Fe–Mn. (Yosimura)..... 660
Caledonite. (Palache, Richmond).. 441
Canyon Diablo iron, identification of diamond in. (Ksanda, Henderson)..... 677
Cesàro, G..... 280
Chao, S. H..... 277
Chemical analyses of minerals, presentation of. (Hey)..... 347
Chlorite veins in serpentine near Kings River, Calif. (Durrell, Macdonald)..... 452
Chrysoberyl occurrence near Golden, Colo. (Waldschmidt, Gaines).....193, 267
Cinnabar, darkening of, in sunlight. (Dreyer)..... 457
Claringbull, G. F.....277, 347
Clay, Hawaiian ceramic, mineral composition of. (Wentworth, Wells, Allen)..... 194
Clay minerals, hydrothermal formation of, in laboratory. (Norton)..... 1
Clays, adsorptive, of Texas Gulf coast. (Hagner).....67, 187
Clerici solution for specific gravity determination of small mineral grains. (Jahns)..... 116
Cliftonite (discredited species).... 280
Colloform ores, European, of Mississippi Valley type. (Behre).. 181
Colusite, its occurrence, paragene-

sis and genetic significance. (Nelson) 369
Colusite, re-examination of. (Berman, Gonyer) 377
Contributions to the knowledge of the chemical composition of the earth's crust in the East Indian Archipelago. (Van Tongeren) [Book review] 172
Cooke, H. B. S. 277
Coombs, H. A. 186
Copiapite, crystallography of. (Peacock) 191
Copiapite, composition and optics of. (Berry) 182
Copperiodate, artificial 390
Corundum in dike at Glen Riddle, Penna. (Tomlinson) 193, 339
Cristobalite in southwestern Yellowstone Park. (Howard) 485
Crystal habit variation in NaF. (Frondel) 185
Crystal space groups determined without x-rays. (Donnay) 184
Cupro-asbolane. (De Leenheer) 657
Cuprorivaite. (Minguzzi) 350

Dakeite, identity with schroeckeringite. (Nováček) 317
DallaValle, J. M. with Goldman, F. H. Determination of components of a heterogeneous particulate mineral system 40
Darapskite 634
Deer, W. A. and Wager, L. R. Olivines from Skaergaard intrusion, Kangerdlugssuak, E. Greenland 18
De Leenheer, L. 657
Density determination, micropycnometric, improved technique in. (Ksanda, Merwin) 482
Descriptive list of new minerals 1892–1938. (English) [Book review] 347
Descriptive petrography of igneous rocks. Vol. IV. Feldspathoid rocks and peridotites and perknites. (Johannsen) [Book review] 64
Determination of components of a heterogeneous particulate mineral system. (Goldman, DallaValle) 40
Devadite. (Fermor) 406
Diamond cutting in terms of atomic structure, explanation of. (Kraus, Slawson) 188
Diamond in Canyon Diable iron, identification of. (Ksanda, Henderson) 677
Diamond, variation in hardness of. (Kraus, Slawson) 661
Dichroism in tourmaline, quantitative measurement of. (Slawson, Thibault) 492
Discredited species 280, 728
Donnay, J. D. H. 184
Dreyer, R. M. Darkening of cinnabar in sunlight 457
Drugman, J. 63
Durrell, C. and Macdonald, G. A. Chlorite veins in serpentine near Kings River, Calif. 452

Eight Mile Park, Colo., minerals of. (Landes) 188
Emery ores, ilmenite-hematite-magnetite relations in. (Bray) 162, 183
Emmons, R. C. and Gates, R. M. New method for determination of feldspar twins. 577
Endothermite (Beliankin) 279
English, G. L. Descriptive list of new minerals 1892–1938. [Book review] 347
Epidesmine and stellerite, relation to stilbite. (Pabst) 63
Evans, R. C. Introduction to crystal chemistry. [Book review] .. 657
Eyepiece micro-planimeter. (Cooke) 277

Fabrics of inclusions and the adjacent intrusive rocks, comparison of. (Ingerson) 187, 607
Fahey, J. J. Shortite, a new carbonate of Na and Ca 514
Fairbairn, H. W. Correlation of quartz deformation with its crystal structure 351

Faratsihite..... 536
Feldspar, resorbed, in a basalt flow. (Fries)..... 782
Feldspar, introduction of, into inclusions, Ellsworth, N. Hamp. (Page)..... 190
Feldspar twins, new method for determination of. (Emmons, Gates)..... 577
Feldspathoids, staining of. (Shand) 508
Fermor, L. L.....279, 406
Fisher, D. J. with Palache, C. Gratonite, a new mineral from Peru..... 136
Fleischer, M.....185, 189
Fluorine, qualitative determination of in minerals. (Foley, West)..... 398
Fluorite, twinned octahedra. (Switzer).....193, 805
Foley, F. C. and West. P. W. Qualitative determination of F in minerals..... 398
Foshag, W. F......185, 728
——— with Gale, W. A. Teepleite, a new mineral from Borax Lake, Calif...... 48
Francolite, composition of (Sandell, Hey, McConnell)..... 277
Fries, C., Jr. Resorbed feldspar in a basalt flow..... 782
Frohberg, M. H. Occurrence of riebeckite in Michipicoten district, Ontario..... 382
Frondel, C..... 185
Fuller, R. E..... 186
Furnival, G. M. Notes on quartz "dikes"..... 499

Gabrielson, O..... 406
Gaines, R. V. with Waldschmidt, W. A. Occurrence of chrysoberyl near Golden, Colo.....193, 267
Gale, W. A. and Foshag, W. F. Teepleite, a new mineral from Borax Lake, Calif...... 48
Gates, R. M. with Emmons, R. C. New method for determination of feldspar twins...... 577
Gems and gem materials. (Kraus, Slawson) [Book review]..... 461
Genesis of polymorphous forms, mechanism of. (Bloom)....182, 281
Glass, J. J. and Schaller, W. T. Inesite..... 26
Glasses, alteration of, to montmorillonite. (Hauser, Reynolds)..... 590
Goldich, S. S. and Kinser, J. H. Perthite from Tory Hill, Ontario.....185, 407
Goldman, F. H. and DallaValle, J. M. Accurate determination of components of a heterogeneous particulate mineral system..... 40
Goldschmidtine, a new antimonide of silver. (Peacock)..... 227
Gonyer, F. A. with Berman, H. Re-examination of colusite... 377
Goodspeed, G. E..... 186
Granite pegmatites of Mt. Antero region, Colorado. (Switzer). 193, 791
Graphic granite. (Wahlstrom).... 681
Gratonite—preliminary description of a new mineral from Cerro de Pasco, Peru. (Palache, Fisher). 136
Gruner, J. W. Ammonium mica synthesized from vermiculite. 428
——— Formation and stability of muscovite in acid solutions at elevated temperatures..... 624
——— 186
Gudmundite, crystal structure of. (Buerger) 183

Hagner, A. F. Adsorptive clays of Texas Gulf coast.....67, 187
Hanksite, composition, space group and unit cell of. (Ramsdell).. 109
Hanley, F. B. New accessibility of Thomsonite Beach, Minn..... 726
Harmotone, association of, with Ba feldspar at Glen Riddle, Penna. (Meier).....189, 540
Harmotone, corundum and hyalophane at Glen Riddle, Penna. (Meier, Tomlinson)..... 189
Hauser, E. A. and Reynolds, H. H. Alteration of glasses to montmorillonite..... 590
Hawaiian ceramic clay, mineral

composition of. (Wentworth, Wells, Allen) 194
Henderson, E. P. 187
——— **with Ksanda, C. J. Identification of diamond in the Canyon Diablo iron** 677
Henricks, S. B. Polymorphism of the micas 729
——— **Random structures of layer minerals as illustrated by cronstedite. Possible iron content of kaolin** 529
Herzenberg, R. 350
Hess, H. H. World distribution of serpentinized peridotites and its geologic significance 275
Hexahedrite meteorites from Chile, chemical study of. (Henderson) 187
Hey, M. H. 66, 277, 280, 347
History of the study of ore minerals. (Thomson) 137, 181
Hopeite, symmetry and unit cell of. (Wolfe) 194
Hata, Shin 66
Howard, A. D. Cristobalite in southwestern Yellowstone Park ... 485
Huckitta meteorite, central Australia. (Madigan, Alderman) . 277
Hunt, W. F. Book reviews 347, 404
Hyalophane 557

Idocrase and certain garnets, chemical similarity of. (McConnell). 62
Ilmenite-hematite-magnetite relations in some emery ores. (Bray) 162, 183
Indices of refraction in anisotropic media, measurement of. (Quirke, Lacy) 705
Inesite. (Glass, Schaller) 26
Ingerson, E. Comparison of the fabrics of inclusions and the adjacent intrusive rock 187, 607
Instituto de Geologia, Caracas, Venezuela. (Knox) 171
Introduction to crystal chemistry. (Evans) [Book review] 657
Iron knebelite. Iron tephroite. (Yosimura) 659

Jahns, R. H. Clerici solution for specific gravity determination of small mineral grains 116
Jarrell, O. W. Marshite and other minerals from Chuquicamata, Chile 188, 629
——— Occurrence of antlerite at Chuquicamata 301
——— **with Palache, C. Salesite, a new mineral from Chuquicamata, Chile** 388
Jefferson, M. E. Optical measurements on micas 729
Johannsen, A. Descriptive petrography of igneous rocks. Vol. IV. [Book review] 64

Kaolin, possible iron content of. (Henricks) 529
Kaolinite in some "eenie" coals. (Claringbull) 347
Kasoite. (Yosimura) 658
Keith, M. L. Selective staining to facilitate Rosiwal analysis 561
Khoharite. (Fermor) 279
Kinser, J. H. with Goldich, S. S. Perthite from Tory Hill, Ontario 185, 407
Klein, I. Microcline in the native copper deposits of Michigan .. 643
Knebelite-Fe, Mn. (Yosimura) 659
Knox, N. B. Instituto de Geologia, Caracas, Venezuela 171
Kornerupine, new occurrence. (Anderson, Payne) 528
Kotoite. (Watanabe) 406
Kraus, E. H. and Slawson, C. B. Variation of hardness in the diamond 189, 661
——— Gems and gem materials. [Book review] 461
Krumbein, W. C. and Pettijohn, F. J. Manual of sedimentary petrography. [Book review] ... 404
Ksanda, C. J. 185, 193
——— **and Henderson, E. P. Identification of diamond in the Canyon Diablo iron** 677
——— **and Merwin, H. E. Improved technique in micro-**

pycnometric density determination 482

Lacy, W. C. with Quirke, T. T. Measurement of indices of refraction in anisotropic media .. 705
Landes, K. K. 188
Larsen, E. S. Presentation of Roebling Medal to W. T. Schaller 53
——— Book review 64
Larsen, E. S. 3rd 188
Legge, J. A. Jr. Vertical illuminator for low magnification photography of polished surfaces 400
Leucite-rich rocks of West Kimberly area, W. Australia, minerals from. (Prider) 277
Libethenite 633
Liquid-vapor equilibria in system K_2O–SiO_2–CO_2–H_2O. (Morey, Fleischer) 189

Macdonald, G. A. with Durrell, C. Chlorite veins in serpentine near Kings River, Calif. 452
Madigan, C. T. 277
Mangan-actinolite 659
Mangan-knebelite 659
Mangan-tremolite. (Yosimura) ... 659
Manual of sedimentary petrography. (Krumbein, Pettijohn) [Book review] 404
Marble, J. P. Analysis of two samples of pitchblende ore from Great Bear Lake, Canada 272
Marshite and other minerals from Chuquicamata, Chile. (Jarrell) 188, 629
Maynard, J. E. Some modes of quartz-bearing plutonites from Derby, Vermont 653
McConnell, D. Chemical similarity of idocrase and certain garnets. 62
——— **Symmetry of phosphosiderite** 189, 636
——— 277
Mechanical twinning in crystals, morphology of. (Bell) 181
Meen, V. B. Santa Luzia de Goyaz meteorite 598
——— 189
Meier, A. E. Association of harmotone and Ba feldspar at Glen Riddle, Penna. 189, 540
Mélon, J. 658
Merosymmetry vs. merohedrism. (Rogers) 63
Merritt, C. A. with Wood, F. C. Soper, Oklahoma, meteorite .. 59
Merwin, H. E. with Ksanda, C. J. Improved technique in micropycnometric density determination 482
——— 193
Metasomatism of shale to an igneous appearing rock. (Goodspeed, Fuller, Coombs) 186
Meteorites:
Hexahedrites from Chile 187
Huckitta, central Australia 277
Rosebud, Milam Co., Texas 184, 242
Santa Luzia de Goyaz 598
Shallowater, Texas 185
Soper, Oklahoma 59
Meyerhofferite 522
Meyers, W. M. Book reviews 461
Miargyrite crystals from Randsburg, Calif. (Murdoch) 772
Micas, polymorphism of, and optical measurements. (Hendricks, Jefferson) 729
Microbalance, torsion, for determination of specific gravities of minerals. (Berman) 182, 434
Microcline in the native copper deposits of Michigan. (Klein) ... 643
Mineralogical Society of America:
Former officers and meeting places 197
List of correspondents, fellows and subscribers 198
Nominations for officers for 1940. 605
Proceedings of 19th annual meeting 174
Mineralogical Society of Great Britain and Ireland.63, 277, 347, 528
Mineralogical trip to Europe. (Rogers) 192
Minguzzi, C. 350
Molengraaffite, identity with lamprophyllite. (Tilley) 728

Monazite, unit cell and space group of. (Parrish) 651
Monothermite. (Beliankin) 279
Monticellite rock from Crestmore, Calif. (Rogers) 192
Montmorillonite, *x*-ray data 94
Morey, G. W. 189
Mountain, E. D. 278
Mounting and remounting detrital minerals grains on slides. (Smith) 602
Murdoch, J. Crystallography of veatchite 130, 190
——— **Miargyrite crystals from Randsburg, Calif.** 772
Muscovite, formation and stability of, in acid solutions at elevated temperatures. (Gruner) 624
Muscovite, optical and chemical studies. (Volk) 255

Nelson, R. Colusite—its occurrence, paragenesis and genetic significance 369
Nepheline-syenite pegmatites in the Bearpaw Mts. of Montana. (Pecora) 191
Nepheline, zonal structure in. (Shand) 508
Newark Mineralogical Society 64
New Haven Mineral Club 405
New minerals
Goldschmidtine 227
Gratonite 136
Overite 188
Salesite 388
Shortite 514
Teepleite 48
New mineral names 66, 278, 350, 406, 657, 728
New York Mineralogical Club 224, 278, 404, 462
Nickel-iron alloy, natural, crystal structure of. (Owen, Burns) ... 528
Norton, F. H. Hydrothermal formation of clay minerals in the laboratory 1
Nováček, R. Identity of dakeite and schroeckingerite 317
——— **and Steinocher, V. β-uranotile** 324

Occurrence of rarer elements in the Netherlands East Indies. (Van Tongeren) [Book review] 172
Olivines from the Skaergaard intrusion, Kangerdlugssuak, East Greenland. (Deer, Wager) ... 18
Olivines, zoned, and their petrogenetic significance. (Tomkeieff) 64
Olivenite 632
Optic properties of organic and inorganic compounds compared. (Winchell) 194
Ore Minerals, history of (Thomson) 137
Overite, a new mineral from Fairfield, Utah. (Larsen) 188
Owen, E. A. 528
Oxyapatite, fluorine and alkaline. (Vlodavetz) 279

Pabst, A. Formula and structure of ralstonite 566
——— 63, 64
Page, L. R. 190
Palache, C. Antlerite 293
——— **Brochantite** 463
——— and Fisher, D. J. Gratonite, a new mineral from Cerro de Pasco, Peru 136
——— **and Jarrell, O. W. Salesite, a new mineral from Chuquicamata, Chile** 388
——— **and Richmond, W. E. Caledonite** 441
Parrish, W. Unit cell and space group of monazite 651
——— 190
Payne, C. J. 528
Peacock, M. A. Goldschmidtine, a newly recognized antimonide of silver 227
——— 191
Pecora, W. T. 191
Penninite—optical data 454
Peridotites, serpentinized, world distribution of, and its geologic significance. (Hess) 275
Perthite from Tory Hill, Ontario. (Goldich, Kinser) 185, 407

Pettijohn, F. J. with Krumbein, W. C. Manual of sedimentary petrography. [Book review]... 404
Phenakite..... 806
Philadelphia Mineralogical Society.....225, 226, 348, 349, 605
Phosphosiderite, symmetry of. (McConnell).....189, 636
Pickeringite..... 522
Picrotephroite. (Yosimura)..... 659
Pike, J..... 528
Pitchblende ore from Great Bear Lake, Canada, analysis of. (Marble)..... 272
Plutonites, quartz-bearing, from Derby, Vermont, some modes of. (Maynard)..... 653
Pollucite, dehydration and *x*-ray study of. (Fleischer, Ksanda). 185
Polymorphous forms, mechanism of the genesis of. (Bloom)..182, 281
Potash-soda feldspar, *x*-ray examination of. (Chao, Smare, Taylor)..... 277
Potassium tetrathionate as an example of monoclinic hemihedral symmetry. (Tunell, Merwin, Ksanda)..... 193
Priceite. (Foshag)..... 728
Prider, R. T..... 277

Quartz-α, with cleavage parallel to prism. (Drugman)..... 63
Quartz-α, with steep rhomohedron as predominant form. (Drugman)..... 63
Quartz deformation, correlation with crystal structure. (Fairbairn)..... 351
Quartz "dikes", notes on. (Furnival)..... 499
Quartz "dikes", discussion of. (Tolman)..... 519
Quensel, P..... 406
Quetenite..... 525
Quirke, T. T. and Lacy, W. C. Measurement of indices of refraction in anisotropic media. 705

Ralstonite, formula and structure of. (Pabst)..... 566
Ramsdell, L. S. Composition, space group and unit cell of hanksite..... 109
——— Book reviews.....276, 657
Random structures of layer minerals as illustrated by cronstedite. (Hendricks)..... 529
Rao, B. R. and Rao, L. R..... 350
Reflectivity and color of minerals, measurement of. (Parrish)... 190
Refractometers employing diamond and other minerals. (Anderson, Payne, Pike)..... 528
Reynolds, H. H. with Hauser, E. A. Alteration of glasses to montmorillonite..... 590
Rhodochrosite, Ca and Fe. (Yosimura)..... 660
Rhyodacite from Tranquille Plateau, B. C. (Stevenson)....192, 446
Richmond, G. M. Serendibite and associated minerals from New City Quarry, Riverside, Calif. 725
Richmond, W. E. X-ray study of antlerite..... 300
——— **X-ray study of brochantite**. 480
——— **X-ray study of salesite**.... 391
——— with **Palache, C. Caledonite**..... 441
Riebeckite, occurrence in Michipicoten District, Ont. (Frohberg)..... 382
Rockville granite, crystallization of. (Tatge)..... 303
Roebling Medal—presentation to W. T. Schaller. (Larsen)..... 53
Rogers, A. F.....63, 192
Rosebud meteorite, Milam Co., Texas. (Bullard).....184, 242
Ross, C. S. and Stephenson, L. W. Calcareous shells replaced by beidellite..... 393
Rotation factor for equi-inclination Weissenberg photographs, (Tunell)..... 448
Russell, A..... 347
Russellite. (Hey, Bannister)..... 66

Salesite, a new mineral from Chuquicamata, Chile. (Palache, Jarrell)..... 388

Sandell, E. B. 277
Santa Luzia de Goyaz meteorite. (Meen) 598
Sapphirine crystals from Blinkwater, Transvaal. (Mountain). 278
Sartorite, crystallography of. (Bannister, Pabst, Vaux) 64
Sawyer, R. A. Book review 172
Schairer, J. F. 192
Schaller, W. T. Roebling Medal presentation 53
——— **with Glass, J. J. Inesite** ... 26
Schroeckingerite, identity with dakeite. (Nováček) 317
Serendibite and associated minerals from New City Quarry, Riverside, Calif. (Richmond). 725
Serpentines, behavior of, between 500°–650°. (Gruner) 186
Shallowater meteorite, petrology of. (Foshag) 185
Shand, S. J. Staining of feldspathoids and zonal structure in nepheline 508
Sharpite. (Mélon) 658
Shells, calcareous, replaced by beidellite. (Ross, Stephenson) 393
Shortite, a new carbonate of Na and Ca. (Fahey) 514
Silicified wood in dolomite. (Barksdale) 181, 699
Singleton, F. A. 63
Slawson, C. B. with Kraus, E. H. Variation in hardness of the diamond 188, 661
——— Gems and gem materials. [Book review] 461
——— **and Thibault, N. W. Quantitative measurement of dichroism in tourmaline** 492
Smare, D. L. 277
Smith, H. T. U. Mounting and remounting detrital mineral grains on slides 602
Soper, Oklahoma, meteorite. (Wood, Merritt) 59
South Victoria Land rocks, petrography of. (Stewart) 155
Spectrographic determination of elements according to arc methods in the range 3600–5000Å. (Van Tongeren) [Book review] 172
Spencer, L. J. 348
Spessartine, Ca-Fe and Fe-Ca. (Yosimura) 660
Sphene crystals, large, from San Jacinto Mts., Calif. (Webb) .. 193, 344
Staining, selective, to facilitate Rosiwal analysis. (Keith) 561
Steinocher, V. with Nováček, R. β-uranotile 324
Stellerite and epidesmine, relation to stilbite. (Pabst) 63
Stephenson, L. W. with Ross, C. S. Calcareous shells replaced by beidellite 393
Stevenson, L. S. Rhyodacite from Tranquille Plateau, B. C. .. 192, 446
Stewart, D., Jr. Petrography of some South Victoria Land rocks 155
Stewart, G. W. Vesuvianite and fluorescent apatite from Center Strafford, N. Hamp. 274
Stone industries. (Bowles) [Book review] 461
Switzer, G. Granite pegmatites of the Mt. Antero region, Colo. 193, 791
System FeO-Al_2O_3-SiO_2, preliminary report on. (Schairer) 192
System K_2O-SiO_2-CO_2-H_2O, liquid vapor equilibria in. (Morey, Fleischer) 189
Szomolnokite 522

Tatge, E. Crystallization of the Rockville granite 303
Taylor, W. H. 277
Teepleite, a new mineral from Borax Lake, Calif. (Gale, Foshag) 48
Teineite. (Yosimura) 658
Tephroite-Fe. (Yosimura) 659
Thaumasite 346
Thibault, N. W. with Slawson, C. B. Quantitative measurement of dichroism in tourmaline 492

Thomson, E. History of the study or ore minerals.....137, 181
Thomsonite Beach, Minnesota, new accessibility of. (Hanley). 726
Tilley, C. E..... 728
Tolman, C. Discussion of quartz "dikes"..... 519
Tomkeieff, S. I..... 64
Tomlinson, W. H. Corundum in dike at Glen Riddle, Penna. 193, 339
——— 189
Tory Hill, Ontario, perthite. (Goldich, Kinser).....185, 407
Trieuite. (De Leenheer)..... 657
Tunell, G. Rotation factor for equi-inclination Weissenberg photographs..... 448
——— 193
Twinned octahedra of fluorite, and associated minerals from Mt. Antero. (Switzer)..... 193

Uranotile-β. (Steinocher, Nováček) 324

Van Tongeren, W. I. Spectrographic determination of elements according to arc methods in the range 3600–5000 Å. II. Occurrence of rarer elements in the Netherlands East Indies. [Book review]..... 172
Vaux, G..... 64
Veatchite, crystallography of. (Murdoch).....130, 190
Verdelite. (Quensel, Gabrielson).. 406
Vertical illuminator for low magnification photography of polished surfaces. (Legge)..... 400
Vesuvianite and fluorescent apatite from Center Strafford, N. Hamp. (Stewart)..... 274
Vesuvianite from Great Slave Lake region, Canada. (Meen). 189
Vlodavetz, V. I..... 279
Volk, G. W. Optical and chemical studies of muscovite..... 255
von Eckermann, H..... 528

Wager, L. R. with Deer, W. A. Olivines from Skaergaard intrusion, Greenland..... 18
Wahlstrom, E. E. Graphic granite. 681
Waldschmidt, W. A. and Gaines, R. V. Occurrence of chrysoberyl near Golden, Colo....193, 267
Watanabe, T..... 406
Webb, R. W. Large sphene crystals from San Jacinto Mts., Calif. 193, 344
——— **New occurrence of alurgite from California**..... 123
Weberite. (Bøgvad)..... 278
Wells, R. C..... 194
Wentworth, C. K..... 194
West, P. W. with Foley, F. C. Qualitative determination of F in minerals..... 398
Winchell, A. N..... 194
Wolfe, C. W..... 194
Wood, F. C. and Merritt, C. A. Soper, Oklahoma, meteorite.. 59
Wulfenite..... 635

Yosimura, T.....658, 659, 660

AUTHOR—TIME PRESENTATION INDEX—NICOLLET HOTEL

Apsouri, Constantin N.	4:07 P.M.	Friday	Grand Ballroom
Ayres, Vincent L.	4:13 P.M.	Thursday	Parlor N
Behre, Charles H., Jr.	2:24 P.M.	Friday	Grand Ballroom
Bell, K. G.	3:12 P.M.	Friday	Grand Ballroom
Berman, Harry	3:37 P.M.	Thursday	Parlor N
Berry, Leonard G.	9:55 A.M.	Friday	Parlor N
Bradley, W. F.	9:22 A.M.	Friday	Parlor N
Buerger, Newton W.	9:41 A.M.	Friday	Parlor N
Bullard, Fred M.	4:41 P.M.	Thursday	Parlor N
Burfoot, J. Dabney, Jr.	11:00 A.M.	Friday	Parlor N
Cuthbert, F. Leicester	2:00 P.M.	Friday	Grand Ballroom
Donnay, J. D. H.	3:59 P.M.	Thursday	Parlor N
Dreyer, Robert M.	3:24 P.M.	Friday	Grand Ballroom
Fisher, D. Jerome	3:13 P.M.	Thursday	Parlor N
Foster, W. R.	4:55 P.M.	Thursday	Parlor N
Frondel, Clifford	5:04 P.M.	Thursday	Parlor N
	10:19 A.M.	Friday	Parlor N
Goldich, Samuel S.	3:53 P.M.	Friday	Grand Ballroom
Gonyer, Forest A.	4:25 P.M.	Thursday	Parlor N
Goodman, Clark	3:12 P.M.	Friday	Grand Ballroom
Kerr, Paul F.	2:55 P.M.	Friday	Grand Ballroom
Kraus, Edward H.	2:49 P.M.	Thursday	Parlor N
Mathews, Edward B.	2:12 P.M.	Friday	Grand Ballroom
McConnell, Duncan	4:48 P.M.	Thursday	Parlor N
Meier, Adolph	By title		
Murdoch, Joseph	11:14 A.M.	Friday	Parlor N
Osborn, E. F.	2:38 P.M.	Friday	Grand Ballroom
Palache, Charles	2:30 P.M.	Thursday	Parlor N
	4:25 P.M.	Thursday	Parlor N
Peacock, Martin A.	3.01 P.M.	Thursday	Parlor N
Philbrick, Shailer S.	3:41 P.M.	Friday	Grand Ballroom
Prince, A. T.	4:32 P.M.	Thursday	Parlor N
Ramsdell, Lewis S.	10:07 A.M.	Friday	Parlor N
Richmond, Wallace E.	9:34 A.M.	Friday	Parlor N
Rogers, Austin F.	10:31 A.M.	Friday	Parlor N
Sandell, E. B.	3:53 P.M.	Friday	Grand Ballroom
Schairer, J. Frank	2:38 P.M.	Friday	Grand Ballroom
Schaller, Waldemar T.	2:37 P.M.	Thursday	Parlor N
	10:48 A.M.	Friday	Parlor N
Slawson, Chester B.	2:49 P.M.	Thursday	Parlor N
Stringham, Bronson	9:15 A.M.	Friday	Parlor N
Taylor, E. D.	3:49 P.M.	Thursday	Parlor N
Tomlinson, W. Harold	5:11 P.M.	Thursday	Parlor N
Tunell, George	3:25 P.M.	Thursday	Parlor N
Vitaliano, Charles J.	By title		
Whitehead, W. L.	3:12 P.M.	Friday	Grand Ballroom
Williams, Norman C.	9:15 A.M.	Friday	Parlor N
Wolfe, C. W.	9:34 A.M.	Friday	Parlor N

THE PEGMATITES OF THE KEYSTONE AREA*

CONSTANTIN N. APSOURI

Detailed mapping of the Hugo, Peerless, Dan Patch, Bob Ingersoll and lesser pegmatites in the Keystone area, supported by critical study of the relations between their minerals and the country rock lead the writer to conclude that:

(1) Some criteria interpreted as favoring replacement need revision, having been used to support two diametrically opposed views; examples are euhedral crystals.

(2) Even a well-established criterion should be employed in the light of spatial and structural relations.

(3) While replacement did take place, its role is over-emphasized. The spodumene "logs" at the Etta mine are not products of replacement.

(4) The common belief that muscovite and muscovite books are replacement products is not supported by the field evidence cited by advocates of replacement. Muscovite forms less than 1% in common pegmatites. The contention that mica occurs at the contact is not strictly correct: mica books are frequently far from a major contact. Not all pegmatites bear mica. The almost constant association of schist xenoliths with an aureole of muscovite books suggests a genetic relationship. The mica probably resulted from the assimilation of the schist by the pegmatitic magma.

(5) Structure and mode of emplacement of pegmatites has not been stressed lately. Pegmatites distend the country rock, or stope their way through, or both, as suggested by xenoliths and the sharp transgression of schistosity by some contacts.

(6) The sequence of mineral paragenesis described by Landes (1928) is revised.

(7) A single mapping of a pegmatite is insufficient. Repeated visits and mapping, concurrent with the progress of mining, are essential to uncover significant data, otherwise irretrievably lost.

* Presented through the Society of Economic Geologists.

STILPNOMELANE, NONTRONITE, AND HALLOYSITE FROM NORTHERN MICHIGAN

VINCENT L. AYRES

Stilpnomelane, nontronite, and halloysite have not heretofore been reported from the Michigan iron mining districts.

The first of these, stilpnomelane, occurs as a *contact* mineral where granite pegmatite has intruded ferruginous slate at Crystal Falls. Notable in the complete analysis is an abnormally high content of ferric iron together with appreciable manganese. The arc spectrograph proves the absence of potash. Refractive indices are: $\alpha = 1.634$, β & $\gamma = 1.730$.

The nontronite superficially resembles chrysocolla. It occurs abundantly with halloysite and limonite lining cracks in a shatter zone at the New Richmond pit east of Palmer on the Marquette Range, and also in a seam in post-Huronian granite five and one-half miles to the west. Nontronite also is to be found at scattered localities on the Menominee and Gogebic Ranges.

The halloysite may not be hydrothermal, but at least it is another example of alumina transported in solution.

STRUCTURAL CONTROL IN EUROPEAN LEAD-ZINC ORES OF THE MISSISSIPPI VALLEY TYPE*

CHARLES H. BEHRE, JR.

This discussion is limited to tectonic, non-mineralogic features, observed during nine months of field work, supplemented with observations by others.

The flat-lying strata of German and Polish Silesia and those of the north Moroccan deposits (Oujda, Toussit) show ore following bedding-partings near normal faults; absence

* Presented through the Geological Society of America.

of obvious trunk channels suggests the Upper Mississippi Valley and Tri-State relationships in the United States. The ores near Alston (northern England) and Djalta (Tunisia) are similar. Somewhat similar also are those of Derbyshire (Mill Close mine), but here mineralized fissures are well exposed.

At Aachen and near-by Limburg (Holland) and Moresnet (Belgium) mineralized large faults, from which the ore spread outward, are well-marked and bedding plane openings are still prominent. But in Wales (Halkyn) and the middle Rhine valley (e.g., Ems) fault openings play the only important role.

At the opposite extreme from the Silesian deposits are replacements and fissure fillings in Alpine limestones at Mezica (Jugoslavia), Cave di Predil (Italy), and Bleiberg (Austria). These show replacements confined to the neighborhood of complex faults, largely thrusts, yet mineralogy and paragenesis are essentially as in the cases first cited.

Summarizing, widespread studies yield transition types between (1) deposits in highly strained rocks and (2) deposits in almost undeformed sediments, in which the direction of mineralization is still actively debated, both here and abroad. The tectonic relations of the less deformed types can therefore scarcely be adduced as arguments against hydrothermal origin.

CLASSIFICATION OF THE NATIVE ELEMENTS, SULPHIDES, AND SULPHO-SALTS

HARRY BERMAN

The classification is that to be followed in the seventh edition of Dana's "*System of Mineralogy.*" Native elements are arranged beginning with the gold group. Sulphides and sulpho-salts are arranged according to a decreasing $A:X$ ratio, where A represents the metallic and X the nonmetallic elements. Groups are based on crystallographic and chemical similarities.

STRUCTURAL CRYSTALLOGRAPHY AND COMPOSITION OF JAMESONITE

L. G. BERRY

Jamesonite with basal cleavage, from Cornwall (type locality), Huanuni, Bolivia, and the Itos Mine near San Felipe de Oruro, Bolivia, give identical x-ray powder photographs. Rotation and Weissenberg photographs of a needle-like crystal from the Itos Mine show monoclinic symmetry; space group $P2_1/a$; a_0 15.68 ± 0.05, b_0 19.01 ± 0.05, c_0 4.03 ± 0.01Å; $\beta = 91°48' \pm 30'$; twinning on (100). The available good analyses on jamesonite with basal cleavage give the cell content:

$$Pb_8Fe_2Sb_{12}S_{28} = 2[4PbS \cdot FeS \cdot 3Sb_2S_3]$$

Specific gravity 5.67 (calc.), 5.63 (meas.). The structural lattice is simply related to the geometrical elements of Slavík (1914); the cell content confirms the empirical formula derived by Loczka (1908) and reached independently by Schaller (1911).

THE STRUCTURAL SCHEME OF ATTAPULGITE

W. F. BRADLEY

The tendency of clays to form aggregates which exhibit preferred orientation can often be made use of to provide x-ray diffraction data not apparent in powder diffraction diagrams. Flaky aggregates of attapulgite formed by sedimentation from a suspension consist of fibrous particles whose fibre axes lie in the plane of the flakes. A series of patterns made with radiation incident at various inclinations to such flakes show fairly well developed arcs for reflections of the type hkO (the fibre axis being c). The c-axis periodicity is about 5.2 Å. Too little data are available for a complete solution of the structure, but a projection on to 001 of an idealized structural scheme consistent with the observed hkO interferences is proposed.

Attapulgite is probably monoclinic, probable space group C_{2h}^3-C2/m with a_0 sin $\beta=12.9$ Å, $b_0=18$ Å. The ideal formula, derived from that of the amphiboles, can be written $(OH_2)_4(OH)_2Mg_5Si_8O_{20}\cdot 4H_2O$, there being two molecules to the unit cell. Partial replacement of Mg^{++} by Al^{+++} on a three for two basis is extensive but such replacement can probably not be complete. The structure is made up of amphibole like chains running parallel to C (at $00\bar{Z}$ and $_{22}{}^{11}\bar{Z}$) with each chain linked through oxygen at its corners to four neighboring chains. Interstitial chains of water molecules also parallel the c-axis and separate the amphibole chains.

The scheme is consistent with the fibrous nature of the material, its clay habit, its optical properties, and its dehydration characteristics.

AN *X*-RAY INVESTIGATION OF THE SOLID PHASES OF THE SYSTEM Cu_2S-CuS

NEWTON W. BUERGER

A systematic x-ray study of the solid phases of the system Cu_2S-CuS has been made. A special camera was designed to make x-ray photographs of powder samples at high temperatures. This camera allows the specimen to remain heated continuously, and the heat treatment can be controlled as in a furnace. The resulting phase diagram shows that the system contains three compounds and six phases. The compounds are:

chalcocite, ideally Cu_2S
digenite, ideally $4Cu_2S\cdot CuS=Cu_9S_5$
covellite, CuS

Chalcocite undergoes three transformations, and none of the high temperature phases is cubic up to at least 250°C. The revised inversion scheme is:

above 105°C.,	non-isometric completely disordered basic structure
78°C. to 105°C.,	non-isometric partially disordered basic structure
52°C. to 78°C.,	non-isometric ordered basic structure
below 52°C.,	orthorhombic superstructure

The superstructure phase is capable of dissolving up to 8 atomic per cent CuS while the ordered basic structure can dissolve only 2 atomic per cent CuS. The experimental evidence indicates a hitherto unrecognized compound Cu_9S_5, whose powder pattern is essentially identical with that of the discredited mineral digenite, to which the formula $2Cu_2S\cdot CuS=Cu_5S_3$ had been assigned. Below approximately 47°C. digenite has the ideal composition Cu_9S_5, but above this temperature it takes increasing amounts of either Cu_2S or CuS into its composition. Evidently digenite has been regarded as the phase of chalcocite stable above 91°C. Certain regions of the phase diagram of this system may be applied to problems of geologic thermometry, providing that proper criteria are recognized.

THE BARTLETT METEORITE, BELL COUNTY, TEXAS

FRED M. BULLARD

This nickel-iron meteorite, weighing 8.59 kilograms, was ploughed up in a field about 5 miles west of the town of Bartlett in Bell County, Texas, about 4 years ago. A polished and etched section showed well developed Widmanstatten figures. The meteorite is a medium octahedrite consisting essentially of grouped kamacite plates with narrow borders of taenite and smaller amounts of plessite, schreibersite, and troilite. A chemical analysis gave 90.41% iron, 8.88% nickel, and small amounts of cobalt and phosphorous. A spectrographic analysis showed small quantities of copper, silicon, and germanium in addition to the elements reported in the chemical analysis.

THE CONCEPT OF UNIQUE DIAMETERS IN CRYSTALLOGRAPHY

J. DABNEY BURFOOT, JR.

A unique diameter is a line, or diameter, unlike any other in the crystal. All parallel lines are the same line crystallographically. All properties, physical, chemical, and crystallographic, along a unique diameter are different from those along any other line in the crystal.

Several criteria based on physical and chemical properties, the groupings of faces and angles between faces, and the dimensions of crystals may be used to recognize unique diameters. Likewise, laws controlling their distribution in crystals and their relations to the various elements of symmetry may be formulated. Since their arrangement in each crystal system is different from that in any other, except that the tetragonal and hexagonal are alike, unique and like diameters may be used to define the six crystal systems independent of symmetry and axes of reference, and the selection and orientation of axes of reference may be based on them.

Some of the applications and relationships of this concept are: (1) the assignment of crystals to systems without the use of symmetry or hypothetical axes of reference; (2) the easy selection of axes of reference; (3) the determination of the crystal system to which a mineral belongs from its cleavage fragment; (4) a clarification of some of the relationships and conditions observed in optical mineralogy; and (5) the simplification of the teaching of crystallography, especially in short courses where it is desirable to present only the commoner forms and not to discuss classes.

This concept elevates systems to a rank of prime importance in crystallography based on independent properties and not on hypothetical axes of reference or groupings of classes.

PETROGRAPHY OF TWO IOWA LOESS MATERIALS

F. LEICESTER CUTHBERT

Two samples of loess material, selected by the Iowa State Highway Commission as being significant in highway construction, were investigated by several methods with the purpose of determining their mineralogical constitution. Although the materials are nearly similar as far as standardized highway laboratory tests are concerned, one affords a stable highway foundation while the other gives considerable difficulty, causing the slab to buckle and dip. Field examination revealed that the materials differed in their relation to a heavy gumbotil; one being located immediately above, and the other about ten feet above the gumbotil. The samples were fractionated by sedimentation and by a supercentrifuge. Chemical, *x*-ray, optical, and base-exchange studies were made on each of the colloidal separates obtained. The results show that one of the samples contains as its principal clay mineral, montmorillonite, while the other contains mixtures of kaolinite and illite. Evidence points to the conclusion that highway engineers must take into consideration both the geological positions of the materials to be used in subgrades and their clay mineral content.

ELEMENTARY DERIVATION OF THE 230 SPACE GROUPS

J. D. H. DONNAY

Elementary derivations of the 32 crystal classes and 14 lattices are known. The extinction criteria of the lattice modes can be established by simple considerations (Friedel's *Leçons*, 1926); the same method holds for deriving the extinction criteria of the various kinds of glide-planes and screw-axes. From these criteria, the different types of zonal distribution (described elsewhere)[1] are graphically derived (with the aid of the reciprocal

[1] J. D. H. Donnay: Le développement des zones cristallines. *Ann. Soc. géol. de Belgique* **61**, B 260–287, 1938.

lattice): *simple zones*, either with unit-face dominant or with dominant shifted, and *double zones*, in which the dominant is always the unit-face. A simple search of all the permissible combinations of such zone types for each lattice mode in each crystal system leads to the 97 *morphological aspects*. Which space-group (or space-groups), in the several classes, correspond to any one aspect then becomes immediately apparent. The method naturally lends itself to the use of the international (Hermann-Mauguin) notation for space-groups, and leads to the appropriate symbols for all alternate crystal settings.

The morphological expression of the space-group symmetry is shown, by means of simple conventions, on a stereographic projection. This projection assumes further value as an unequivocal graphic representation of the *aspect* in a certain setting.

SPECTROGRAPHIC STUDY OF CINNABAR

ROBERT M. DREYER

A quantitative spectrographic study of cinnabar from twenty quicksilver deposits has indicated the elemental content of quicksilver mineralizing solutions and the extent to which various impurities exist in solid solution in cinnabar. The study indicates that certain heavy metals are invariably associated with cinnabar ores (viz., iron, chromium, manganese, silver, copper, zinc, nickel, germanium, lead, and cobalt). Of these elements, certain are markedly differentially concentrated (presumably in solid solution) in the cinnabar—namely, copper, lead, cobalt, germanium, and silver. Such concentrations are found regardless of geological or geographical occurrence. The varying shades of cinnabar coloration are found to be independent of the elements differentially concentrated in the cinnabar.

A NEW PROJECTION-PROTRACTOR

D. JEROME FISHER

This projection protractor is made for either the stereographic or gnomonic projections. It is designed for general use with these projections, rather than solely for crystallographic purposes. It should therefore appeal to the field and laboratory geologist. Besides the usual stereographic and gnomonic scales drawn to spheres of radii 5 and 2 centimeters, it embraces a meridional stereographic half-net and a centimeter scale. It may be used as an ordinary protractor, straight-edge, scale, and right-angle triangle. It is available as an 8×20 centimeter rectangle on colorless transparent cellulose acetate .025 inch thick.

THE BINARY SYSTEM: $NaAlSiO_4$-$CaSiO_3$

W. R. FOSTER

A study of the equilibrium relations of the binary system carnegieite, nephelite-pseudowollastonite, wollastonite has been made as part of an investigation of the ternary system carnegieite, nephelite-pseudowollastonite, wollastonite-albite. The liquidus and sub-liquidus relations, and their petrological significance, are discussed.

EXSOLUTION GROWTHS OF ZINCITE IN MANGANOSITE

CLIFFORD FRONDEL

Manganosite crystals from Franklin, N. J., contain thin plates of zincite intergrown along octahedral planes. The two minerals are mutually oriented, with zincite {0001} [10$\bar{1}$0] parallel to manganosite {111} [110]. This position of orientation marks an exact coincidence in crystal structure of the two minerals. The zincite apparently has exsolved from the manganosite.

REDEFINITION OF TELLUROBISMUTHITE

CLIFFORD FRONDEL

Tellurobismuthite, long considered a variety of tetradymite, is a distinct species. Composition of unit cell Bi_2Te_3; rhombohedral, with $a_0=4.43$ Å and $\alpha=57°11'$; G = 7.66 (calc.), 7.65 (meas.); perfect cleavage {0001}. Ten localities are cited. Vandiesitte, a supposed telluride of Bi and Ag from Colorado, is shown to be a mixture of tellurobismuthite and hessite. *X*-ray powder data and polished section data are summarized for tellurobismuthite, tetradymite, gruenlingite, joseite and wehrlite.

THE RADIOACTIVITY OF SEDIMENTARY ROCKS AND ASSOCIATED PETROLEUM*

CLARK GOODMAN, K. G. BELL, AND W. L. WHITEHEAD

Determinations of the radioactivity of 21 sedimentary rocks and 7 associated crude oils have been made by the precision method developed by R. D. Evans. (1) The specimens consisted of cuttings and cores from wells in the Bartlesville, Cromwell, Frio, Woodbine and Viola-Simpson formations. Considerable variability in radioactivity was found in the sandstones (1.4 to 0.19×10^{-12} gms Ra/gm) and limestones (1.3 to 0.18×10^{-12} gms Ra/gm). The radium content of limestones decreases with increasing purity. The shales were quite uniform (1.2 to 1.0×10^{-12} gms Ra/gm). Apparently, discrete mineral particles in sandstone and impurities in limestone account for their occasional high radioactivity. The radon content of the crude oils (0.47 to 0.05×10^{-12} curies/gm of oil) was in one sample 38 times, and averaged 10 times, the amount in equilibrium with the radium present. The results corroborate the inferences of former investigators that radon tends to concentrate in crude oils. Maximum radon content and maximum ratio of radon to radium were found in petroleum produced from a permeable, Oligocene (Frio) sandstone of high radioactivity. Cracking of hydrocarbons with generation of hydrogen has been proved by S. C. Lind (2) to result from bombardment with alpha rays. The amounts of radioactivity found in these crude oils are quantitatively sufficient to cause appreciable cracking by alpha radiation during geologic time. These reactions, together with subsequent hydrogenation, may account for important changes in petroleum. This hypothesis would also explain the presence of hydrogen in some natural gases. The hydrogen content of soil gases is suggested as a possible method of geophysical prospecting for oil fields.

(1) Evans, R. D. Rev. of Sci. Inst. **6**, 99–112 (1935).

(2) Lind, S. C. "The Chemical Effects of Alpha Particles and Electrons," Chemical Catalog Co. (1928).

* Presented through the Society of Economic Geologists.

TUNGSTEN ARCS*

PAUL F. KERR

The tungsten deposits of the Cordillera of the United States define three belts for convenience designated as *tungsten arcs:* (1) extending from southern California to eastern Washington; (2) extending from southern Arizona to eastern Idaho; and (3) extending from Silverton, Colorado, to the Black Hills. More important tungsten localities along the arcs are:

Western arc—California: Atolia, Posey, Pine Creek, Tungsten Hills.
Nevada: Silver Dyke, Nightingale, Oreana, Mill City.
Oregon: Baker-Wallowa Mountain.
Washington: Germania.

* Presented through the Geological Society of America.

Central arc—Arizona: Dragoon, Las Guijas, Boriana.
Nevada: Snake Range.
Idaho: Lemhi
Eastern arc—Colorado: San Juan, Boulder.
South Dakota: Black Hills.

The western arc is perhaps connected with later phases of Nevadian orogeny, the central and perhaps the eastern arcs with Laramide. In each district the mineralization shows a relationship to the trend of the respective arc and suggests influence of an underlying igneous source.

Deposits are apparently confined to areas of actual or proximate igneous activity. The immediate contact is frequently barren. Aplite and pegmatite dikes or quartz veins favor concentration evidently as conduits from magmatic sources. Conduit bodies frequently contain traces but rarely concentrations of tungsten minerals. Field examination with ultra-violet light evidences the connection between ore formation in a host rock, scheelite bearing aplitic conduits, and adjacent granitic intrusives.

Considerable deposits may consist chiefly of scheelite, wolframite, hubnerite or ferberite ores but the psilomelane or limonite type may prove to be important. Tungsten bearing minerals occur in hot spring deposits, in quartz veins, in pegmatite dikes, in greisen zones and in contact metamorphic deposits. Ca-tungstate predominates in the western arc with the exception of Germania. Ca-, Fe-Mn-, and Mn-tungstates are important in the central arc. Fe-, Mn-, and Fe-Mn-tungstates are most abundant in the eastern arc.

FURTHER STUDIES ON THE VARIATION OF HARDNESS IN THE DIAMOND

EDWARD H. KRAUS AND CHESTER B. SLAWSON

Approximate hardness curves for certain crystal faces of the diamond are indicated, and the areas of optimum cutting and those which resist cutting are delimited.

THE GEOGRAPHIC CLASSIFICATION OF ANALYSES OF METAMORPHIC AND IGNEOUS ROCKS*

EDWARD B. MATHEWS

The ambitious undertaking supported by grants from the Geological Society is now well advanced and it has been deemed advantageous to present to the Fellows of the Society something of the manner of procedure and the results obtained and how the results may be serviceable before the undertaking is completed.

One of the largest published collections of chemical analyses of rocks is that in Professional Paper 99 which carried analyses published before 1913. This contains something over 9000 analyses. The present collection which is to be carried to 1940 already contains between 30,000–40,000 analyses grouped in single degree units. Since the sources are indicated this work may well serve as a series of bibliographies of small geographical units and a geologist going into a new region may readily secure a clue to practically all the available literature sufficiently detailed to have analyses of rocks.

The method of classification, some of the difficulties encountered in securing the location of the samples analyzed and some suggested improvements which can be made by authors in the future will be discussed if time permits.

---

* Presented through the Geological Society of America.

THE ISODIMORPHOUS SERIES, VARISCITE-METAVARISCITE

DUNCAN MCCONNELL

Through the use of x-ray methods the minerals starred have been referred definitely to an isodimorphous series.

Orthorhombic	Monoclinic ($\beta \rightarrow 90°$)	Composition
*Variscite	Metavariscite	$AlPO_4 \cdot 2H_2O$
*Barrandite	—	$(Al, Fe)PO_4 \cdot 2H_2O$
—	Vilateite	$(Fe, Mn)PO_4 \cdot 2H_2O$
*Strengite	*Phosphosiderite	$FePO_4 \cdot 2H_2O$
*Scorodite	—	$FeAsO_4 \cdot 2H_2O$

The axial ratios, optical properties, etc., permit the classification of the substances for which x-ray data have not been obtained. A more complete investigation will probably reveal that several poorly known substances are to be associated with this series.

DESCENT OF PLAGIOCLASE-RICH CORUNDUM BEARING PEGMATITES FROM DESILICATED GRANITE AT GLEN RIDDLE, PA.

ADOLPH E. MEIER

Two divergent opinions are held on the origin of albitites and plumasites (corundum-plagioclase bearing dikes). Du Toit, Gordon and Cobb favor a process of desilication of high silica pegmatites by reaction with basic wall rock. Larsen believes that they possess a hydrothermal mode of origin. Analogous types occurring as dikes or hydrothermal veins at Glen Riddle are rich in oligoclase where flanked by serpentine (meta-pyroxenite), and rich in andesine, oligoclase and corundum where associated with narrow dikes of gabbro previously emplaced in pyroxenite.

On the basis of a recent study of relations between the local hornblende granite, meta-pyroxenite and gabbro[1] and of more detailed work on the granite now in progress, it is believed that desilication and hydrothermal replacement have both played a significant role in the formation of the plagioclase-rich dikes and of the corundum found in the types mentioned.

Sufficient data has been collected thus far in three typical exposures to show that in comparatively large masses of granite the magnesium content increases and the quartz content of the latter decreases from the center of the mass to the bordering meta-pyroxenite. Where granite stringers or tongues narrow down to ten feet or less the quartz content is reduced to two per cent.

The conclusions to be drawn are that a process of desilication took place during an early stage of granitic intrusion as a direct result of assimilation of the invaded pyroxenite. As a result of this chemical conditioning the granitic exudates carried a high concentration of alkalies which filtered into the country rock, and produced veins analogous to plumasites by hydrothermal reaction with previously emplaced gabbro, and types analogous to albitites where pyroxenite alone was the host rock.

---

[1] Corundum in a Dike at Glen Riddle, Pa: W. H. Tomlinson, *Amer. Min.*, **24,** 339–343, 1939.

Association at Harmotome and Barium Feldspar at Glen Riddle, Pa.: A. E. Meier, *Amer. Min.*, **24,** 540–560, 1939.

THE CRYSTALLOGRAPHY OF ULEXITE

JOSEPH MURDOCH

Measurable crystals of ulexite discovered at Kramer, California, show that the mineral is triclinic, with the following elements:

a:b:c	0.68553:1:0.51911	
α90°16′	β109°08′	γ105°07′
$p_0:q_0:r_0$	0.78523:0.50804:1	
λ84°20½′	μ70°05½′	ν73°53½′
p_0′ 0.83514	q_0′ 0.54032	
x_0′ 0.34662	y_0′ 0.10483	

The crystals occur as an irregular network of prismatic forms in a matrix of borax and clay. They are sometimes as much as five mm. long, though few terminated crystals are this size. In general the shape of the crystals is lathlike, with elongation 3–4 times the short dimension. The consistently broad face in the prism zone is (100), and other common faces here are (010) (110) and (1$\bar{1}$0). (130) (350) (3$\bar{1}$0) and (12$\bar{0}$) were also seen. Terminal faces, in order of frequency, are ($\bar{1}\bar{1}$1) (0$\bar{1}$1) (001) ($\bar{1}$11) ($\bar{1}$01), the form ($\bar{1}\bar{1}$1) appearing on practically every crystal.

THE TERNARY SYSTEM AKERMANITE--GEHLENITE--PSEUDO-WOLLASTONITE

E. F. OSBORN AND J. F. SCHAIRER

Phase equilibrium studies on the ternary system with the melilite molecules akermanite and gehlenite and a simple pyroxene, $CaSiO_3$, have just been completed. Akermanite and gehlenite form a complete series of solid solutions, but no appreciable solid solution exists between $CaSiO_3$ and either akermanite or gehlenite. There is no ternary eutectic, but a minimum at 1302 $\pm$2° with two solid phases present—a melilite (solid solution of akermanite and gehlenite) and pseudo-wollastonite. For some mixtures in this system, as crystallization proceeds melilite crystals are first enriched in akermanite, then reverse and become enriched in gehlenite.

CUPROBISMUTITE—A MIXTURE

CHARLES PALACHE

Cuprobismutite is shown by a study of the type material to be a mixture of three minerals—emplectite, bismuthite, and chalcopyrite. Crystals of the two first-named minerals were measured.

MICROLITE FROM TOPSHAM, MAINE

CHARLES PALACHE AND F. A. GONYER

An analysis and physical description is given of a new occurrence of microlite which had previously been mistaken for gahnite.

RAMMELSBERGITE AND PARARAMMELSBERGITE, DISTINCT ORTHORHOMBIC FORMS OF $NiAs_2$

M. A. PEACOCK

Rammelsbergite from Schneeberg, Saxony (type locality) and Eisleben, Thuringia, gives identical x-ray powder photographs. The specimen from Eisleben is compact, fibrous to lathy, tin-white, with bright narrow cleavage planes. The polished section is white, homogeneous, hard, strongly anisotropic. With the fibre axis vertical Weissenberg photographs give orthorhombic symmetry; holohedral space group *Pmnn;* a_0 3.53, b_0 4.78, c_0 5.78 Å. Twin plane (110); cleavage {110}. The unit cell contains Ni_2As_4. G 7.06 (calc.), 6.9–7.158 (Dana). These structural data conform to the meagre geometrical data (Dürrfeld, 1911), and show the expected similarity to those of marcasite (Buerger, 1931).

Recently described materials provisionally named rammelsbergite (Peacock and Michener, 1939), from Cobalt, Ontario, and Elk Lake, Ontario, give identical x-ray powder photographs unlike those of from Schneeberg and Eisleben. The specimens are compact,

tin-white, with small bright cleavage areas. The polished sections are white, homogeneous, hard, strongly anisotropic. Analysis: Ni 28.1, Co 0.4, As 68.5, S 2.6=99.6. Weissenberg photographs give orthorhombic (or pseudo-orthorhombic) symmetry; apparent holohedral space group *Pbma;* a_0 5.74, b_0 5.81, c_0 11.405 Å; twinning not observed; cleavage {001}. The unit cell contains Ni_8As_{16}. *G* 7.24 (calc.); 7.12 (meas.). The Canadian mineral is thus a distinct species for which the name *pararammelsbergite* is proposed.

The cell-edges of rammelsbergite and pararammelsbergite are not simply related to the cube-edge of smaltite-chloanthite (Oftedal, 1925), supposed to have the composition (Co, Ni)As_2.

RECONNAISSANCE OF THE CONTACT METAMORPHISM OF THE KATAHDIN GRANITE

SHAILER S. PHILBRICK

The Katahdin granite, an intrusive some 60 miles long, in Piscataquis and Penobscot counties, Maine, has been found to have metamorphosed its country rock, a series of slates and thin interbedded quartzitic sandstones of varying composition, with the development of hornfels and schist. Near the igneous contact considerable aplitic material has been injected in veinlets and ptygmatic folding and brecciation have been produced in the hornfels. The reconnaissance has been confined to the southern and southwestern portions of the intrusive where a belt of metamorphics some 35 miles in length has been noted outcropping on several mountain ranges. The metamorphics are strikingly similar in general character to those found about 10 miles to the south in the three zoned aureole surrounding the Onawa pluton, a small body about 11 miles long. The greater size of the Katahdin granite, as far as can be determined at this time, seems not to have comparably influenced the degree or lateral extent of the metamorphism.

Keith has mapped a belt of Cambrian or Ordovician rocks along the boundaries of the Katahdin granite in the area under consideration and also surrounding the Onawa pluton. In the latter case the writer believes that these rocks are the common Silurian of central Maine metamorphosed by the Onawa pluton. Those bounding the Katahdin granite here may, or may not, be pre-Silurian but since their metamorphic character is attributed mainly to contact with the granite it is assumed, in the absence of paleontologic evidence to the contrary, that they are Silurian and the same age as the common slate series of central Maine.

THE BINARY SYSTEM: ALBITE ($NaAlSi_3O_8$)-SPHENE ($CaTiSiO_5$)

A. T. PRINCE

The liquidus curve of the binary system, albite-sphene, has been determined as part of an investigation of the ternary system, albite-anorthite-sphene. The character of the curve and its petrological significance are discussed.

THE CRYSTAL SYSTEM AND UNIT CELL OF ACANTHITE, Ag_2S

LEWIS S. RAMSDELL

Preliminary data obtained from twinned acanthite crystals by means of Weissenberg photographs indicate a monoclinic unit cell, with $a=4.20$, $b=6.93$, $c=9.50$ Å, and $\beta=55°$.

CRYSTALLOGRAPHY OF DOLEROPHANITE

W. E. RICHMOND AND C. W. WOLFE

Dolerophanite, Cu_2SO_5, from the type locality has been re-examined. An *x*-ray study establishes the validity of the Goldschmidt orientation. The mineral is figured in his position.

ZONES, ZONE-BUNDLES, AND CRYSTAL SYSTEMS

AUSTIN F. ROGERS

Zones are not sufficiently emphasized in elementary work. The use of a linear projection combined with a front elevation provides a simple method of showing the relation between face-indices and zone-indices.

All the possible zones of crystals are included under four types: clinogonal, orthogonal, hexagonal, and tetragonal, which are defined in terms of the interfacial angles that remain constant with a change of temperature.

A zone-bundle is a series of zones with one face in common and may be defined by its interzonal angles. Six kinds of zone-bundles are recognized: tetragonal, hexagonal, orthogonal of two kinds, and clinogonal of two kinds.

Zones furnish a simple, accurate method of defining crystal systems:

Triclinic:	All zones are clinogonal.
Monoclinic:	A symmetry direction (a symmetry axis or a line normal to a symmetry plane) is a clinogonal zone-axis.
Orthorhombic:	Three orthogonal zones at right angles to each other.
Tetragonal:	A single tetragonal zone.
Hexagonal:	A single hexagonal zone.
Isometric:	Three tetragonal zones and four hexagonal zones.

All crystals of a given crystal system have the same kind of normal zone-pattern, which may be defined as the complex of nine zones with the simplest indices or 13 zones if four axes of reference are used.

Since the 12 symmetry classes with a single hexagonal zone all have the same kind of normal zone-pattern, there are six crystal systems and not seven.

THE RARER METALLIC CONSTITUENTS OF SOME AMERICAN IGNEOUS ROCKS

E. B. SANDELL AND S. S. GOLDICH

This paper is a preliminary report of an investigation of the less abundant heavy metals in igneous rocks. Copper, lead, zinc, cobalt, nickel, and molybdenum were determined in 31 samples using semi-micro-chemical methods. The analyzed samples represent three igneous areas in central United States and are distributed as follows: from the Llano (Central Mineral) region of Texas, 7; from the St. Francois Mountains of Missouri, 7; from central and northern Minnesota, 17. In addition cobalt and nickel determinations were made on 19 samples of the Keweenawan flows from the Michigan copper district. The distribution of cobalt and nickel in the Kearsarge and in the Greenstone flows is discussed and correlated with Broderick's findings for copper and for the major rock constituents. The data are presented in tables and in a series of diagrams.

A PROBABLY NEW PHOSPHATE-SULPHATE OF ALUMINUM FROM UTAH

WALDEMAR T. SCHALLER

A scaly white mineral, like alunogen in appearance and in its properties, was collected in the Tintic Standard mine, Dividend, Utah, along with many other secondary sulphates. The mineral, intimately associated with halotrichite, siderotile, and szomolnokite, is readily soluble in cold water from which solution when warmed a curdy white precipitate forms. On cooling, the precipitate disappears, the solution becoming clear again.

Analyses of two different samples yielded the same formula, $2Al_2O_3 \cdot 4SO_3 \cdot P_2O_5 \cdot 24H_2O$ which might be interpreted as a phosphorian alunogen, with one-third of the sulphate replaced by phosphate on the basis of considering $[SO_4]$ and $[HPO_4]$ as equivalent, as follows:

Alunogen	$Al_2(SO_4)_3 \cdot 16H_2O$	or $2Al_2O_3 \cdot 6SO_3 \cdot 32H_2O$
Phosphorian alunogen	$Al_2(SO_4)_2(HPO_4) \cdot 16H_2O$	or $2Al_2O_3 \cdot 4SO_3 \cdot P_2O_5 \cdot 33H_2O$
Mineral	$Al_2(SO_4)_2(HPO_4) \cdot 11\frac{1}{2}H_2O$	or $2Al_2O_3 \cdot 4SO_3 \cdot P_2O_5 \cdot 24H_2O$

The mineral however contains less total water than a phosphorian alunogen, the ratio of P_2O_5 to SO_3 is definite (1:4), two different samples have the same composition, and most important, the mineral loses no water at 105° whereas alunogen loses 30 per cent or $\frac{2}{3}$ of its total water at 105°. The mineral therefore seems to be a new species and not merely a variety of alunogen.

A METHOD FOR MAKING ACCURATE DRAWINGS OF CRYSTALS

WALDEMAR T. SCHALLER

Accurate crystal drawings may be made by photographing a crystal in the positions corresponding to the orthographic and clinographic projections. The crystal is adjusted in polar position on the goniometer and its correct position before the camera determined by various means. The photographs are enlarged to the proper size and the lengths of the intersection edges measured and transferred to the drawing or they may be inked in on the enlargement and the crystal drawing traced off. Illustrated by examples.

LARGE SANIDINE CRYSTALS FROM UTAH

BRONSON STRINGHAM AND NORMAN C. WILLIAMS

Sanidine is often present in small monzonite intrusives of the Stockton-Tooele area of the Oquirrh Mountains, Utah. Two localities are of special interest because of the large size of the crystals and the ease with which they are separated from the parent rock. One mile south of Tooele in a small sill, sanidine crystals averaging three centimeters in length are easily procured. These crystals, grayish in color, exhibit faces conventional to orthoclase which is elongated parallel to *a*. Carlsbad twins are abundant and of unusual shape since the elongation of *a* is not sacrificed for elongation parallel to the prism. The gray color is due chiefly to inclusions consisting of calcite and small andesine crystals. The latter are often grouped in rows parallel to the growth lines of the host.

The second occurrence has been exposed by a water development tunnel in Pine Canyon north of Tooele. Large single crystals elongated parallel to *a*, and Carlsbad twins are abundant. They are gray in color and average eight centimeters in length with some reaching eleven centimeters. Although most crystals exhibit excellent forms, many are rounded due to resorbtion.

THE MORPHOLOGY OF COLUMBITE CRYSTALS

E. D. TAYLOR

By the morphological method of Donnay (1938), the space-group of columbite (Fe, Mn) (Nb, Ta)$_2O_6$ is found to be *Pman*, in a new setting ($a:b:c=0.4023:1:0.3580$) chosen so as to comply with the convention $c<a<b$. (Transformations: Taylor to Dana $=0\bar{1}0/\bar{3}00/00\bar{3}$. Taylor to Sturdivant $=00\bar{1}/0\bar{1}0/\bar{1}00$.) According to *x*-ray results (Sturdivant, 1930; confirmed by Peacock, 1939, unpublished), the space-group is *Pcan* (in the same setting). The conflict lies in the interpretation of the zone [100]: the morphology indicates (100) to be a mirror plane of symmetry, whereas *x*-rays unquestionably show it to be a *c* glide-plane. This is the first clear case of disagreement between the morphological and the structural results.

Although the available data concerning the faces (0*kl*) are scarce, they cannot be reconciled with a *c* glide-plane at all. That the structural arrangement might simulate a

mirror plane where a glide-plane actually exists is a plausible hypothesis which, however, cannot be substantiated at present.

As to the prediction of relative form importances, the classical Law of Bravais does not agree with the observed facts as well as the generalized law (Donnay-Harker, 1937) which, although not perfect, is decidedly better.

SLIDES SHOWING MINERAL ASSOCIATIONS OF CORUNDUM

W. HAROLD TOMLINSON

Three slides showing association of corundum in ultra-basic rocks.
Three slides showing association of corundum in syenites.

THE RELATIONSHIP BETWEEN THE CRYSTAL STRUCTURES OF THE GOLD-SILVER TELLURIDE MINERALS, SYLVANITE, KRENNERITE, AND CALAVERITE

GEORGE TUNELL

The crystal structures of the gold-silver telluride minerals, sylvanite, krennerite, and calaverite, are fundamentally related, although they crystallize in three different space-groups. In all three minerals pairs of tellurium atoms occur between metal atoms (gold or silver) along a set of parallel lines. The coordination is octahedral in all three minerals, but the nearest neighbors of a tellurium atom are in some cases three metal atoms and three telluriums, in others one metal and five telluriums, and finally in others five metal atoms and one tellurium; the nearest neighbors of each metal atom are in all cases six telluriums. New chemical analyses* of krennerite and new pycnometric determinations of its density have been carried out on pure faceted crystals identified by measurement on the two-circle reflection goniometer in order to clear up uncertainties in the literature concerning these points.

* The chemical analyses were made by K. J. Murata in the U. S. Geological Survey.

CONTACT METAMORPHISM AT RYE PATCH, NEVADA

CHARLES J. VITALIANO

The area under discussion is situated in the west central part of the Humboldt Range.

Westward dipping sediments occur, consisting largely of Triassic (?) limestone interbedded with an occasional thin layer of a more shaly nature. These sediments have been intruded by two different types of igneous rocks. The earlier intrusive is of a granitic nature. It occurs as a small, irregular intrusive, sill-like in part, probably connected in depth with the Rocky Canyon intrusive which occurs farther south in the Humboldt Range. The second intrusive type is a porphyry of a basic nature occurring in dikes which cut across the bedding of the limestone.

Both types of intrusives are surrounded by an aureole of contact metamorphism. In addition, a long narrow area of contact metamorphism extends northward a considerable distance from the granitic intrusive. The changes produced in the sediments range from the recrystallization of the limestone to the development of typical contact silicates. The area has been mapped in detail in order to establish the areal distribution of metamorphism with relation to the intrusive. Microscopic studies have been made to establish the sequence of mineralization and selectivity of metamorphism for certain strata.

SCHEDULE OF PRESENTATION OF PAPERS

Thursday, December 28, 1939 AFTERNOON SESSION Parlor N

Chairman: Max N. Short

1	2:30	C. Palache	Cuprobismutite—a mixture. (5 minutes)
2	2:37	W. T. Schaller	A probable new phosphate-sulphate of aluminum from Utah. (Lantern slides; 10 minutes)
3	2:49	E. H. Kraus and C. B. Slawson	Further studies on the variation of hardness in the diamond. (Lantern slides; 10 minutes)
4	3:01	M. A. Peacock	Rammelsbergite and pararammelsbergite, distinct orthorhombic forms of $NiAs_2$ (Lantern slides; 10 minutes)
5	3:13	D. J. Fisher	A new projection-protractor. (Lantern slides; 10 minutes)
6	3:25	G. Tunell	The relationship between the crystal structures of gold-silver telluride minerals, sylvanite, krennerite, calaverite. (Lantern slides; 10 minutes)
7	3:37	H. Berman	Classification of the native elements, sulphides, and sulpho-salts. (Lantern slides; 10 minutes)
8	3:49	E. D. Taylor	The morphology of columbite crystals. (Lantern slides; 8 minutes)
9	3:59	J. D. H. Donnay	Elementary derivation of the 230 space groups (Lantern slides; 12 minutes)
10	4:13	V. L. Ayres	Stilpnomelane, nontronite, and halloysite from northern Michigan. (10 minutes)
11	4:25	C. Palache and F. A. Gonyer	Microlite from Topsham, Maine. (5 minutes)
12	4:32	A. T. Prince	The binary system: albite ($NaAlSi_3O_8$)—sphene ($CaTiSiO_5$). (Lantern slides; 7 minutes)
13	4:41	F. M. Bullard	The Bartlett meteorite, Bell County, Texas. (Lantern slides; 5 minutes)
14	4:48	D. McConnell	The isodimorphous series, variscite—metavariscite. (5 minutes)
15	4:55	W. R. Foster	The binary system: $NaAlSiO_4$-$CaSiO_3$. (Lantern slides; 7 minutes)
16	5:04	C. Frondel	Exsolution growths of zincite in manganosite, (5 minutes)
17	5:11	W. H. Tomlinson	Slides showing mineral associations of corundum. (6 minutes)
18		A. E. Meier	Descent of plagioclase-rich corundum bearing pegmatites from desilicated granite at Glen Riddle, Pennsylvania. (Presented by title)
19		C. J. Vitaliano	Contact metamorphism at Rye Patch, Nevada. (Presented by title)

Friday, December 29, 1939 MORNING SESSION Parlor N

Chairman: Max N. Short

1	9:15	B. Stringham and N. C. Williams	Large sanidine crystals from Utah. (Lantern slides; 5 minutes)
2	9:22	W. F. Bradley	The structural scheme of attapulgite. (Lantern slides; 10 minutes)
3	9:34	W. E. Richmond and C. W. Wolfe	Crystallography of dolerophanite. (5 minutes)
4	9:41	N. W. Buerger	An x-ray investigation of the solid phases of the system Cu_2S-CuS. (Lantern slides; 12 minutes)
5	9:55	L. G. Berry	Structural crystallography and composition of jamesonite. (Lantern slides; 10 minutes)
6	10:07	L. S. Ramsdell	The crystal system and unit cell of acanthite, Ag_2S. (Lantern slides; 10 minutes)
7	10:19	C. Frondel	Redefinition of tellurobismuthite. (10 minutes)

8	10:31	A. F. Rogers	Zones, zone-bundles, and crystal systems. (Lantern slides; 15 minutes)
9	10:48	W. T. Schaller	A method for making accurate drawings of crystals. (Lantern slides; 10 minutes)
10	11:00	J. D. Burfoot, Jr.	The concept of unique diameters in crystallography. (Lantern slides; 12 minutes)
11	11:14	J. Murdoch	The crystallography of ulexite. (Lantern slides; 10 minutes)

Friday, December 29, 1939 **AFTERNOON SESSION** **Grand Ballroom**

Chairman: Ellis Thomson

Geological Society of America—Mineralogical Society of America—Society of Economic Geologists

1	2:00	F. L. Cuthbert	Petrography of two Iowa loess materials. (Lantern slides; 10 minutes)
2	2:12	E. B. Mathews	The geographic classification of analyses of metamorphic and igneous rocks. (10 minutes)
3	2:24	C. H. Behre, Jr.	Structural control in European lead-zinc ores of the Mississippi Valley type. (Lantern slides; 12 minutes)
4	2:38	E. F. Osborn and J. F. Schairer	The ternary system akermanite--gehlenite--pseudo-wollastonite. (Lantern slides; 15 minutes)
5	2:55	P. F. Kerr	Tungsten arcs. (Lantern slides; 15 minutes)
6	3:12	C. Goodman, K. G. Bell, and W. L. Whitehead	The radioactivity of sedimentary rocks and associated petroleum. (Lantern slides; 10 minutes)
7	3:24	R. M. Dreyer	Spectographic study of cinnabar. (Lantern slides; 15 minutes)
8	3:41	S. S. Philbrick	Reconnaissance of the contact metamorphism of the Katahdin granite (Maine). (Lantern slides; 10 minutes)
9	3:53	E. B. Sandell and S. S. Goldich	The rarer metallic constituents of some American igneous rocks. (Lantern slides; 12 minutes)
10	4:07	C. N. Apsouri	The pegmatites of the Keystone area, South Dakota. (Lantern slides; 15 minutes)